

AD-A186 419

THE SYNTHESIS OF STABLE FORCE-CLOSURE GRASPS(U)
MASSACHUSETTS INST OF TECH CAMBRIDGE ARTIFICIAL
INTELLIGENCE LAB V NGUYEN JUL 86 AI-TR-985

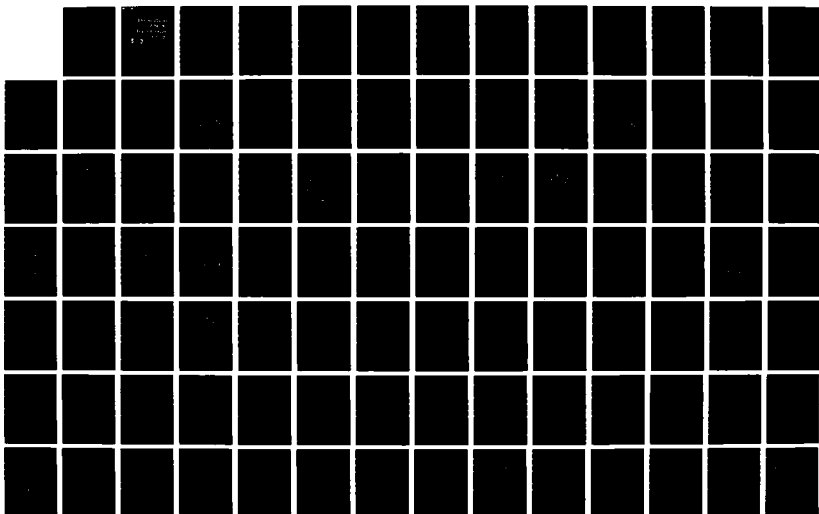
1/2

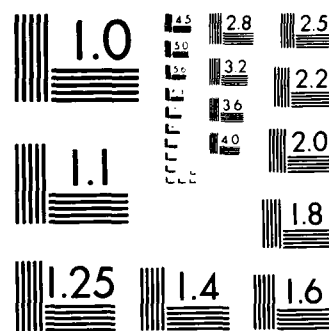
UNCLASSIFIED

N00014-85-K-0124

F/G 23/1

NL





MICROCOPY RESOLUTION TEST CHART
NATIONAL BUREAU OF STANDARDS 1963 A

AD-A186 419

Technical Report 905

The Synthesis of Stable Force-Closure Grasps

DTIC
ELECTE
OCT 22 1987
S D

Van-Duc Nguyen

MIT Artificial Intelligence Laboratory

DISTRIBUTION STATEMENT A
Approved for public release
Distribution Unlimited

87 10 13 022

UNCLASSIFIED

SECURITY CLASSIFICATION OF THIS PAGE (When Data Entered)

REPORT DOCUMENTATION PAGE		READ INSTRUCTIONS BEFORE COMPLETING FORM
1. REPORT NUMBER AI-TR 905	2. GOVT ACCESSION NO. 14-00000-107	3. RECIPIENT'S CATALOG NUMBER
4. TITLE (and Subtitle) The Synthesis of Stable Force-Closure Grasps		5. TYPE OF REPORT & PERIOD COVERED Technical Report
		6. PERFORMING ORG. REPORT NUMBER
7. AUTHOR(s) Van-Duc Nguyen		8. CONTRACT OR GRANT NUMBER(s) N00014-85-K-0124
9. PERFORMING ORGANIZATION NAME AND ADDRESS Artificial Intelligence Laboratory 545 Technology Square Cambridge, MA 02139		10. PROGRAM ELEMENT, PROJECT, TASK AREA & WORK UNIT NUMBERS
11. CONTROLLING OFFICE NAME AND ADDRESS Advanced Research Projects Agency 1400 Wilson Blvd. Arlington, VA 22209		12. REPORT DATE July 1986
		13. NUMBER OF PAGES 134
14. MONITORING AGENCY NAME & ADDRESS (if different from Controlling Office) Office of Naval Research Information Systems Arlington, VA 22217		15. SECURITY CLASS. (of this report) UNCLASSIFIED
		15a. DECLASSIFICATION/DOWNGRADING SCHEDULE
16. DISTRIBUTION STATEMENT (of this Report) Distribution is unlimited.		
17. DISTRIBUTION STATEMENT (of the abstract entered in Block 20, if different from Report)		
18. SUPPLEMENTARY NOTES None		
19. KEY WORDS (Continue on reverse side if necessary and identify by block number) Grasp synthesis Grasp analysis Force-closure Stability Slip Active stiffness control		
20. ABSTRACT (Continue on reverse side if necessary and identify by block number) The thesis addresses the problem of synthesizing grasps that are force-closure and stable. The synthesis of force-closure grasps constructs independent regions of contact for the fingertips, such that the motion of the grasped object is totally constrained. The synthesis of stable grasps constructs virtual springs at the contacts, such that the grasped object is stable, and has a desired stiffness matrix about its stable equilibrium. (cont. on back)		

DD FORM 1473
1 JAN 73EDITION OF 1 NOV 65 IS OBSOLETE
S/N 0102-014-6601

UNCLASSIFIED

SECURITY CLASSIFICATION OF THIS PAGE (When Data Entered)

Block 20 cont.

A grasp of an object is force-closure if and only if we can exert, through the set of contacts, arbitrary forces and moments on the object. So force-closure implies equilibrium exists because zero force and moment is spanned. In the reverse direction, ~~we prove that~~ a non-marginal equilibrium grasp is also a force-closure grasp, if it has at least two point contacts with friction in 2D, or two soft-finger contacts or three hard-finger contacts in 3D.

~~Next, we prove that~~ all force-closure grasps can be made stable, by using either active or passive springs at the contacts. The thesis develops a simple relation between the stability and stiffness of the grasp and the spatial configuration of the virtual springs at the contacts. The stiffness of the grasp depends also on whether the points of contact stick, or slide without friction on straight or curved surfaces of the object.

The thesis presents fast and simple algorithms for directly constructing stable force-closure grasps based on the shape of the grasped object. The formal framework of force-closure and stable grasps provides a partial explanation to why we stable grasp objects so easily, and to why our fingers are better soft than hard.

The Synthesis of Stable Force-Closure Grasps

by

Van-Duc Nguyen

©Massachusetts Institute of Technology, 1986.



Accession For	
NTIS CRA&I	<input checked="checked" type="checkbox"/>
DTIC TAB	<input type="checkbox"/>
Unannounced	<input type="checkbox"/>
Justification	
By	
Distribution /	
Acquisition Codes	
A-1	

This report is a revised version of a thesis submitted to the Department of Electrical Engineering and Computer Science on May 16, 1986 in partial fulfillment of the requirements for the degree of Master of Science.

Acknowledgements. This report describes research done at the Artificial Intelligence Laboratory of the Massachusetts Institute of Technology. Support for the Laboratory's Artificial Intelligence research is provided in part by the System Development Foundation and in part by the Advanced Research Projects Agency of the Department of Defense under Office of Naval Research contract N00014-85-K-0124.

The Synthesis of Stable Force-Closure Grasps

by

Van-Duc Nguyen

Abstract

The thesis addresses the problem of synthesizing grasps that are force-closure and stable. The synthesis of force-closure grasps constructs independent regions of contact for the fingertips, such that the motion of the grasped object is totally constrained. The synthesis of stable grasps constructs virtual springs at the contacts, such that the grasped object is stable, and has a desired stiffness matrix about its stable equilibrium.

A grasp on an object is force-closure if and only if we can exert, through the set of contacts, arbitrary forces and moments on the object. So force-closure implies equilibrium exists because zero force and moment is spanned. In the reverse direction, we prove that a non-marginal equilibrium grasp is also a force-closure grasp, if it has at least two point contacts with friction in 2D, or two soft-finger contacts or three hard-finger contacts in 3D.

Next, we prove that all force-closure grasps can be made stable, by using either active or passive springs at the contacts. The thesis develops a simple relation between the stability and stiffness of the grasp and the spatial configuration of the virtual springs at the contacts. The stiffness of the grasp depends also on whether the points of contact stick, or slide without friction on straight or curved surfaces of the object.

The thesis presents fast and simple algorithms for directly constructing stable force-closure grasps based on the shape of the grasped object. The formal framework of force-closure and stable grasps provides a partial explanation to why we stably grasp objects so easily, and to why our fingers are better soft than hard.

Thesis Supervisor: Professor Tomás Lozano-Pérez

Title: Associate Professor of Electrical Engineering and
Computer Science

Acknowledgements

I am grateful to Tomás Lozano-Pérez for his warm guidance and encouragement, and for many helpful discussions. Tomás has been my advisor, my professor and research supervisor over the five years I spent at MIT. He has made a great influence on me, both as a person and as a professional.

I am fortunate to learn from dedicated professors: William Siebert, Gerald Sussman, Patrick Winston, Gilbert Strang, and Eric Grimson. I am grateful for the dedication they put in teaching and preparing lectures which open up my horizons.

Above all, I am blessed with such caring parents. My deepest gratitude goes to my parents for their love and support. Thanks go to my parents and fiancée for encouraging me to learn and educate myself.

I would like to thank Tomás Lozano-Pérez for his careful reading of this thesis. I would like to thank Kenneth Salisbury for helping me setup experiments with the three-finger hand, and for sharing my enthusiasm over new ideas and results.

The Artificial Intelligence Laboratory has been a great place to learn and do research. I am grateful to Patrick Winston for nurturing the open and flexible environment at the laboratory, and to my friends Alain Lanusse, Sundar Narasimhan, Bruce Donald, John Canny, Mike Erdmann, Robert Hall, Gil Etinger, for making this place so pleasant to be in.

My first year of research is supported by a fellowship from the System Development Foundation. My second year is supported by a grant from the National Science Foundation, Grant DMC-8451218. Part of the research on 2D stable grasps is done over the summer of 1985 at the General Motors Research Laboratories.

Contents

1	Introduction	1
1.1	How to Grasp an Object?	1
1.2	Framework and Assumptions	2
1.3	Examples	3
1.4	Contributions	6
1.5	Other Related Works	8
2	Constructing Force-Closure Grasps	10
2.1	Where Should the Fingertips Be Placed?	10
2.2	Background Theory of Twists and Wrenches	12
2.2.1	Plücker Line Coordinates	12
2.2.2	Virtual Work and Total Freedom	13
2.2.3	Convexes and Operations on Convexes	15
2.2.4	Dual Subsystems	17
2.3	Force-Closure Grasps in 2D	19
2.3.1	Representing Contacts and Grasps	19
2.3.2	Resisting Translation and Rotation	22
2.3.3	Finding All Force Closure Grasps	25
2.3.4	Finding Independent Regions of Contact	30
2.3.5	Force-Closure with Redundant Contacts	35
2.4	Force-Closure Grasps in 3D	37
2.4.1	Primitive Contacts	37
2.4.2	Grasps with Two Soft-Finger Contacts	37
2.4.3	Grasps with Three Hard-Finger Contacts	43
2.4.4	Grasps with Seven Frictionless Point Contacts	46
2.5	Conclusion	50
2.5.1	Main Results	50
2.5.2	Extensions	50
3	Constructing Stable Grasps	52
3.1	How Should the Fingers Be Servoed?	52
3.2	Stable Grasps in 2D	54
3.2.1	Planar Grasps with Linear Springs	54
3.2.2	Compliance about Stable Equilibrium	56
3.2.3	Finding Virtual Springs at the Fingertips	64

3.3	Stable Grasps in 3D	70
3.3.1	Ideal Independent Springs	70
3.3.2	Equilibrium and Stability Conditions	74
3.3.3	Compliance about Stable Equilibrium	80
3.4	Conclusion	86
3.4.1	Main Results	86
3.4.2	Experiments	86
4	Grasping With Slip	91
4.1	How to Deal with Slip?	91
4.2	Analysis of Slip in 2D	92
4.2.1	When Do the Fingers Slip?	92
4.2.2	Where Will The Fingers Slip To?	93
4.3	Effect of Slip on Force-Closure and Stability	97
4.3.1	Grasps without Friction	97
4.3.2	Grasps with Friction	99
4.4	Slip on Circular Arcs	101
4.4.1	Model Local Curvatures with Wide Circular Arcs	101
4.4.2	Effect of Local Curvature on Stability	103
4.5	Conclusion	107
5	Conclusion	108
5.1	A Review	108
5.2	Open Problems	109
A	110
A.1	Force-Direction Closure With Planar Forces	110
A.2	Torque Closure With Planar Forces	113
A.3	Stiffness Matrix When the Fingertips Stick	118

List of Figures

1.1	Examples of force-closure grasps found by the synthesis.	4
1.2	Examples of stable grasps found by the synthesis.	5
2.1	Examples of force-closure grasps in 2D and 3D.	11
2.2	Total freedom of a box lying on a frictionless plane.	14
2.3	A 2D friction cone is represented by a two-wrench convex.	16
2.4	Planar contacts and their twist and wrench convexes.	20
2.5	Duality between twist and wrench spaces.	22
2.6	A geometrical view of force-direction closure.	23
2.7	A geometrical view of torque closure.	24
2.8	Finding frictionless grasps on four edges.	26
2.9	Finding grasps with friction on two edges.	29
2.10	Finding the independent regions of contact on two edges.	31
2.11	Independent regions for four frictionless point contacts.	32
2.12	Search for the optimum vertex of the two-sided cone.	33
2.13	Primitive contacts in 3D.	38
2.14	Complex contacts in 3D.	39
2.15	Force-closure with two soft-finger contacts.	41
2.16	Two distinct soft-finger contacts give six independent wrenches. . . .	42
2.17	Force-closure grasps with three hard-finger contacts.	44
2.18	Sequence of two-point and three-point grasps.	45
2.19	Force-closure grasps with seven frictionless contacts.	46
3.1	Examples of stable grasps in 2D and 3D.	53
3.2	A frictionless fingertip modeled as a linear spring.	55
3.3	Compliance of the grasped object about its stable equilibrium. . . .	59
3.4	Compliance polygon of a grasp.	61
3.5	Compliance polygon always exists for force-closure grasps.	61
3.6	Outside-in / inside-out / mixed grasps.	63
3.7	Pin and hole insertion with passive and active stiffness.	65
3.8	Linked chains and their loop equations.	67
3.9	Models for linear and angular springs in 3D.	71
3.10	Two hard-finger contacts versus two soft-finger contacts.	79
3.11	Compliance polyhedron in a grasp with 2 hard-finger contacts. . . .	84
3.12	A sequence of commands which executes a grasp.	87
3.13	The Stanford JPL hand.	89

4.1	A fingertip modeled as two independent springs.	93
4.2	Places where slip occurs as the object is displaced.	94
4.3	Stick and slip regions for the fingertip.	95
4.4	Places where the fingers will slip to.	95
4.5	Effect of large displacements on a frictionless grasp.	98
4.6	Point contacts slipping on curved segments.	102
4.7	Model local curvature with a wide circular arc.	103
4.8	Two frictionless point contacts pressing at two concave half-circles. .	104
A.1	A geometrical view of force-direction closure.	111
A.2	A geometrical view of torque closure.	114
A.3	A fingertip which sticks is modeled by two linear springs.	119

Notation

O	Origin of the reference frame.
P_i	Point of contact.
e_i	Edge of contact.
s_i	Independent region of contact for point P_i .
ψ	Angle between two grasping edges or faces.
ϕ	Half angle of the friction cone.
C_i	Local center of curvature.
r_i	Local radius of curvature.
$G = (P_1, \dots, P_n)$	Grasp on object.
$\mathbf{f} = (f_x, f_y, f_z)^T$	Force applied on object at O .
$\mathbf{m} = (m_x, m_y, m_z)^T$	Moment applied on object about O .
$\hat{\mathbf{w}} = (\mathbf{f}^T, \mathbf{m}^T)^T$	Wrench applied on object, and resolved at origin O .
$\delta = (\delta_x, \delta_y, \delta_z)^T$	Infinitesimal rotation of object about O .
$\mathbf{d} = (d_x, d_y, d_z)^T$	Infinitesimal translation of object at O .
$\hat{\mathbf{t}} = (\delta^T, \mathbf{d}^T)^T$	Twist displacement of object resolved at origin O .
$\hat{\mathbf{t}}^S = (\mathbf{d}^T, \delta^T)^T$	Spatial transpose of twist $\hat{\mathbf{t}}$.
$C^<$	Convex cone, or non-negative combinations of vectors in C .
$W^<$	Wrench convex, or range of forces and moments applied on object.
$T^<$	Twist convex, or range of unconstrained motions of object.
$C_1^< \cup C_2^<$	Convex addition of $C_1^<$ and $C_2^<$.
$C_1^< \cap C_2^<$	Intersection of $C_1^<$ and $C_2^<$.
$\overline{C^<}$	Dual of convex $C^<$.
C	Sector or range of directions.
k_i	Stiffness constant of spring k_i .
σ_i	Compression of spring k_i .
$\mu_i = \mathbf{p}_i \times \mathbf{k}_i$	Moment of linear spring k_i about z -axis.
$d_i = \mathbf{p}_i \cdot \mathbf{k}_i$	Distance to point of contact P_i , along the line of action of k_i .
$f_i = k_i \sigma_i$	Force of contact exerted by spring k_i on object.
\mathbf{k}_i	Direction of force (resp. torque) of linear (resp. angular) spring k_i .
$\hat{\mathbf{k}}_i$	Spatial vector representing the line of action of spring k_i .
U	Potential function of the grasp.
K	Stiffness matrix of the grasp.
\mathcal{K}	Diagonal matrix containing all the stiffness constants k_i 's.
$S = [\hat{\mathbf{k}}_1 \dots \hat{\mathbf{k}}_n]$	Spatial configuration matrix of the springs.
$K_S = S \mathcal{K} S^T$	Stiffness matrix from the spatial configuration of the springs.
K_P	Stiffness matrix describing the effect of the fingertips sticking, or sliding without friction on the edges or faces of the object.
K_C	Stiffness matrix describing the effect of the fingertips sliding without friction on curved segments of the object.

Chapter 1

Introduction

1.1 How to Grasp an Object?

Robot end effectors have evolved from simple parallel grippers to multi-finger hands to provide greater flexibility and dexterity in manipulation and assembly operations. Robot hands come in many shapes, but they all have in common the ability of being programmed and servoed from a computer. To take full advantage of the dexterity offered by multi-purpose hands, we need to be able to not only *analyze* a grasp but *synthesize* it. In other words, we would like to *construct* grasps that have such features as feasibility, reachability, force-closure, equilibrium, stability, compliance, etc...

- Feasibility — A grasp is kinematically feasible if there exist joint configurations for the individual fingers, such that the fingertips contact the grasped object at the desired grasp points.
- Reachability — A grasp is reachable if there exist collision-free paths for the fingers from their current configurations to their respective grasp configurations.
- Force-Closure — A grasp on an object is a force-closure grasp if and only if we can exert, through the set of contacts, arbitrary forces and moments on this object. Equivalently, any motion of the object is resisted by a contact force, which means that the object cannot break contact with the fingers without some non-zero external work.
- Equilibrium — A grasp is in equilibrium if and only if the sum of the forces and moments acting on the object is zero. There is a balance between the weight of the object and the contact forces exerted by the fingers.
- Stability — A grasp is stable if and only if the grasped object is always pulled back to its equilibrium configuration, whenever it is displaced from this configuration.

- Compliance — A grasp is compliant if the grasped object behaves as a generalized spring, damper, or impedance, in complying with external constraints such as a hard surface, or in reacting to errors between controlled and actual state variables, such as position, velocity, or force. Common examples are generalized springs and dampers.

The thesis addresses the problem of synthesizing grasps that are force-closure, equilibrium, stable, and compliant. Synthesizing a force-closure grasp is equivalent to finding places to put the contacts, such that these contacts totally constrain the motion of the grasped object. Constructing an equilibrium grasp is synthesizing the forces and moments at the contacts, such that the object is in equilibrium. Constructing a stable grasp is finding the virtual springs at the contacts, such that the grasp has a positive definite stiffness matrix. Constructing a compliant grasp is mapping the desired stiffness matrix at the grasped object into the stiffness matrices at the fingertips and at the finger joints. The compliance model used is a generalized spring. The grasped object behaves as though there are independent linear and angular springs attached at its compliance center.

1.2 Framework and Assumptions

A grasp is defined by a set of contacts. From a force-closure point of view, a contact is described by either a wrench convex or a twist convex. The wrench convex captures the range of forces and moments that can be applied through the contact. The twist convex captures the set of motions that are unrestrained by the contact. The wrench convexes from the individual contacts are 'added', until we get the whole space, or the twist convexes are intersected until we get the null space. The force-closure constraint is formalized by the theory of convexes and the theory of systems of linear inequalities.

Finding n independent regions of contact for the fingertips is formalized as finding n disjoint wrench convexes, such that any n -tuple of wrenches from these convexes is force-closure. By exploiting the line-based geometry of twists and wrenches, the independent regions of contact can be constructed based on the shape of the grasped object. Force-closure grasps on polygons and polyhedra are particularly simple, especially with friction at the contacts.

Chapter 2 explores the analysis and synthesis of force-closure grasps, in both 2D and 3D. The focus is grasps on polygonal and polyhedral objects. The contacts between the fingertips and the grasped object are modeled as point contacts with or without friction in 2D, and as frictionless point contacts, hard-finger or soft-finger contacts with friction in 3D.

From a stability point of view, each contact is described by a virtual spring. It can be a linear or an angular spring, or a combination of linear and angular springs. The virtual spring captures the passive stiffness at the fingertip and tendons, or the

active stiffness control at the finger joints. All the virtual springs are independent, and their potential functions are added into the potential of the grasp.

Chapter 3 assumes conservation of the grasp potential. So, the fingertips either stick or slide without friction on the edges or faces of the grasped object. The equilibrium condition of the grasp is obtained from zeroing the first partial derivatives of the grasp potential. The second partial derivatives gives the stiffness matrix of the grasp. This stiffness matrix depends on the spatial configuration of the virtual springs, and on whether the fingertips stick or slide without friction on the object.

Chapter 4 explores the effect of slip on force-closure and stability of the grasp. It shows slip makes grasps become more stable when there is friction. The effect of slip on curved objects are also analyzed. The model is a set of linear springs sliding without friction on arcs of circle.

1.3 Examples

Figure 1.1 shows examples of force-closure grasps found by the algorithms. The independent regions of contact are highlighted with bold segments and circles. The grasp is force-closure no matter where the fingertips are placed in these regions. This flexibility is of great importance in manipulation since we always have positioning errors and many other uncertainties. The first two grasps are 2D grasps: one with four frictionless point contacts, and one with two point contacts with friction. The third and fourth grasps are 3D grasps: one with two soft-finger contacts, and one with three hard-finger contacts with friction. The number of contacts shown are the minimum number of contacts required for force-closure.

Figure 1.2 shows examples of stable grasps constructed by the algorithms. The stiffness matrix at the grasped object is mapped into the virtual springs at the contacts. These virtual springs are responsible for generating restoring forces and moments whenever the grasped object is displaced from its stable equilibrium.

A Grasp Planner can construct a stable grasp G on a set of n edges or faces as follows:

- Synthesize a set of grasp points $\{P_1, \dots, P_n\}$ for which the grasp G at these grasp points is force-closure.

Better yet, we find the optimal set of independent regions of contact $\{s_1, \dots, s_n\}$ for the given n grasping edges or faces. The regions are independent from each other, in the sense that as long as we pick grasp point P_i in region s_i the resulting grasp $G = \{P_1, \dots, P_n\}$ is always force-closure. The set is optimal in the sense that the set of independent regions has the largest minimum radius for the given set of grasping edges or faces. We then pick the mid point of the region s_i as the optimal grasp point P_i .

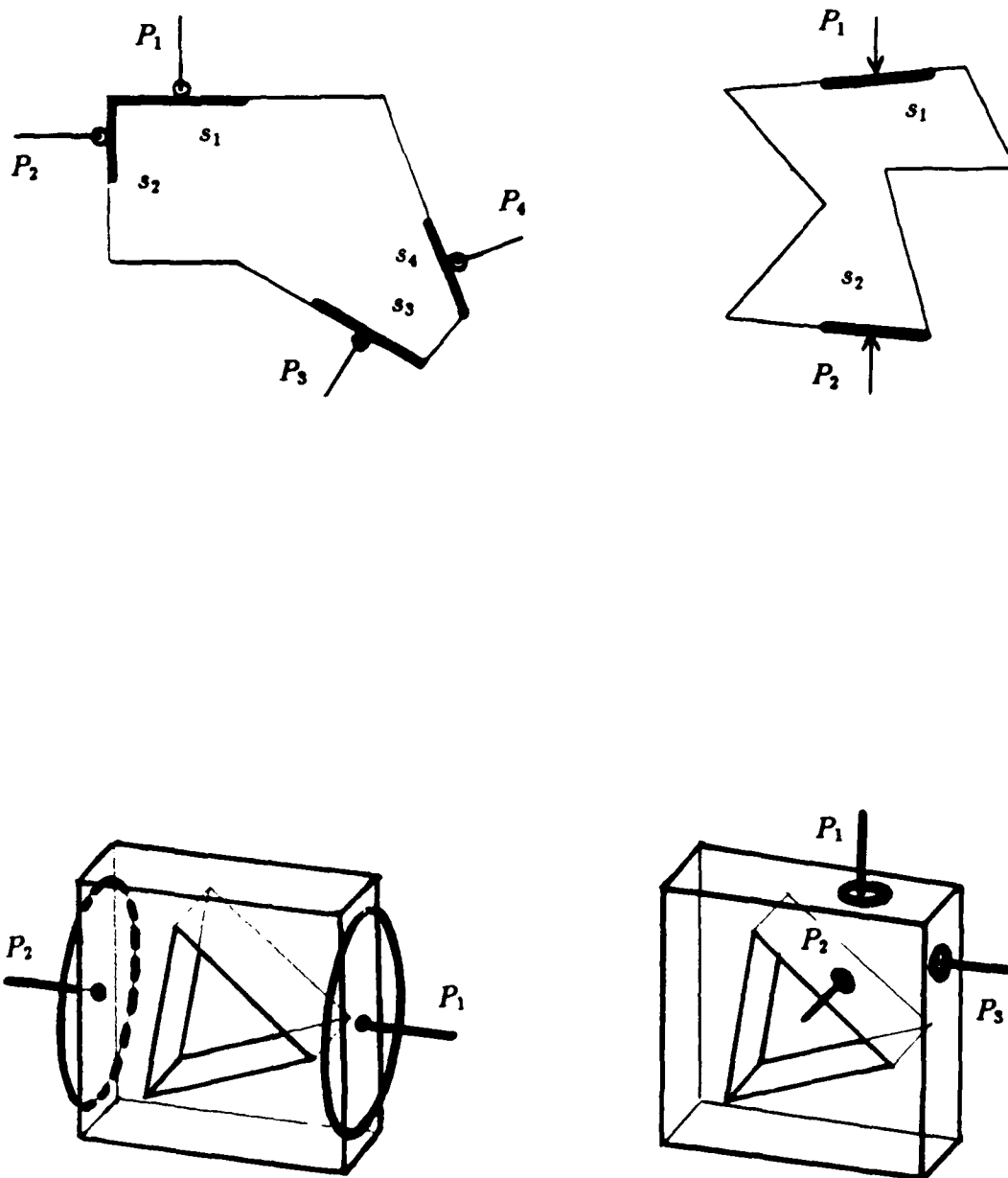


Figure 1.1: Examples of force-closure grasps found by the synthesis. The independent regions of contact are highlighted with bold segments and circles.

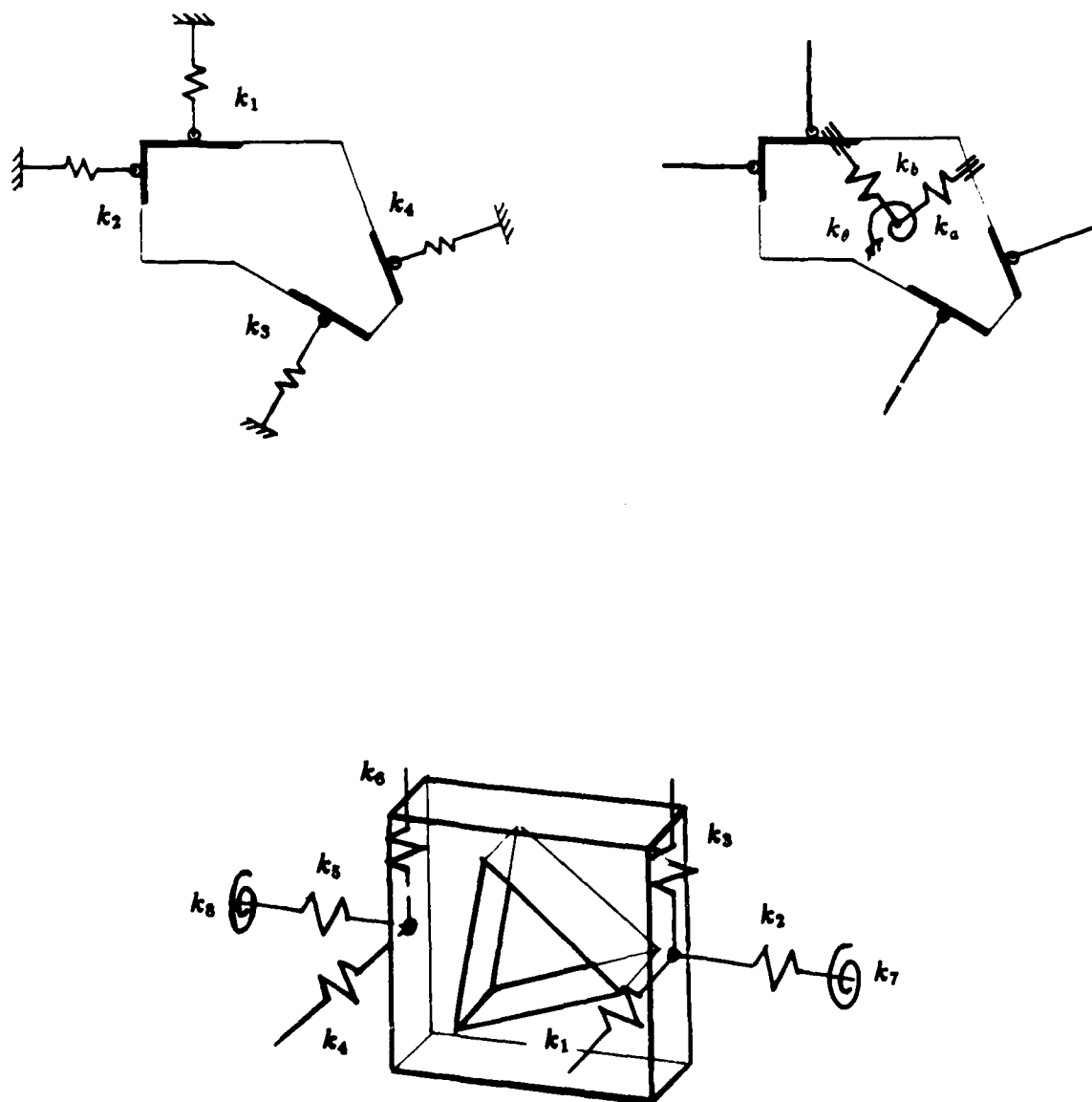


Figure 1.2: Examples of stable grasps found by the synthesis.

- Synthesize a corresponding set of virtual springs, such that grasp G is stable. Each virtual spring has stiffness k_i and compression $\sigma_{i,0}$. We prove that the stiffnesses k_i 's and compressions $\sigma_{i,0}$'s of the virtual springs can always be chosen so as to make the grasp stable. We can also construct the set of virtual springs such that the grasp has some desired compliance center and stiffness matrix.

1.4 Contributions

The thesis presents a formal framework for analyzing and synthesizing grasps in both 2D and 3D. Research is done in three areas: force-closure grasps, stable grasps, and grasps with possible slip at the contacts.

The research on force-closure grasps leads to:

- Fast and simple algorithms for directly constructing force closure grasps. We find not only single grasps but the complete set of all force-closure grasps on a set of edges in 2D (resp. faces in 3D). We can also construct the independent regions of contact for the finger tips. The construction of the independent regions of contact is very simple for polygonal and polyhedral objects.
- A representational framework for describing contacts and grasps. A grasp is described as the combination of individual contacts, which in turn are modeled as the combination of a few primitive contacts: point contacts without and with friction in 2D, and frictionless point contacts, hard-finger and soft-finger contacts in 3D.
- A proof that non-marginal¹ equilibrium grasps are also force-closure grasps, if each grasp has at least two points contacts with friction in 2D, or two soft-finger contacts or three hard-finger contacts in 3D. This proof supports a very simple heuristic for grasping: "Increase friction at the contacts by covering the finger tips with soft rubber. Then grasp the object on two opposite sides."

The research on stable grasps leads to:

- A proof that all force-closure grasps can be made stable. The algorithm for constructing stable grasps is both simple and efficient. It costs $O(n)$ time to synthesize a set of n virtual springs such that a given force-closure grasp is stable.
- A relation between the stability of a grasp and the spatial configuration of the virtual springs at the contacts. We show that the stiffness matrix K of the grasp is the sum of two matrices K_S and K_P . The matrix K_S depends

¹An equilibrium grasp is non marginal if the forces of contact point strictly within their respective friction cones.

on the spatial configuration of the virtual springs. $K_S = SKS^T$, where the columns of S are the spatial vectors describing the lines of action of the springs. The geometric relation can be viewed as a similarity transformation from the stiffnesses at the contacts K to the stiffnesses in the frame of the grasped object K_S . The stiffness matrix K_S is positive definite if and only if there are at least three (resp. six) virtual springs with independent spatial vectors for 2D (resp. 3D) grasps.

- A relation between the angular stiffness of the grasp and whether the fingers stick or slide without friction on the object. We show that the stiffness matrix K_P depends on whether the finger stick or slide on the straight edges or flat faces of the object. K_P makes outside-in grasps more stable than inside-out grasps, if the fingers slide without friction on the object. The reverse holds if there is friction and the fingers stick.
- A relation between the position of the compliance center of the grasp and the lines of action of the linear springs. We show that the compliance center of the grasp must be inside a region delimited by the lines of action of the linear springs. So a placement of the compliance center implies either a relative orientation of the linear springs, or a placement of the points of contact, or both.

A brief analysis of slip shows that:

- Virtual springs at the contacts can be synthesized such that the finger tips are guaranteed to stick inside their respective grasping edges, after they slip.
- Frictionless grasps remain force-closure and stable for arbitrarily large translations and for small rotations of the grasped object. Grasps with friction remain force-closure and stable, as long as the grasped object is in equilibrium, with the contact forces pointing strictly inside their respective friction cones.
- Slip without friction on circular arcs affects the stability of the object. The stiffness matrix K of the grasp is the sum of K_S and K_C . The stiffness matrix K_S comes from the spatial configuration of the springs. The matrix K_C plays the role of the position-dependent matrix K_P . It describes the effect of the fingers slipping on the circular arcs. It is negative (resp. positive) for convex (resp. concave) arcs.
- Point contacts which stick or slide without friction on straight edges are good approximations to finger tips slipping without friction respectively on convex and concave arcs.

1.5 Other Related Works

Related works can be grouped as follows:

- **Feasible and reachable grasps.** — Feasibility and reachability problems can be solved using the Configuration Space approach (Lozano-Pérez 1983), which grows the grasped object into a configuration obstacle in higher dimensional space, and inversely shrinks the fingers into a configuration point. The two problems become a search respectively for a feasible configuration point, and a path to that feasible point, such that the path does not intersect the configuration obstacle (Lozano-Pérez 1976, 1983). Related problems are finding the workspace of the hand and fingers, and finding the forward and inverse kinematics of the fingers (Paul 1981, Chiu 1985).
- **Force-closure grasps** — Force-closure and total freedom capture the main constraint between the fingers and the grasped object. Ohwovoriole analyzed the geometry of the different repelling screw systems, and use the results to analyze systems of contacting bodies such as an object grasped by a set of fingers, or a pin being inserted into a hole (Ohwovoriole 1980, 1984). Related to force-closure are the notion of degree of freedom (Bottema and Roth 1979), (Hunt 1978), and the solution of systems of linear inequalities (Kuhn and Tucker 1956).
- **Form-closure grasps** — A grasp is form-closure if the grasped object is totally constrained by the set of contacts, irrespective of the magnitude of the contact forces. A 2D grasp can be force-closure with two point contacts with friction. Translations of the object tangential to the contact normals are resisted by frictional forces. The magnitude of this resistance depends on the magnitude of the normal contact forces. In a form-closure grasp, the constraints on the object comes only from geometry of the contacts. Reuleaux (1875) proved that a 2D grasp needs at least four point contacts for form-closure. Lakshminarayana (1978) showed that a 3D grasp needs at least seven point contacts. Form-closure can be viewed as force-closure with frictionless contacts only.
- **Equilibrium grasps** — There are many works on analyzing the equilibrium of forces in a grasp with different types of contact (Salisbury 1982), with flexible contacts (Cutkosky 1984), or with friction (Abel, Holzmann and McCarthy 1985). Finding a good grasp is often formalized as a search of the space of all grasps with some goal function, such as optimum for internal forces (Kerr 1984), or security of grasp (Jameson 1985).
- **Stable grasps** — A stable prehension of a planar hand on a polygon can be found by centering the hand on the center of mass, and check for grasps that are stable with respect to rotation, then stable with respect to translation (Hanafusa and Asada 1977), (Asada 1979). Baker, Fortune and Grosse (1985) proved that stable grasps on a convex polygon exist, and presented efficient algorithms that require no incremental search.

- *Compliant grasps* — We can have active stiffness control of the fingers and the grasped object by using the Grip and Jacobian matrices as in (Salisbury and Craig 1981), (Salisbury 1984, 1982), or build in some proximity damping as in (Jacobsen, Wood, Knutti and Biggers 1984, 1985). Grasps can be achieved easily with active compliance and bounded slip at the fingers as in (Fearing 1984), or by exploiting the friction and passive compliance of the object with the fingers and the environment as in (Mason 1982, Brost 1986). Grasping a peg and inserting it into a hole is currently done best with a passive compliance wrist known as the Remote Center of Compliance (Whitney 1982).

This thesis is different from previous work on grasping in that it emphasizes the synthesis rather than the analysis of grasps.

Chapter 2

Constructing Force-Closure Grasps

2.1 Where Should the Fingertips Be Placed?

Grasping an object is exerting force and moment on the object, to move it or to keep it in stable equilibrium. Grasping is also constraining the motion of the object by a set of contacts. These two descriptions are dual of each other. They correspond respectively to a force-closure grasp and to zero total freedom of the object. A grasp on an object is force-closure if and only if we can exert, through the set of contacts, arbitrary force and moment on this object. Equivalently, any motion of the object is resisted by a contact force. The object cannot break contact with the fingertips without some non-zero external work.

The forward problem is to analyze whether a grasp, defined by a set of contacts, is force-closure or not. The reverse problem is to find places to put the fingertips, such that the grasp is force-closure. The synthesis method we develop finds large independent regions of contact for the fingertips. We'll explore the analysis and the synthesis of force-closure grasps, in both 2D and 3D. The focus will be grasps on polygonal and polyhedral objects. Extension to grasps on curved objects is also discussed.

In 2D, grasped objects are arbitrary polygons. The contacts between the fingertips and the grasped object are modeled as point contacts with or without friction. In 3D, grasped objects are arbitrary polyhedra. The fingertip contacts are modeled as frictionless point contacts, hard-finger contacts, or soft-finger contacts.

Figure 2.1 shows examples of force-closure grasps in 2D and 3D. The independent regions of contact for the fingertips are highlighted by bold segments and circles.

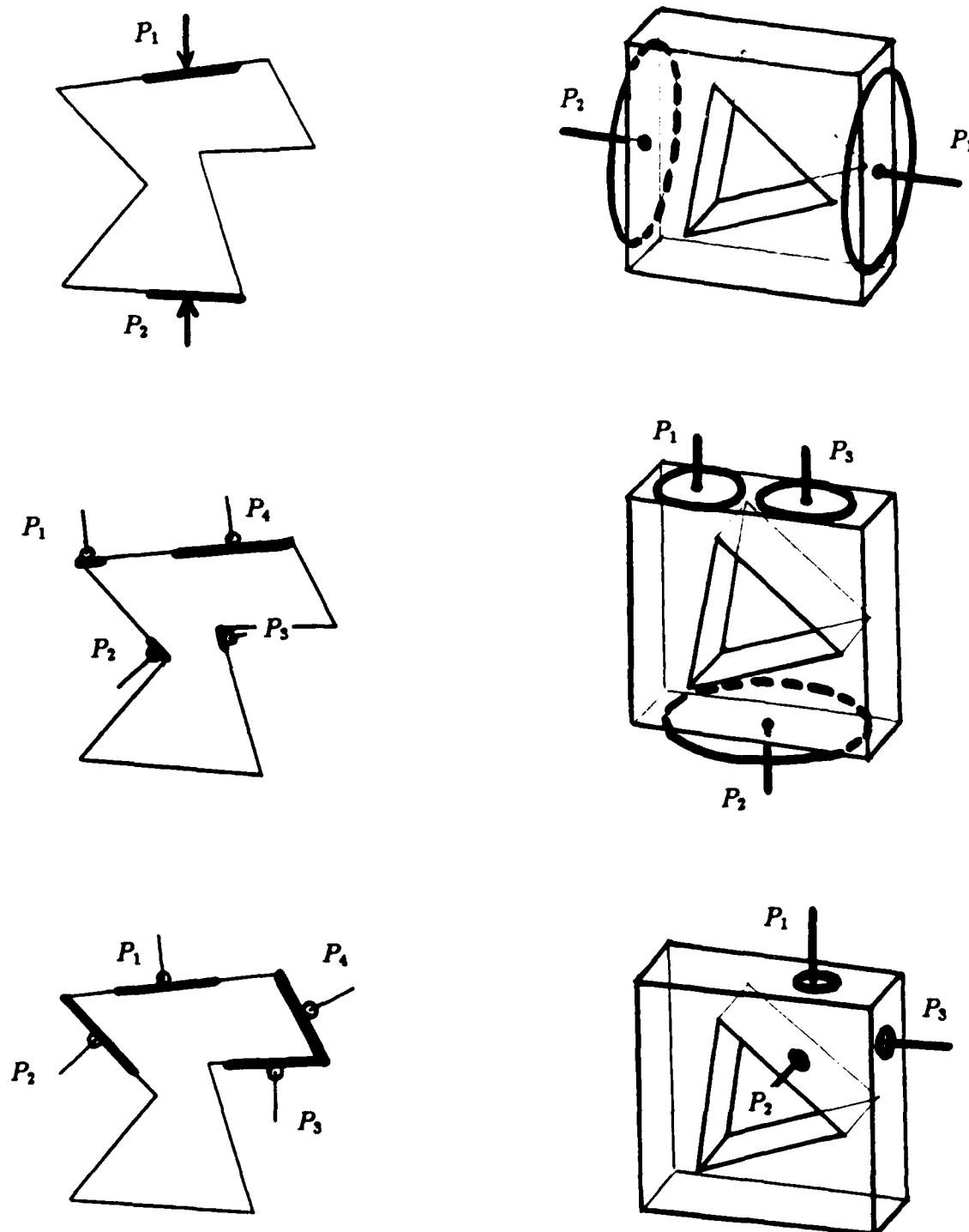


Figure 2.1: Examples of force-closure grasps in 2D and 3D.

2.2 Background Theory of Twists and Wrenches

The instantaneous motion of an object is described by a twist. A twist is a spatial vector which captures the angular and linear displacements of the object. A wrench describes the force and moment exerted by a contact on the object. Twists and wrenches are represented in Plücker coordinates.

The following mechanics review looks at Plücker line coordinates, virtual work, total freedom, and dual subsystems of twists and wrenches in 2D and 3D. A mathematics review looks at systems of linear inequalities, at convexes and operations on convexes: convex addition, intersection and dual. For more extensive materials on these topics, the reader is referred to (Featherstone 1983, 1984), (Ball 1900), (Ohwovoriohle 1980, 1984), (Kuhn and Tucker 1956), and (Lakshminarayana 1978).

2.2.1 Plücker Line Coordinates

A general spatial vector is the sum of a line vector and a free vector. A line vector has a magnitude and a line of action, whereas a free vector has magnitude and direction only. In rigid body mechanics, line vectors represent quantities like force and rotation, which have a definite line of action. The line of action is respectively the line of force and the axis of rotation. Free vectors describe quantities like torque and translation, which are invariant respective to the point of application.

A free vector is a spatial vector with zero upper part. For example, a translation \mathbf{d} is represented in Plücker coordinates by the following translational twist:

$$\hat{\mathbf{t}} = \begin{bmatrix} \mathbf{0} \\ \mathbf{d} \end{bmatrix}$$

The $\hat{\mathbf{t}}$ notation is borrowed from (Featherstone 1984), to denote a 6-dimensional spatial vector.

A line vector is a spatial vector with both upper and lower parts, called Plücker vectors. The upper part represents the magnitude and direction of the vector. The lower part represents the moment of the vector about the origin of the reference frame. Concretely, a line vector $\hat{\mathbf{s}}$ is represented as:

$$\hat{\mathbf{s}} = \begin{bmatrix} \mathbf{s} \\ \mathbf{r} \times \mathbf{s} \end{bmatrix} = \begin{bmatrix} s_x \\ s_y \\ s_z \\ r_y s_z - r_z s_y \\ r_z s_x - r_x s_z \\ r_x s_y - r_y s_x \end{bmatrix} \quad (2.1)$$

where \mathbf{r} is a vector from the origin of the reference frame to any point on the line of action of $\hat{\mathbf{s}}$. For example, a rotation δ about an axis Δ is represented by the

following twist in Plücker coordinates:

$$\hat{\mathbf{t}} = \begin{bmatrix} \boldsymbol{\delta} \\ \mathbf{r} \times \boldsymbol{\delta} \end{bmatrix} \quad (2.2)$$

$\boldsymbol{\delta}$ is the rotation vector, whose normalized vector is the direction of the axis of rotation Δ , and whose magnitude is the equivalent angle of rotation. \mathbf{r} is a vector from the origin of the reference frame to any point on the axis of rotation Δ . We recognize the upper and lower parts of the twist as the angular and linear displacements of the origin of the reference frame.

Only instantaneous and infinitesimal twists can be composed and resolved like vectors. The composition of finite twists is in general non-commutative. Finite twists are commonly represented by transformation matrices (Paul 1981), and these are composed by matrix multiplications. From now on, a twist will be written as $\hat{\mathbf{t}} = (\boldsymbol{\delta}^T, \mathbf{d}^T)^T$ to designate an infinitesimal displacement of the object.

A force \mathbf{f} is a line vector which is represented in Plücker coordinates by the following wrench:

$$\hat{\mathbf{w}} = \begin{bmatrix} \mathbf{f} \\ \mathbf{r} \times \mathbf{f} \end{bmatrix} \quad (2.3)$$

The upper and lower parts of the wrench are respectively the equivalent force going through the origin of the reference frame, and the moment of the force \mathbf{f} about the origin. Wrench $\hat{\mathbf{w}}$ can be written as the sum of a line vector and a free vector:

$$\hat{\mathbf{w}} = \begin{bmatrix} \mathbf{f} \\ \mathbf{0} \end{bmatrix} + \begin{bmatrix} \mathbf{0} \\ \mathbf{r} \times \mathbf{f} \end{bmatrix}$$

The same force \mathbf{f} has a different wrench when its line of action is translated to the origin. By representing the contact forces and the motion of the grasped object in Plücker coordinates, we make explicit the line-based geometry of the domain.

2.2.2 Virtual Work and Total Freedom

A twist and a wrench are related by a spatial scalar product which describes the virtual work done by the wrench against the infinitesimal twist (Featherstone 1984). The virtual work is defined as follows:

Definition 2.1 *The virtual work of a wrench $\hat{\mathbf{w}} = (\mathbf{f}^T, \mathbf{m}^T)^T$ against an infinitesimal twist displacement $\hat{\mathbf{t}} = (\boldsymbol{\delta}^T, \mathbf{d}^T)^T$ is the sum of the virtual work due separately to the linear and angular components:*

$$\hat{\mathbf{w}} : \hat{\mathbf{t}} = \mathbf{f} \cdot \mathbf{d} + \mathbf{m} \cdot \boldsymbol{\delta} \quad (2.4)$$

We can define the virtual work as a scalar multiplication of the wrench $\hat{\mathbf{w}}$ with the spatial transpose of the twist $\hat{\mathbf{t}}$, denoted $\hat{\mathbf{t}}^S$:

$$\begin{aligned} \hat{\mathbf{w}} : \hat{\mathbf{t}} &= \hat{\mathbf{w}} \cdot \hat{\mathbf{t}}^S \\ &= \begin{bmatrix} \mathbf{f} \\ \mathbf{m} \end{bmatrix} \cdot \begin{bmatrix} \mathbf{d} \\ \boldsymbol{\delta} \end{bmatrix} \end{aligned}$$

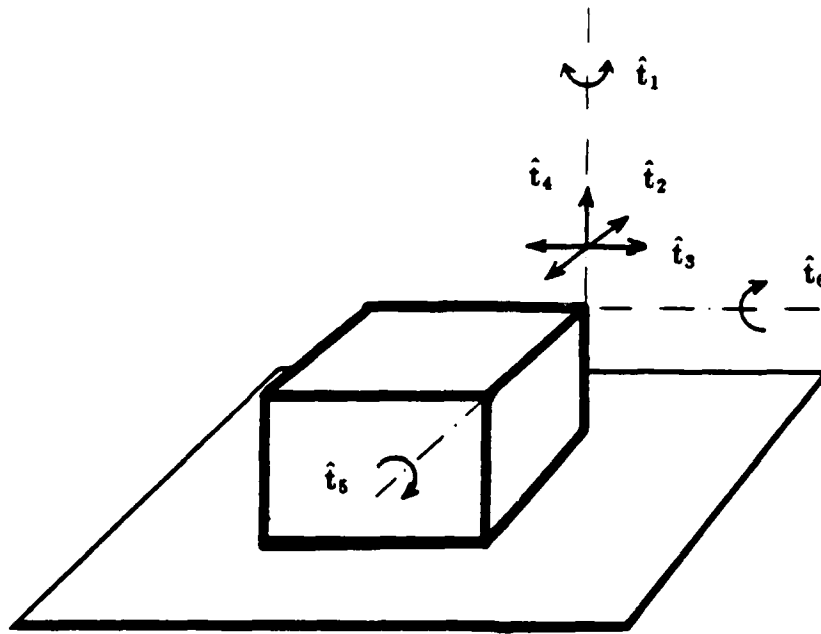


Figure 2.2: Total freedom of a box lying on a frictionless plane.

The spatial transpose of twist $\hat{t} = (\delta^T, d^T)^T$ is the twist $\hat{t}^S = (d^T, \delta^T)^T$ with the upper and lower parts permuted.

The concept of total freedom (Ohwovori 1980) emerges from the sign of the virtual work. We'd like to know not only the degrees of freedom of the object, but also whether and when the object breaks contact or pushes against the other bodies contacting it.

Definition 2.2 (Ohwovori 1980) A twist \hat{t} and a wrench \hat{w} are reciprocal to each other if and only if their virtual work is zero. The pair (\hat{t}, \hat{w}) is repelling (resp. contrary) if and only if their virtual work is strictly positive (resp. negative).

Let W be a set of wrenches acting on an object. The set of twists reciprocal to W is represented as linear combinations of n linearly independent twists. The object is said to have n degrees of freedom.

Similarly, the set of twists reciprocal or repelling to W is represented by non-negative combinations of non-zero twists. These twists form a convex basis which describes the total freedom of the object.

A reciprocal twist corresponds to a degree of freedom in the system. For example, look at the box in Figure 2.2. The box lies on a frictionless horizontal plane. It has a reciprocal rotational twist about any vertical axis. In other words, it can freely rotate about any vertical axis, and therefore has one degree of freedom. The box can also translate in the plane, and so has two other degrees of freedom.

The above three degrees of freedom do not completely describe the set of motions possible to the object. For example, the box can be raised from the plane and break contact. This half-free motion is different from the usual concept of degree of freedom in that it is *unisense*. The upward motion is a twist repelling to the contact force exerted by the plane onto the box. The downward motion is a twist contrary to this contact force. Note that the plane will oppose the downward motion with an upward reaction force, resulting in a negative virtual work. Finally, the box can rotate about two horizontal axes, provided that the box does not enter the plane. These two rotations define two other unconstrained motions. The box has three degrees of freedom, but its total freedom or range of unconstrained motions is much larger.

2.2.3 Convexes and Operations on Convexes

In grasping, the goal is to have force closure, or to fully constrain the motion of the grasped object with a set of finger contacts. Through each contact, we can exert a range of forces and moments, represented by a wrench convex. Just as many contacts are combined to form a grasp, many wrench convexes are "added" until their sum spans the whole space, or until we have force closure. Each contact can also be described by a twist convex. The twist convexes are intersected until we get the null space, or until the grasped object has zero total freedom. Let's first define convexes and three operations on convexes: convex addition, intersection, and dual.

Definition 2.3 Let C be a non-empty set of vectors. We define by convex $C^<$, the set of all non-negative combinations of vectors in C , formally:

$$C^< = \left\{ \hat{s} \mid \hat{s} = \sum_i \alpha_i \hat{s}_i, \alpha_i \geq 0, \hat{s}_i \in C \right\} \quad (2.5)$$

The vectors \hat{s}_i in C are called generating vectors of the convex $C^<$. A convex is polyhedral when the set of generating vectors is finite.

A convex is null when it contains only the zero vector. A convex is total when it is the entire space.

The convexes just defined are open-ended sets. They are also called convex cones (Goldman and Tucker 1956) to differentiate them from convex sets, such as convex polygons and polyhedra. An example of a convex is the friction cone in the plane, Figure 2.3. The range of forces inside the friction cone can be represented as the set of all positive combinations of the two extreme rays of the friction cone. So, a 2D friction cone can be represented by a two-wrench convex. The friction cone is no longer a polyhedral convex in 3D, because the set of generating vectors is infinite.

Definition 2.4 Let $C_1^<$, $C_2^<$ be two convexes. The convex addition of $C_1^<$ and $C_2^<$, denoted $C_1^< \cup C_2^<$, is the least convex that contains both $C_1^<$ and $C_2^<$. Formally:

$$C_1^< \cup C_2^< = \left\{ \hat{s} \mid \hat{s} = \alpha \hat{s}_1 + \beta \hat{s}_2, \right. \\ \left. \alpha \geq 0, \beta \geq 0, \hat{s}_1 \in C_1^<, \hat{s}_2 \in C_2^< \right\} \quad (2.6)$$

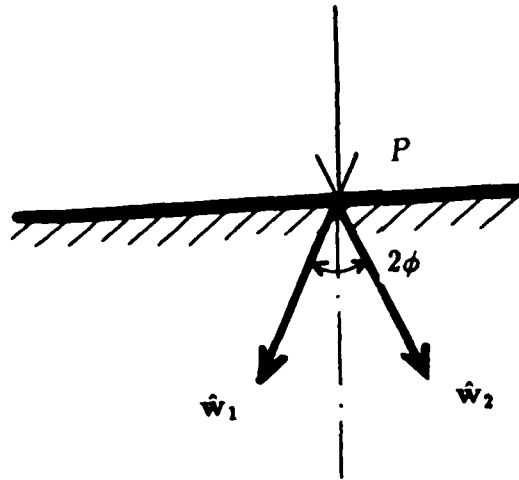


Figure 2.3: A 2D friction cone is represented by a two-wrench convex.

Convex addition¹ is also known as the Minkowski sum. Convex addition is used to combine wrench convexes from the various contacts on the grasped object. For example, each point contact with friction in the plane gives a two-wrench convex, Figure 2.3. A grasp with two point contacts with friction has a wrench convex which is the Minkowski sum of the two convexes, describing the friction cones at the two points of contact. From the above equation, the resulting convex can be generated by the four wrenches, each is a force along an edge of the two friction cones. The convex sum of polyhedral convexes can be represented by the union of the generating vectors, except that the concatenated set of generating vectors may not be minimal.

Convexes are closed under convex addition and intersection. The intersection of two convexes is defined as follows:

Definition 2.5 Let $C_1^<$, $C_2^<$ be two convexes. The intersection of $C_1^<$ and $C_2^<$, denoted $C_1^< \cap C_2^<$, is the largest convex inside both $C_1^<$ and $C_2^<$. Formally:

$$C_1^< \cap C_2^< = \{ \hat{s} \mid \hat{s} \in C_1^<, \hat{s} \in C_2^< \} \quad (2.7)$$

Twist and wrench convexes are duals of each other. The dual operation on twist or wrench convexes is defined as follows:

¹Convex addition is *not* set union. We borrow the union sign \cup to emphasize the duality of the convex addition and the set intersection of two convexes, denoted \cap .

Definition 2.6 Let $C^<$ be a twist or wrench convex. The dual of $C^<$, denoted $\overline{C^<}$, is the convex of vectors that are either reciprocal or repelling to all the vectors in $C^<$. Formally:

$$\overline{C^<} = \{ \hat{s} \quad C^T \hat{s}^S \geq 0 \} \quad (2.8)$$

where C is the matrix whose columns are generating vectors of the convex $C^<$.

One use of the dual operation is to calculate the twist convex $T^<$ which describes the total freedom of an object. Solving for the twist convex is equivalent to solving the following system of linear inequalities:

$$W^T \hat{t}^S \geq 0 \quad (2.9)$$

where \hat{t}^S is the spatial transpose of the unknown twist, and each column of matrix W is a generating wrench of $W^<$. The product of \hat{t}^S and the i th row of W^T gives the virtual work of twist \hat{t} against wrench \hat{w}_i of W . This virtual work must be either zero or positive. Similarly for all other rows.

The duality between twists and wrenches allows us to compute in the wrench-space and deduce equivalent result in the twist-space, and vice versa. See Figure 2.5. The following Lemma summarizes important facts about the dual operation, the convex addition and intersection of twist and wrench convexes. For a proof see (Goldman and Tucker 1956).

Lemma 2.1 Let $W^<$, $T^<$ be respectively a wrench and a twist convex. Let $C^<$ be either a wrench or twist convex.

1. $\overline{\overline{C^<}} = C^<$
2. $\overline{W^<} = T^<$; $\overline{T^<} = W^<$
3. $C^< \cap \overline{C^<} = \text{null space}$; $C^< \cup \overline{C^<} = \text{total space}$
4. $\overline{C_1^<} = \overline{C_2^<}$ if and only if $C_1^< = C_2^<$ (2.10)
5. $\overline{C_1^<} \cap \overline{C_2^<} = \overline{C_1^< \cup C_2^<}$
6. $\overline{C_1^<} \cup \overline{C_2^<} = \overline{C_1^< \cap C_2^<}$

2.2.4 Dual Subsystems

We have seen that twists and wrenches form dual systems. In planar mechanics, a twist can be represented by a 3-dimensional spatial vector as follows:

$$\hat{t} = \begin{bmatrix} \delta_z \\ d_x \\ d_y \end{bmatrix} \quad (2.11)$$

δ_z is the infinitesimal rotation about the z -axis, and (d_x, d_y) is the infinitesimal translation of the origin in the xy -plane. Similarly, a planar wrench can be represented by:

$$\hat{\mathbf{w}} = \begin{bmatrix} f_x \\ f_y \\ m_z \end{bmatrix} \quad (2.12)$$

where (f_x, f_y) are the two force-direction components in the xy -plane, and m_z is the moment component about the z -axis.

In this 3-dimensional space, we can identify two pairs of subspaces which form interesting dual subsystems:

- The space of xy -translations, and its dual which is the space of all force directions in the xy -plane.
- The space of pure moments or torques about the z -axis, and its dual which is the space of clockwise and counter-clockwise rotations about the z -axis.

It is well known that any planar motion can be decomposed uniquely into a translation and a rotation about the origin. So, the space of clockwise and counter-clockwise rotations, and the space of xy -translations are two independent subspaces of the space of planar twists. Similarly, the space of torques and the space of force directions are two independent subspaces of the space of planar wrenches.

Force closure for these two pairs is very simple for polygonal objects. Edges of a polygonal object have constant normals, so force-direction closure becomes a simple test of the angles between the edge normals. Only torque closure depends on the position of the points of contact on the grasping edges. The same observations hold for polyhedral objects in 3D.

2.3 Force-Closure Grasps in 2D

2.3.1 Representing Contacts and Grasps

Primitive Contacts

Figure 2.4 depicts the different types of planar contacts. The first column describes the physical contact with the finger on top and the grasped object below it. The second and third columns describe respectively the wrench convex, representing the range of forces that can be applied to the object, and the twist convex, representing the total freedom of the object. Each convex is represented by a minimal set of generating vectors. The twist convex is computed by taking the dual of the wrench convex.

a. *Frictionless point contact* — We can apply only a single pure force, normal to the segment, through a frictionless point contact. The wrench convex has a single wrench. The twist convex has three twists: a rotation about the point of contact, a translation along the edge of the object, and an unisense downward translation which breaks contact with the finger. This downward translation is a repelling twist whereas the first two twists are reciprocal ones.

b. *Point contact with friction* — The friction cone at the point of contact shows the range of pure force that can be applied through the point contact. The wrench convex has two wrenches which are along the two extreme rays of the friction cone. Any force pointing inside this friction cone can be written uniquely as a positive combination of the these two wrenches. The twist convex has two unisense translations, each reciprocal to one wrench and repelling to the other. It also has a free rotation about the point of contact as above.

c, d. *Edge contact with/without friction* — It is well known that, for rigid objects, any force distribution along the segment of contact is equivalent to a unique force at some point inside the segment. This unique force is mathematically the positive combination of two ranges of force at the two ends of the segment of contact. Specifically, the wrench convex of an edge contact with/without friction is equivalent to the convex sum of two wrench convexes, each represents a point contact with/without friction at one end of the edge of contact.

e. *Soft finger contact* — From a force closure point of view, a soft finger contacting an edge is the same as an edge contact with friction. The pressure distribution is irrelevant to our current focus, which is concerned with whether the object can be constrained with the given contacts, rather than how much force should the fingers apply to the object.

A soft finger becomes more useful when it contacts on the inside or outside of a corner. Figure 2.4.e shows a soft finger contacting on the outside of a corner. The wrench convex is the convex addition of two convexes, each describes the edge contact with friction on one side of the corner. The object can only break contact by sliding downward.

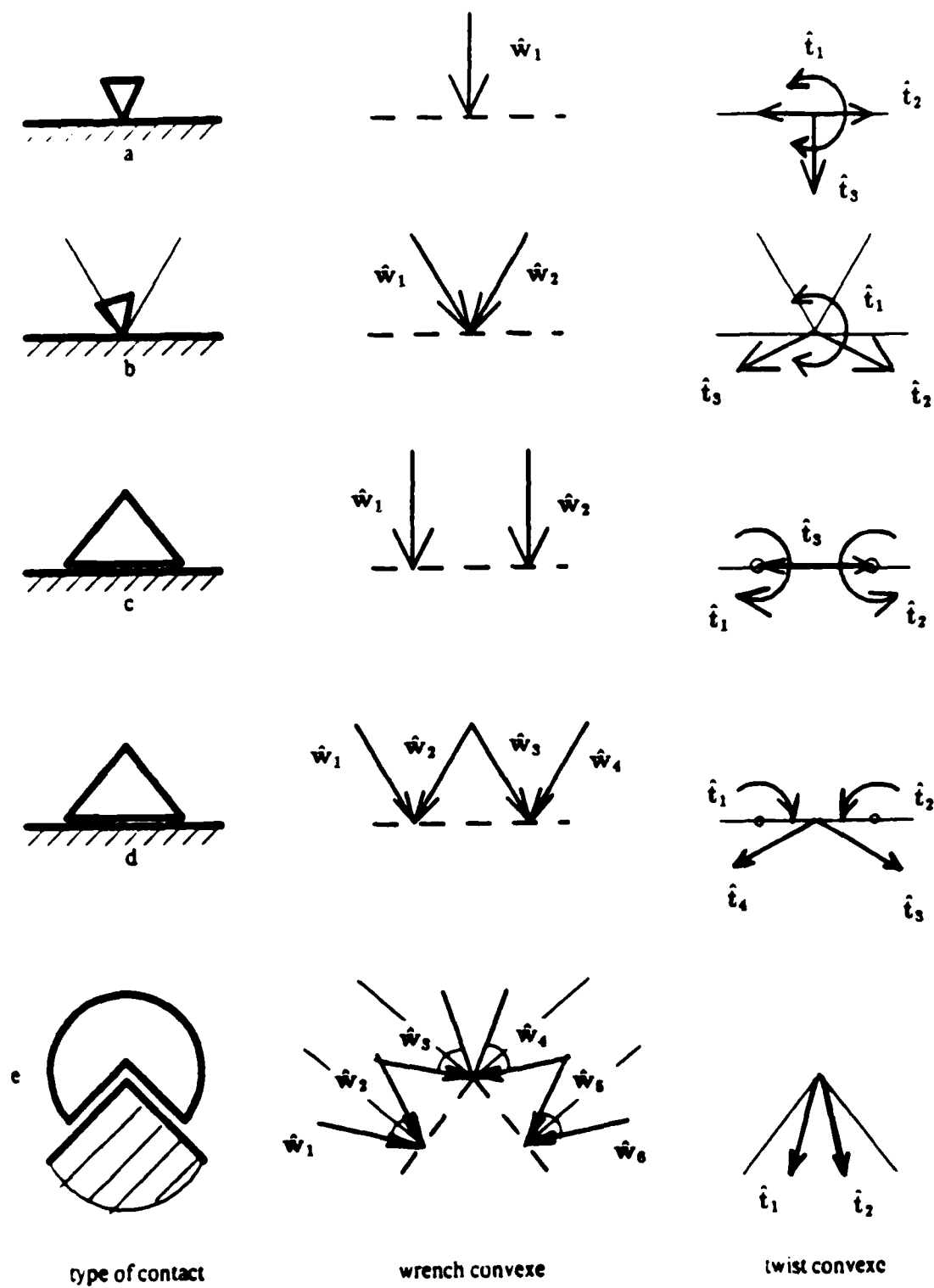


Figure 2.4: Planar contacts and their twist and wrench convexes.

People tend to grasp at the edges and corners if there is no reachable pair of parallel faces. Why? One among many plausible answers is the availability of a larger wrench convex, which means not a more stable grasp but a greater ability to constrain and move the object, by applying necessary forces through the soft contacts. A soft contact pressing at a vertex can be approximated as a point contact with a much larger friction cone. So a grasp with two soft contacts is better than a grasp with two point contacts with friction.

Gravity is not a contact, but it does play a role in constraining the total freedom of the object. For example, the box of Figure 2.2 is immobile on the table because the force of gravity is holding it down to the table. We can view the box as being grasped, or more exactly constrained, by two contacts: a plane contact between the bottom of the box and the table, and an imaginary point contact at the center of gravity of the box. Gravity is useful in this case, because without gravity the box can freely float upwards!

We conclude that point contacts without and with friction are the two primitive contact types. A contact over a finite segment is the combination of all point contacts over this segment. This infinite set of point contacts is the convex sum of two point contacts at the two ends if the segment is straight. The straight segment is a convex set, whereas the wrench convex is a convex cone. The description of a contact over a finite segment is split into two independent parts: a convex set for the point contact, and a convex cone for the range of force directions. This property applies only to polygonal and polyhedral objects.

Dual Representations For Grasps

Twist and wrench convexes are two dual representations for contacts. We can add wrench convexes from all the contacts or intersect the corresponding twist convexes to find the resulting wrench or twist convex of the grasp. We have here two dual view points:

- A constraint view point. -- Wrench convex describes the set of forces and moments which constrain the object. A total wrench convex means we can arbitrarily apply any force and moment on the object, and so we can grasp it, instantaneously rotate or translate it in any way we want.
- A freedom view point. - Twist convex describes the total freedom of the object. A total twist convex means the object can freely move relative to the fingers. A null twist convex means the object cannot break contact without external work against the contact forces exerted by the fingers.

Which representation, twist or wrench convexes, is better? For planning grasps, wrench convexes are definitely more efficient since generating wrenches can be deduced readily from the type of contact, and we can just take the union of all the generating wrenches to describe the grasp (Figure 2.5). The twist convex representation is more efficient for describing the total freedom at the end effectors of linked manipulators. The infinitesimal motions and the velocities of the end effector due

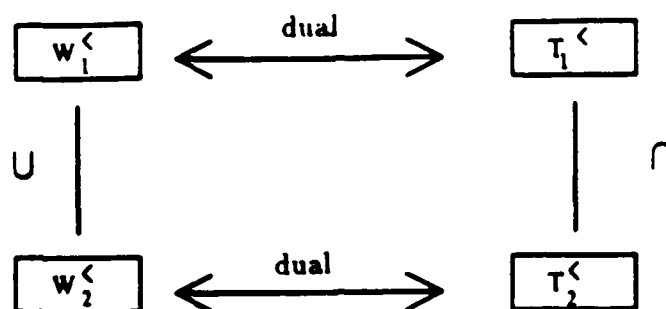


Figure 2.5: Duality between twist and wrench spaces.

to each joint are 'added'. The end effector can have arbitrary motion if the twist convexes of all the joints 'add up' to a total convex.

2.3.2 Resisting Translation and Rotation

The force closure problem can be formulated as solving a system of linear inequalities:

$$W^T \hat{t}^S \geq 0 \quad (2.13)$$

where the columns of W are generating wrenches collected from all the contacts of the grasp. We can design a generate-and-test algorithm which enumerates all the possible grasps, and test each grasp by solving the above system of linear inequalities. We get a force-closure grasp if and only if there is no non-zero solution to the above system, i.e. zero total freedom. There are two main objections to this scheme: first, the set of possible grasps is infinite; second, the grasp synthesis uses an analytical formulation which does not exploit the geometry of the domain. Polygonal objects have straight edges; contacts on straight edges have wrench convexes which can be split into position-dependent and position-independent parts. A force (resp. infinitesimal rotation) is a line vector while a torque (resp. infinitesimal translation) is a free vector which does not depend on the point of contact. Our key contribution is to make the force-closure constraint explicit for polygonal and polyhedral objects.

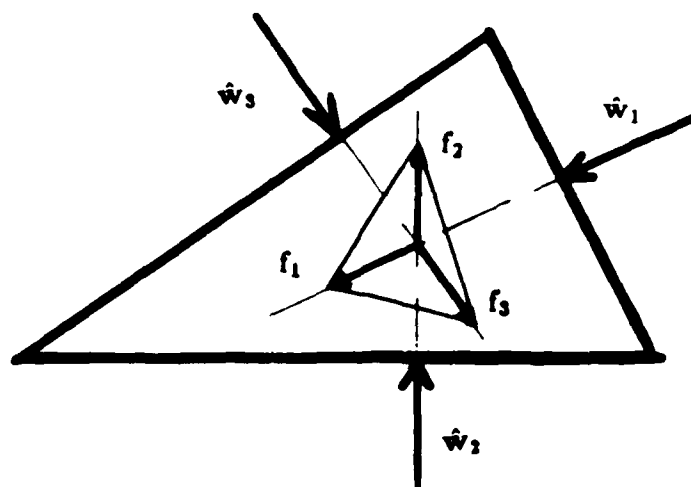


Figure 2.6: A geometrical view of force-direction closure.

Force-Direction Closure With Planar Forces

When can a grasp resist arbitrary planar translation of the object? Informally, the contact forces of the grasp must have directions that span the space of all directions in the plane, Figure 2.6. Formally:

Theorem 2.1 *A set of wrenches W can generate force in any direction if and only if there exists a three-tuple of wrenches $(\hat{w}_1, \hat{w}_2, \hat{w}_3)$ whose respective force directions f_1, f_2, f_3 satisfy:*

- *Two of the three directions f_1, f_2, f_3 are independent.*
- *A strictly positive combination of the three directions is zero.*

$$\alpha f_1 + \beta f_2 + \gamma f_3 = 0$$

The first (resp. second) condition corresponds to no homogeneous (resp. particular) solutions to the system $W^T \hat{t}^S > 0$, where twist $\hat{t} = (0, d_x, d_y)^T$ is an infinitesimal translation of the object. For detailed proofs the reader is referred to Appendix A.1. Theorem 2.1 can be captured in a more suggestive and compact way as follows:

Corollary 2.1 *A set of wrenches W can generate forces in any arbitrary direction if and only if there exists a three-tuple of force-direction vectors (f_1, f_2, f_3) whose end points draw a nonzero triangle that includes their common starting point.*

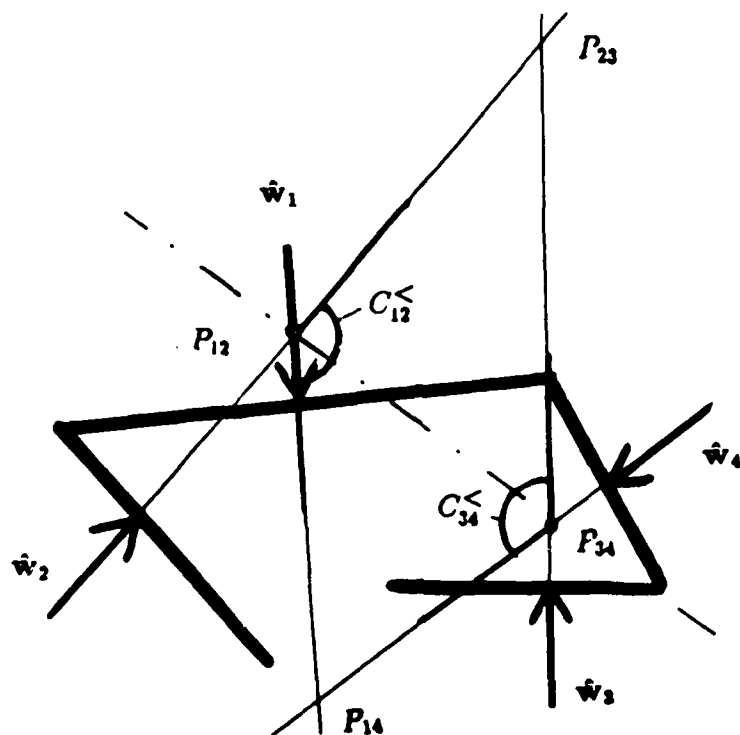


Figure 2.7: A geometrical view of torque closure.

Torque Closure With Planar Forces

Torque closure can be achieved easily by creating enough friction on some axis of rotation of the object. The friction between the rotating object and its supporting axis will create a torque which resists any clockwise or counter-clockwise rotation of the object. Unfortunately, in most grasp configurations, we have only point contacts, and through a point contact, a finger can exert only a pure force on the object and not torque. The more interesting problem is to achieve torque closure with only pure forces.

Theorem 2.2 *A set of planar forces W can generate clockwise and counter-clockwise torques if and only if there exists a four-tuple of forces $(\hat{w}_1, \hat{w}_2, \hat{w}_3, \hat{w}_4)$ such that:*

- *Three of the four forces have lines of action that do not intersect at a common point or at infinity*
- *Let $\mathbf{f}_1, \dots, \mathbf{f}_4$ be the force directions of $\hat{w}_1, \dots, \hat{w}_4$. Let \mathbf{p}_{12} (resp. \mathbf{p}_{34}) be the point where the lines of action of \hat{w}_1 and \hat{w}_2 (resp. \hat{w}_3 and \hat{w}_4) intersect. There*

exist $\alpha, \beta, \gamma, \delta$ all greater than zero, such that:

$$\begin{aligned} \mathbf{p}_{34} - \mathbf{p}_{12} &= \pm (\alpha \mathbf{f}_1 + \beta \mathbf{f}_2) \\ &= \mp (\gamma \mathbf{f}_3 + \delta \mathbf{f}_4) \end{aligned}$$

The first (resp. second) condition corresponds to no homogenous (resp. particular) solutions to system $W^T \hat{\mathbf{t}}^S \geq \mathbf{0}$, where twist $\hat{\mathbf{t}} = (\delta_z, d_x, d_y)^T$ is an infinitesimal rotation of the object. For detailed proofs the reader is referred to Appendix A.2. Theorem 2.2 can be formulated in more geometrical terms as follows:

Corollary 2.2 *A set of planar forces W can generate clockwise and counter-clockwise torques if and only if there exists a four-tuple of forces $(\hat{\mathbf{w}}_1, \hat{\mathbf{w}}_2, \hat{\mathbf{w}}_3, \hat{\mathbf{w}}_4)$ such that the segment $P_{12}P_{34}$, or $P_{34}P_{12}$, points out of and into the 2 cones $C_{12}^<$, $C_{34}^<$, formed by the two pairs $(\hat{\mathbf{w}}_1, \hat{\mathbf{w}}_2)$, and $(\hat{\mathbf{w}}_3, \hat{\mathbf{w}}_4)$.*

From Figure 2.7, the reader can check for torque closure in the plane by drawing a quadrilateral delimiting the overlapping region of the two cones $C_{12}^<$, $C_{34}^<$. From this quadrilateral, he can generate clockwise and counter-clockwise torques from positive combinations of the four pure forces.

2.3.3 Finding All Force Closure Grasps

Theorem 2.3 *Let G be a planar grasp described by the set of wrenches W . Let's denote by $W^<$ the wrench convex spanned by W , and by $T^<$ the twist convex reciprocal or repelling to W . The following clauses are equivalent:*

1. G is a force closure grasp.
2. W can generate force with arbitrary direction, and moment.

$$W^< = \infty [f_x, f_y, m_z]$$

3. There is neither translational nor rotational twist that is free, or that breaks contact with G .

$$T^< = \mathbf{0} \delta_z, d_x, d_y$$

We know from Section 2.2.4 that the convex addition of the convex of all force directions $\infty [f_x, f_y]$ and the convex of all torques ∞m_z is the convex of all planar forces $\infty [f_x, f_y, m_z]$. So, from the above theorem, the necessary and sufficient condition for force closure is contained in both Theorems 2.1 and 2.2. If we assume that through any contact we can only exert force and not torque, then Theorem 2.2 subsumes Theorem 2.1. A translation can be viewed as a rotation with point of rotation at the infinity. So, if there is no free rotation for the grasped object constrained by a set of contact forces, then there exists also no free translation. Thus Corollary 2.2 describes the geometrical necessary and sufficient condition for force closure with planar forces only.

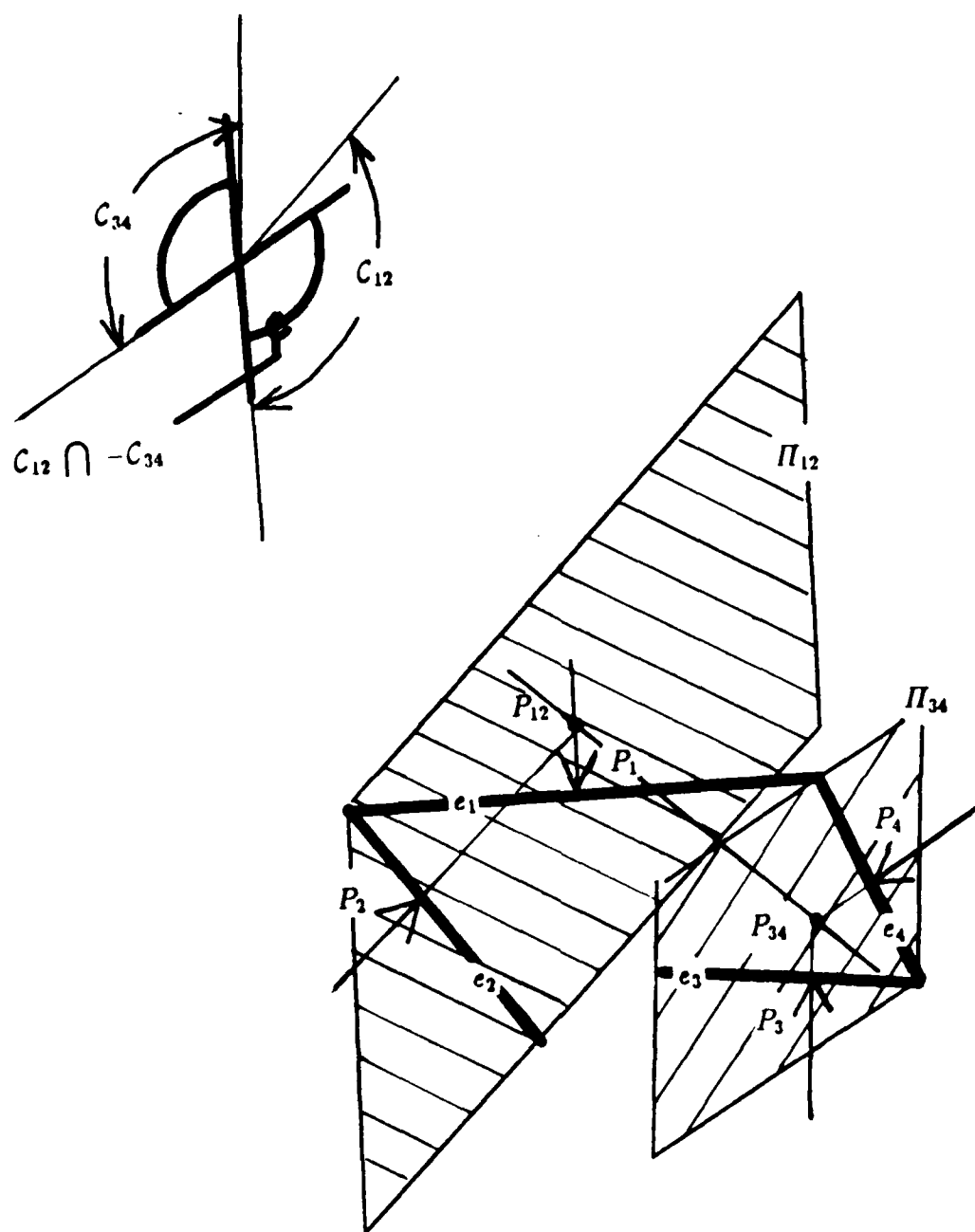


Figure 2.8: Finding frictionless grasps on four edges.

Grasps on Two Edges Require Friction

Corollary 2.3 *Two point contacts with friction at P and Q form a force closure grasp if and only if the segment PQ , or QP , points strictly into and out of the two friction cones respectively at P and Q .*

Proof: This is a well known fact of planar mechanics. Let's however prove the above corollary using a reduction from a grasp with 2 point contacts with friction to a grasp with 4 point contacts without friction. A friction cone at P (resp. Q) is equivalent to two forces \hat{w}_1, \hat{w}_2 (resp. \hat{w}_3, \hat{w}_4) along the edge of friction cone and going through P (resp. Q), Figure 2.9. We recognize that point P (resp. Q) is nothing more than the point P_{12} (resp. P_{34}). So the above corollary is a special case of Corollary 2.2. ■

Now, let's find the set of possible grasps from two edges e_1 , and e_2 . Since the point of contact P , (resp. Q), must lie on edge e_1 , (resp. e_2), the parallelogram Π_{12} , (resp. Π_{34}) reduces to the edge e_1 , (resp. e_2). The construction of the set of grasps from two edges e_1, e_2 is similar to the construction given in Algorithm 2.1.

Lemma 2.3 *The set of all possible grasps with friction on two edges e_1, e_2 , denoted $\mathcal{G}(e_1, e_2)$, is completely described by the two edges e_1, e_2 , and the counter-overlapping sector $\mathcal{C} = \mathcal{C}_1 \cap -\mathcal{C}_2$ of the two friction cones resp. from edge e_1 and e_2 .*

By definition, a force-closure grasp is a set of contacts which allows us to exert arbitrary force and moment on the object by pushing at the contacts. So, we can exert zero force and moment, i.e. have an equilibrium grasp. In the other direction, it turns out that most equilibrium grasps with point contacts with friction are also force-closure grasps:

Corollary 2.4 *Let G be a grasp with at least two distinct point contacts with friction. G is a force closure grasp if it is an equilibrium grasp, and has contact forces pointing strictly within their friction cones.*

Proof: The two friction cones gives three lines of force which are not all parallel because the friction cones are not null. These three lines of forces do not all intersect at the same point because the two points of contact are distinct. So, we have three planar wrenches with independent spatial vectors. The set of contact wrenches is also force closure, or vector closure,² if there exists a strictly positive combination of four contact wrenches that results in the zero wrench, or equilibrium. The coefficients of the contact wrenches must be strictly positive, i.e. the contact forces must point strictly inside their respective friction cones. ■

How does a soft finger contact compare with a point contact with friction? Due to the non-zero segment, a soft finger contacting an edge gives us a range of friction

The general vector closure theorem, Theorem 2.5, has the same form as Theorem 2.1, and is given in Section 2.4.4.

Grasps With Frictionless Contacts

Algorithm 2.1 A force closure grasp between four edges e_1, \dots, e_4 can be constructed as follows:

1. Pair up two edges e_1, e_2 against e_3, e_4 such that the two sectors C_{12}, C_{34} are non null. By sector C_{12} , we denote the smallest sector between the normals $-\mathbf{n}_1, -\mathbf{n}_2$.

2. Check that the two sectors C_{12}, C_{34} counter-overlap, i.e.:

$$C_{12} \cap -C_{34} \neq \emptyset \quad (2.14)$$

3. Find the parallelogram Π_{12} by intersecting the two infinite bands perpendicular to and containing the edges e_1 and e_2 . Parallelogram Π_{12} is the locus of points P_{12} where the lines of force of $\hat{\mathbf{w}}_1, \hat{\mathbf{w}}_2$ intersect. Similarly, we find the parallelogram Π_{34} which represents the locus of points P_{34} where lines of force of $\hat{\mathbf{w}}_3, \hat{\mathbf{w}}_4$ intersect.

4. Pick two points P_{12}, P_{34} respectively from the parallelograms Π_{12}, Π_{34} , such that the direction of the line joining P_{12} and P_{34} is in the counter-overlapping sector $C = C_{12} \cap -C_{34}$.

5. From point P_{12} , backproject along the normal \mathbf{n}_1 , (resp. \mathbf{n}_2), to find the grasp point P_1 , (resp. P_2), on edge e_1 , (resp. e_2). Similarly, we find the grasp points P_3 , and P_4 by backprojecting P_{34} respectively along the normals $\mathbf{n}_3, \mathbf{n}_4$.

6. The four grasp points P_1, P_2, P_3, P_4 found as above form a force closure grasp $G(P_1, P_2, P_3, P_4)$ between the four edges.

Lemma 2.2 The set of all possible grasps on four edges e_1, \dots, e_4 , denoted $\mathcal{G}(e_1, \dots, e_4)$, is completely described by the two parallelograms Π_{12}, Π_{34} , and the counter-overlapping sector $C = C_{12} \cap -C_{34}$.

It is obvious from the construction, and from Corollary 2.2 that the set of grasps characterized as above is complete for the pairing of edges e_1, e_2 against e_3, e_4 . The reader may wonder whether the different pairings in step 1 of the above construction give different sets of grasps. The answer is No. Different pairings certainly give different parallelograms and counter-overlapping sectors. However, they all describe the same set of grasps. This is supported by Lemma A.1 in Appendix A.2, which says informally that the three pairings are equivalent to each other.

From Corollary 2.1, we must have at least three non-parallel forces to have force-direction closure. So we need at least four contacts on three non-parallel edges, if there is no friction between the fingers and the grasped object. With two of the four contacts on the same edge, there are possibly three grasp-sets between three edges e_1, e_2, e_3 : $\mathcal{G}(e_1, e_2, e_1, e_3), \mathcal{G}(e_1, e_2, e_2, e_3), \mathcal{G}(e_1, e_3, e_2, e_3)$. The problem reduces to one of finding grasp sets between four edges. From Section 2.3.1, we can replace two frictionless point contacts on the common edge with a frictionless edge contact. This is a good illustration of how we can grasp a same object with fewer fingers by using edge contacts instead of point contacts.

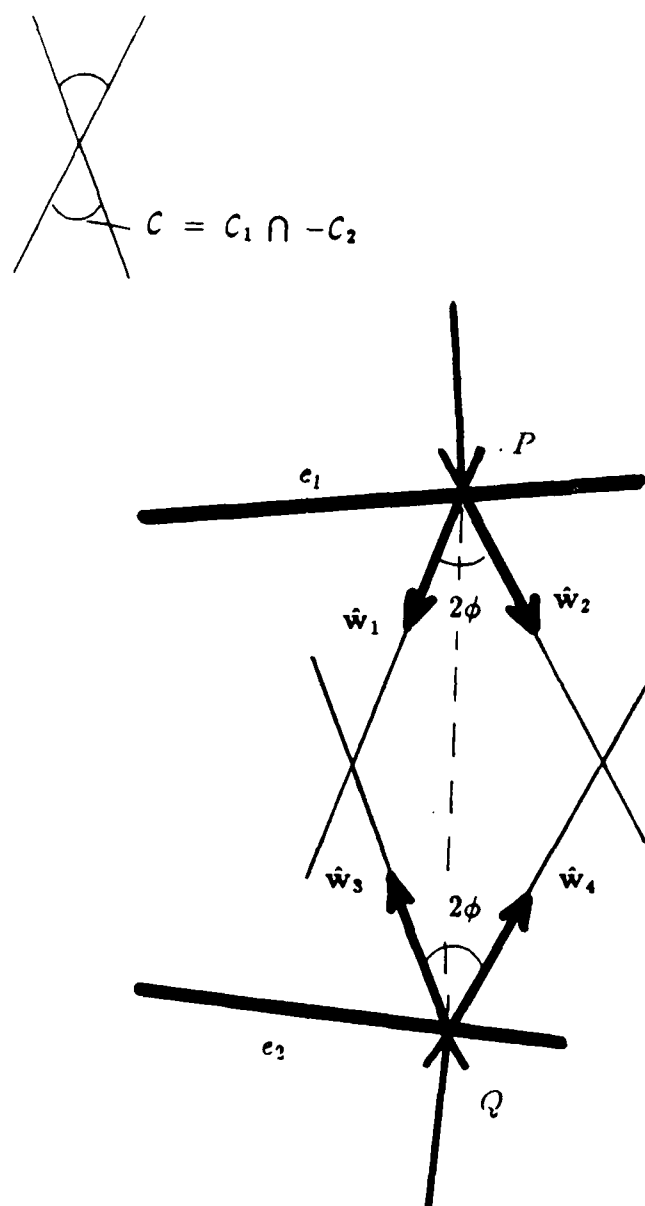


Figure 2.9: Finding grasps with friction on two edges.

cones instead of a single friction cone (Figure 2.4.e). A more interesting comparison is to compare the range of force directions when the soft-finger contacts a vertex. A soft finger contacting at a vertex can be approximated as a point contact with a much wider friction cone. From Corollary 2.3, we have seen that the larger the friction cones at the points of contacts, the greater is the likelihood that they counteroverlap, or that the grasp is force closure. So a soft finger gives us more flexibility than a point contact with friction. This partially explains why people grasp objects at edges and corners, and also why the contacting surface of human fingers had better be soft than hard like the finger nails.

2.3.4 Finding Independent Regions of Contact

Independent Regions For Two Point Contacts With Friction

In task planning, we are interested in finding grasps that require as little accuracy as possible. One aspect of that goal is to have grasps such that the fingers can be positioned independently from each other, not at discrete points, but within large regions of the edges.

Corollary 2.3 allows us to cast the problem of finding the independent regions of contact on two edges into a problem of fitting a two-sided cone cutting these two edges into two segments of largest minimum length. Figure 2.10.

Definition 2.7 A two-sided cone $C^\times(I, \pm C)$ with vertex I and sector C , is the set of points P such that the segment IP has orientation inside $\pm C$.

Algorithm 2.2 The independent regions of contact on two edges e_1 and e_2 can be constructed as follows:

1. Find the two-sided cone $C^\times(I_1, \pm C)$ that cuts all of edge e_1 and very little or none of edge e_2 . We get a triangle Δ_1 formed by edge e_1 and vertex I_1 . This triangle represents the set of vertices I , where the two-sided cone $C^\times(I, \pm C)$ monotonically cuts larger segment e'_1 and smaller segment e'_2 as we move from edge e_1 to e_2 . Similarly, we find the two-sided cone $C^\times(I_2, \pm C)$ such that this later cuts exactly the edge e_2 and very little or none of edge e_1 . We get a triangle Δ_2 formed by edge e_2 and vertex I_2 .

2. Find the trade-off region for vertex I by intersecting the triangle Δ_1 with Δ_2 . The trade-off region describes the locus of vertex I , for which the two-sided cone $C^\times(I, \pm C)$ cuts both edges e_1 and e_2 into segments e'_1 and e'_2 . The length of the independent segments e'_1 and e'_2 is proportional to the distance from vertex I of the two-sided cone to the respective edges.

3. We cut the trade-off region with the bisector of the two edges e_1 , and e_2 . The intersection is the locus of vertex I for which the two segments e'_1 and e'_2 have the same length. The optimal vertex I^* is at one of the two endpoints of the intersecting segment, or anywhere on this segment, depending on the angle between the two edges. If no intersecting segment exists, then the optimal vertex is the point of the trade-off region which is nearest to the bisector.

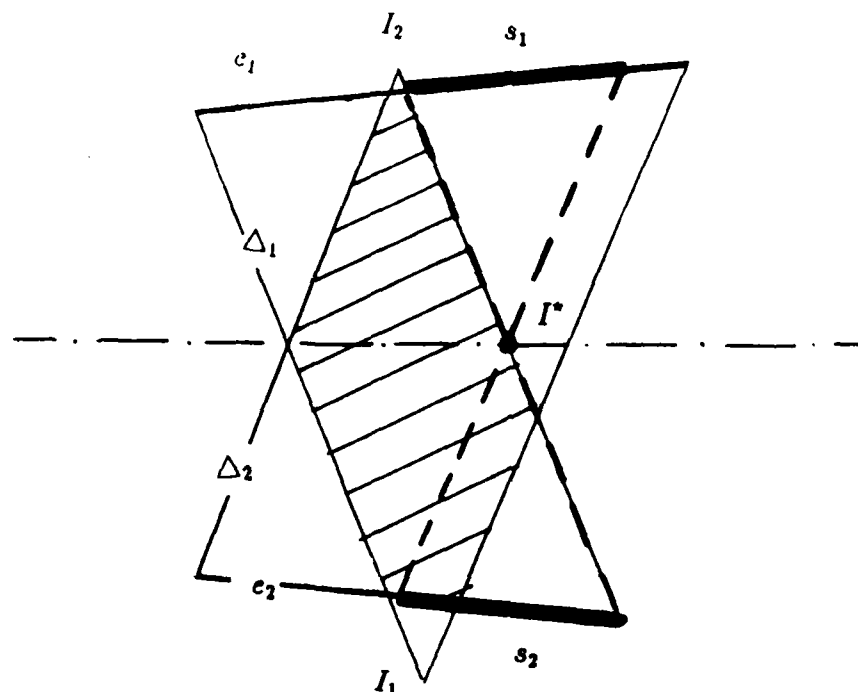


Figure 2.10: Finding the independent regions of contact on two edges.

4. From the optimal vertex I^* , the independent regions of contact s_1 and s_2 are found by cutting the two-sided cone $C^\times(I^*, \pm C)$ with the grasping edges e_1 and e_2 .

The computation of the optimum independent regions of contact for two point contacts with friction on two edges takes about 0.05 seconds. The code is written in Zeta Lisp, compiled and run on a Symbolics machine.

Independent Regions For Four Frictionless Point Contacts

Using Corollary 2.2, the problem of finding the independent regions of contact on three or four edges becomes a problem of fitting a two-sided cone between two parallelograms. Figure 2.11 illustrates the fitting of a two-sided cone between the two parallelograms Π_{12} and Π_{34} . The two-sided cone has vertex at I , and sector $C = C_{12} \cap -C_{34}$. This two-sided cone cuts the two parallelograms Π_{12} and Π_{34} into two disjoint regions, for which Corollary 2.2 is satisfied for any pair of points (P_{12}, P_{34}) from these two regions. Better, we restrict the two disjoint regions to two smaller parallelograms Π'_{12} and Π'_{34} , so that the point of contact P_1 (resp. P_3) can be independently placed from P_2 (resp. P_4). The problem is to find the optimum position of the vertex I such that the parallelograms Π'_{12} and Π'_{34} have largest minimum distance between parallel edges. The independent contact regions are

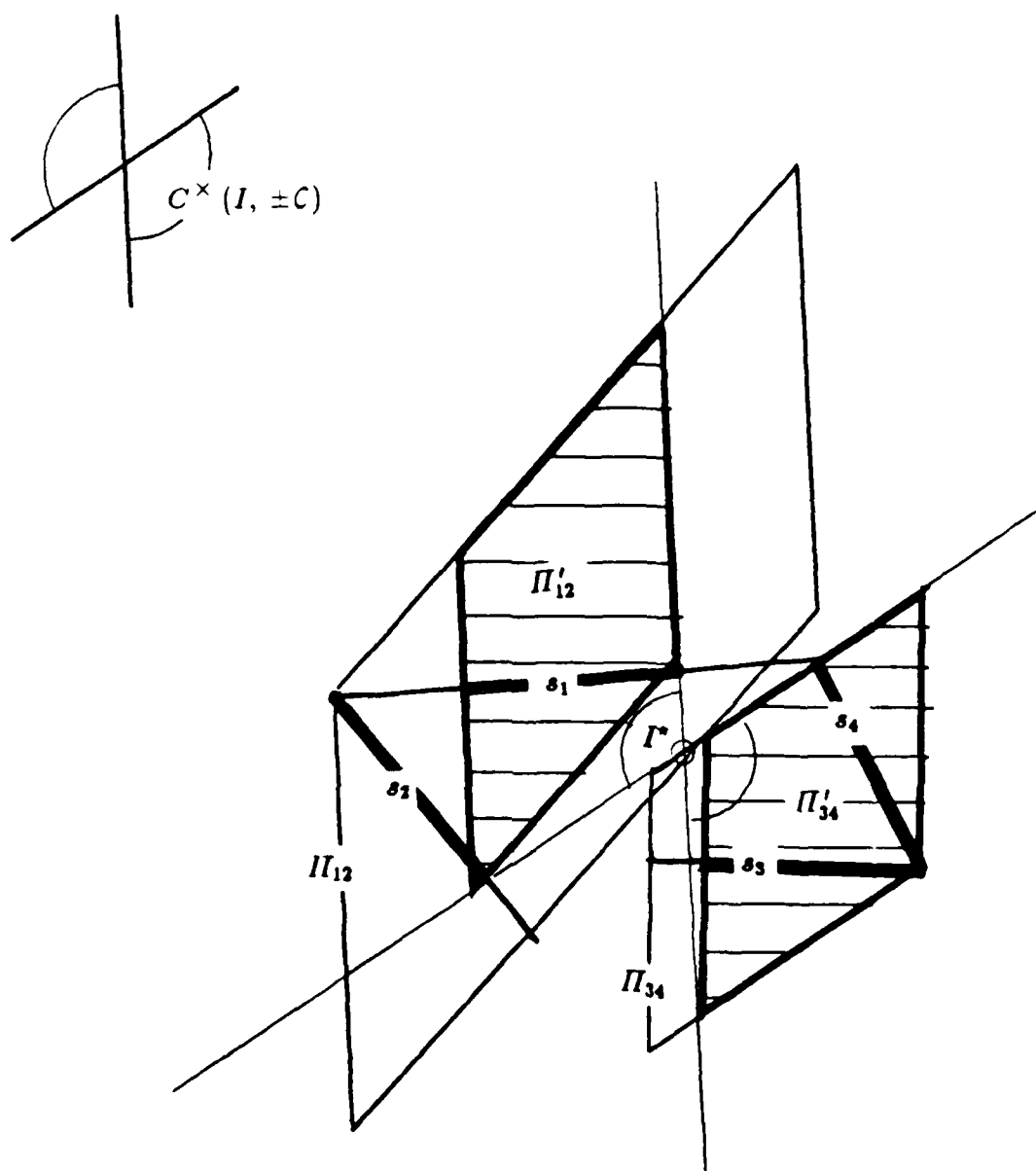


Figure 2.11: Independent regions for four frictionless point contacts.

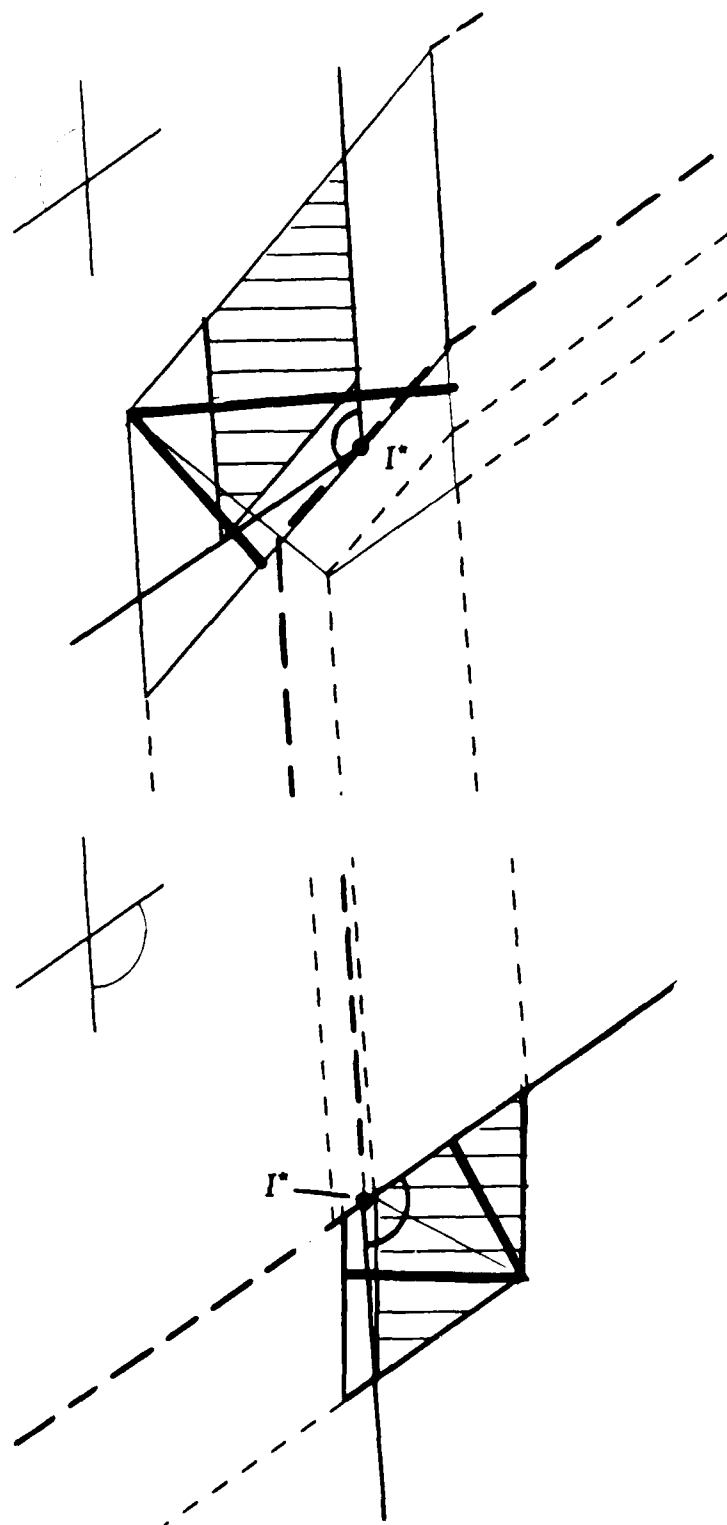


Figure 2.12: Search for the optimum vertex of the two-sided cone.

found by backprojecting the smaller parallelogram Π'_{12} on edges e_1 and e_2 , similarly for Π'_{34} . The algorithm is similar to Algorithm 2.2.

As we translate one of the edges of the cone $C'(I, \pm \mathcal{C})$, the parallelograms Π'_{12} and Π'_{34} vary monotonically in opposite directions. This monotonicity allows us to consider only a finite number of boundary cases. We partition the plane into regions R_i 's depending on how the two-sided cone cuts the parallelogram Π_{12} . In each region R_i , the loci of vertex I , for which Π'_{12} has constant area, form parallel lines shown by dashed lines in Figure 2.12. We find similar regions R_j 's and loci, for parallelogram Π_{34} . The problem then reduces to computing all pairwise intersections $R_i \cap R_j$, from the two sets of regions, and for each intersection, compute the locally optimum vertex I from the two corresponding loci.

The computation of the four optimal independent regions of contact takes about 0.25 seconds on a Symbolics machine.

The synthesis of the four independent regions of contact can be viewed as finding four convexes $C_1^<, \dots, C_4^<$, such that any 4-tuple of wrenches $(\hat{\mathbf{w}}_1, \dots, \hat{\mathbf{w}}_4)$ is vector closure or:

$$\sum_{i=1}^4 \alpha_i \hat{\mathbf{w}}_i = \hat{\mathbf{0}} \quad \alpha_i > 0 \quad (2.15)$$

assuming that three of the four wrenches are always independent. The wrench $\hat{\mathbf{w}}_i$ and the convex $C_i^<$ correspond respectively to a point contact and a range of point contacts on edge e_i .

The above equation can be rewritten as follows:

$$\begin{aligned} (\alpha_1 \hat{\mathbf{w}}_1) &= -(\alpha_2 \hat{\mathbf{w}}_2 + \alpha_3 \hat{\mathbf{w}}_3 + \alpha_4 \hat{\mathbf{w}}_4) \\ (\alpha_1 \hat{\mathbf{w}}_1 + \alpha_2 \hat{\mathbf{w}}_2) &= -(\alpha_3 \hat{\mathbf{w}}_3 + \alpha_4 \hat{\mathbf{w}}_4) \end{aligned} \quad (2.16)$$

which have the following necessary conditions:

$$\begin{aligned} (C_1^<) \cap -(C_2^< \cup C_3^< \cup C_4^<) &\neq \emptyset \\ (C_1^< \cup C_2^<) \cap -(C_3^< \cup C_4^<) &\neq \emptyset \end{aligned} \quad (2.17)$$

By permutating the indexes, we get five other necessary conditions:

$$\begin{aligned} (C_2^<) \cap -(C_3^< \cup C_4^< \cup C_1^<) &\neq \emptyset \\ (C_3^<) \cap -(C_4^< \cup C_1^< \cup C_2^<) &\neq \emptyset \\ (C_4^<) \cap -(C_1^< \cup C_2^< \cup C_3^<) &\neq \emptyset \\ (C_1^< \cup C_3^<) \cap -(C_2^< \cup C_4^<) &\neq \emptyset \\ (C_2^< \cup C_3^<) \cap -(C_4^< \cup C_1^<) &\neq \emptyset \end{aligned} \quad (2.18)$$

The intersection of two convexes generally gives a smaller convex, so the above necessary conditions restrict the edges e_1, \dots, e_4 into smaller segments s_1, \dots, s_4 . These segments represent the independent regions of contact if their convexes are also disjoint.

In a plane, two non parallel lines always intersect. This is why $C_1^< \cup C_2^<$ can be geometrically represented by point P_{12} and the sector C_{12} . The geometric representation is exact, because it captures all the strictly positive combinations of vectors in $C_1^<$ and $C_2^<$. The fitting of the two-sided cone in between the two parallelograms Π_{12} and Π_{34} , captures the operation $(C_1^< \cup C_2^<) \cap -(C_3^< \cup C_4^<)$. The enumeration of the regions R_i 's and R_j 's and the pairwise intersection of these regions, $R_i \cap R_j$, is just a geometric construction of the optimum set of four disjoint convexes that satisfy the above seven necessary conditions. The geometric construction makes explicit the location of the points of contact. The number of intersections to test is exponential in the number of convexes, or the minimum number of required contacts, c . So the optimal set of independent regions of contact costs $O(2^c)$.

2.3.5 Force-Closure with Redundant Contacts

Redundant contacts do not change the force closure property of the grasp, and so can be placed anywhere on the object. For example, a frictionless force-closure grasp needs at least four contacts. Grasping regions on n given edges, $n > 4$, can be found by finding the four optimal independent regions of contact for all $\binom{n}{4}$ 4-tuples of the n grasping edges. The first four fingers must be inside the four independent regions found, while the other $n - 4$ fingers can be anywhere in the remaining grasping edges. So, the other $n - 4$ independent regions of contact are the grasping edges that have not been used. We can pick the set of n independent regions of contact with the largest minimum length, and this is the optimal set.

In general, finding the best set of independent regions of contact for n fingertips on m edges requires an enumeration of $\binom{\max(n, m)}{c}$ combinations, and so costs $O(\max(n, m)^c)$ time. c is the minimum number of required contacts, and $c \leq \max(n, m)$. It is four for frictionless point contacts, and is two for point contacts with friction. Finding the set of all force-closure grasps for n fingers on m edges costs $O(\max(n, m)^c)$ time, because we also need to enumerate all $\binom{\max(n, m)}{c}$ combinations.

There is another constant factor in the construction of the independent regions of contact. The constant factor comes from the optimal trade-off between the independent regions of contact, for all possible combinations of c wrench convexes from the c edges. The number of such combinations is $O(2^c)$.

Complexity 2.1 *Let B be a polygonal object grasped by n contacts on m edges. Let c be the minimum number of required contacts. For $c \leq \max(n, m)$:*

- *Finding the set of all force-closure grasps, for n fingertips on m edges, costs $O(\max(n, m)^c)$ time.*
- *Finding the optimal set of independent regions of contact, for n fingertips on m edges, costs $O(\max(n, m)^c 2^c)$ time.*

In the minimal case where both the number of contacts and the number of edges are minimal, the force-closure grasps can be constructed in constant time.

The independent regions of contact are also computable in constant time, with a constant factor exponential in the number of required contacts. Friction is crucial in reducing the number of required contacts. So grasps with friction are not only easier to execute but also easier to construct.

2.4 Force-Closure Grasps in 3D

2.4.1 Primitive Contacts

The contacts between the fingertips and the object can be modeled as frictionless point contacts, hard-finger contacts, or soft-finger contacts with friction. See Figure 2.13.

- Frictionless point contact. -- The finger can only exert a normal force through the point of contact. The wrench convex has a single wrench, with line of action going through the point of contact, and with direction the negative of the contact normal.
- Hard-finger contact. -- This is a point contact with friction. The finger can exert any force pointing into the friction cone at the point of contact. This friction cone describes the wrench convex, which mathematically has an infinite number of generating wrenches. This friction cone can be approximated by a polyhedral convex, with vertex at the point of contact (Kerr 1985).
- Soft-finger contact. -- The friction over the area of contact allows the finger to exert pure torques in addition to pure forces pointing into the friction cone. The finger can exert torques in both directions, about the normal axis at the point of contact. So the wrench convex is described by a one-sided friction cone plus a two-sided torque.

Any complex contact can be described as a convex sum of the above primitive contacts. Figure 2.14 shows an edge contact without friction whose wrench convex is the convex sum of two wrench convexes, each describes the frictionless point contact at one end of the edge of contact. Similarly, a face contact is the convex sum of point contacts at the vertices of the face. If the face is non convex, then its wrench convex is equivalent to the convex sum of point contacts on the convex hull of the face only. The convex hull has fewer vertices than the non convex face.

Similar to the planar case, a soft finger contacting at a vertex (or an edge) of a polyhedron can be approximated by a point contact (or an edge contact) with a much larger friction cone. For a grasp with two soft finger contacts, the larger the friction cone, the more likely the grasp is force closure. This explains why people tends to grasp at sharp corners and edges.

2.4.2 Grasps with Two Soft-Finger Contacts

Figure 2.15.a shows two soft-finger contacts on two faces of a polyhedron. The angle between the two contact planes is ψ . The positive combination of the two friction cones generate rays in any direction if and only if $\psi < 2\phi$, where $\tan \phi$ is the coefficient of friction.

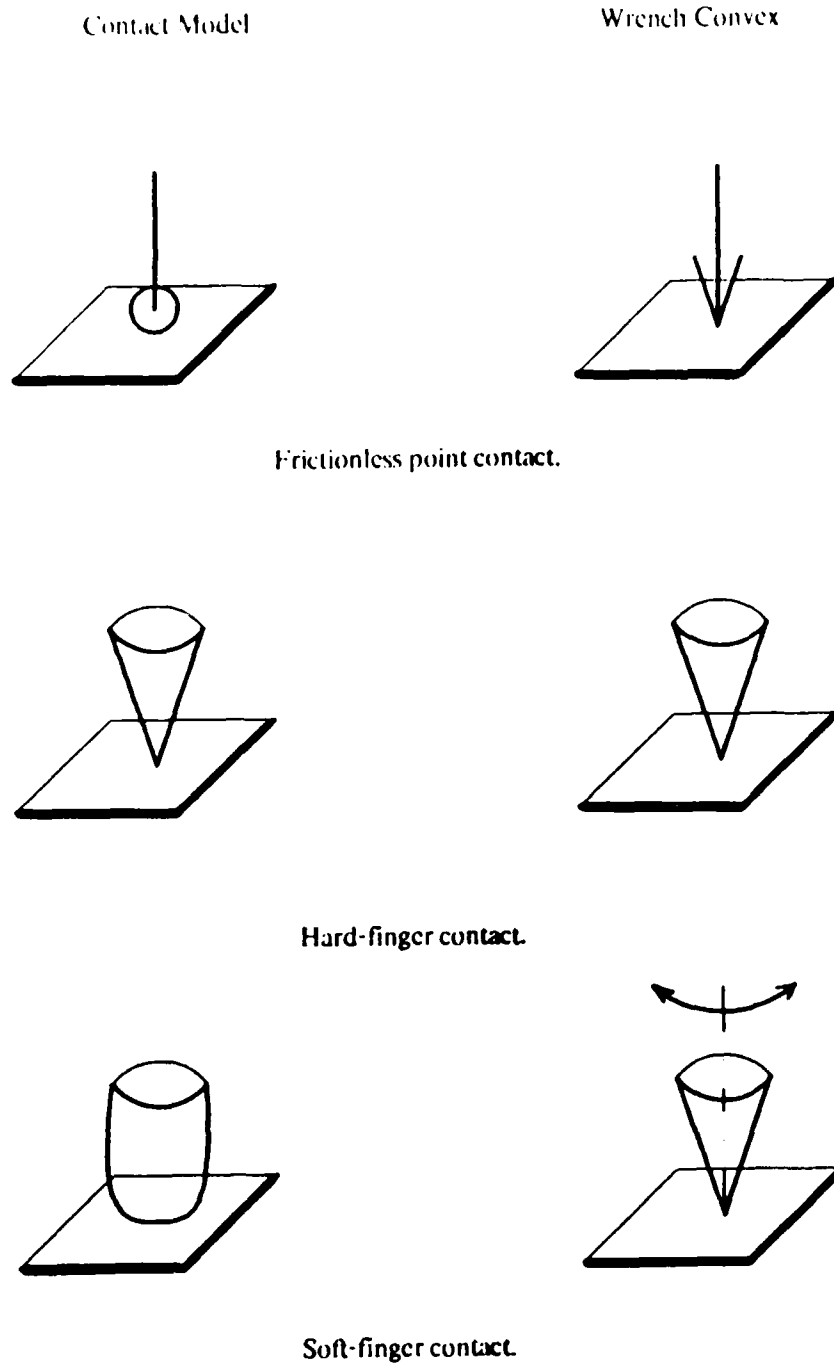
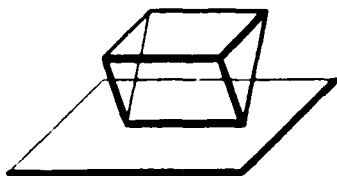
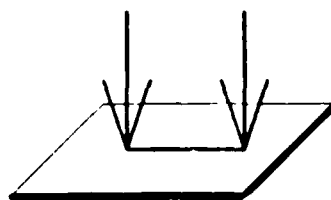


Figure 2.13: Primitive contacts in 3D.

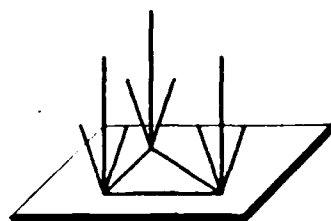
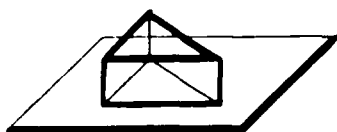
Contact Model



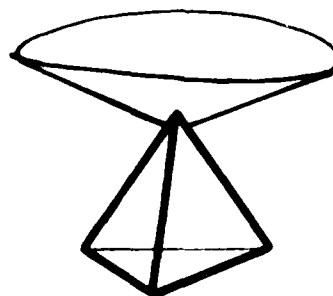
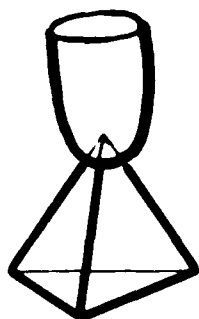
Wrench Convex



Frictionless edge contact



Frictionless face contact



Soft-finger on a vertex.

Figure 2.14: Complex contacts in 3D.

Lemma 2.4 *A grasp with 2 soft-finger contacts is force-direction closure if and only if the angle ψ between the two planes of contact is strictly less than the angle of the friction cone 2ϕ .*

By coupling opposite contact forces, we can generate arbitrary pure torques perpendicular to the segment P_1P_2 joining the two points of contact, Figure 2.15.a. These torques can be generated if (1) $\psi < 2\phi$, and (2) the segment P_1P_2 , or P_2P_1 , points strictly into and out of the two friction cones at the two points of contact P_1 and P_2 . The pure torques about P_1 and P_2 have projections on the segment P_1P_2 , so the grasp drawn is also torque closure. The first condition is a prerequisite of the second condition. The second condition is both a sufficient and necessary condition for the case of two soft-finger contacts:

Theorem 2.4 *A grasp with 2 soft-finger contacts is force-closure if and only if: The segment P_1P_2 , or P_2P_1 , joining the two points of contact P_1 and P_2 , points strictly into and out of the friction cones respectively at P_1 , P_2 .*

For polyhedral objects, the faces have constant normals, so the force-direction closure condition reduces to a simple test of the angle between the two plane normals. Once the force-direction closure is satisfied, the two friction cones counter-overlap, and the counter-overlapping range is $C_2 \cap -C_1$. The torque closure condition is satisfied if and only if the segment P_1P_2 , or P_2P_1 , has orientation inside the counter-overlapping range $C_2 \cap -C_1$. The independent contact regions can be constructed by cutting the two faces with a two-sided cone, having cone angle $\pi(C_2 \cap -C_1)$, and vertex in between the two faces.

Figure 2.15.b shows examples of force-closure grasps with two soft-finger contacts. The coefficient of friction used is 0.8. The construction is similar to its 2-dimensional analogue given in Algorithm 2.2. The faces are approximated by their bounding circular disks. The counter-overlapping range $C_2 \cap -C_1$ is approximated by the maximum cone inside $C_2 \cap -C_1$. The two-sided cone is positioned in between the two disks bounding the two faces. The intersection between the two disks and their respective cones give the independent contact regions. The approximate computation of the independent regions for two soft-finger contacts on two faces takes about 0.05 seconds.

If the face has holes, or if it is non convex, then the the circular disk bounding the face no longer preserves the compactness or convexity property of the face. A non-convex face is approximated by a set of overlapping circular disks, each disk approximates a local convex region of the face. Local convex regions can be computed from the Voronoi Diagram of the face (Shamos 1978). They can be approximated by the generalized cones between facing edges as in (Nguyen 1984).

A force-closure grasp implies that equilibrium grasps exist since zero force and moment is spanned by the set of contact forces. In the reverse direction, it turns out that equilibrium grasps with soft-finger contacts are usually force-closure grasps:

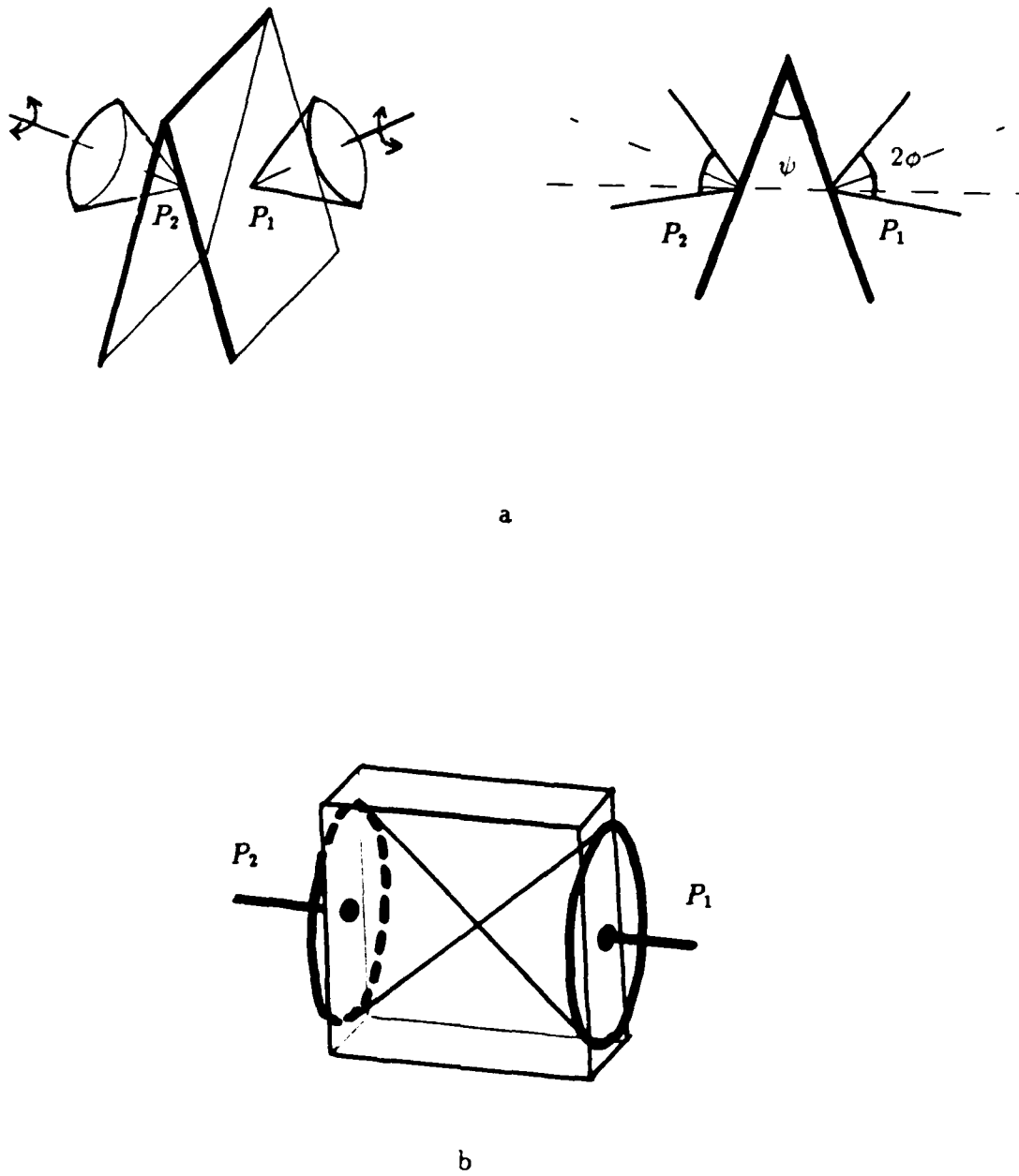


Figure 2.15: Force-closure with two soft-finger contacts.

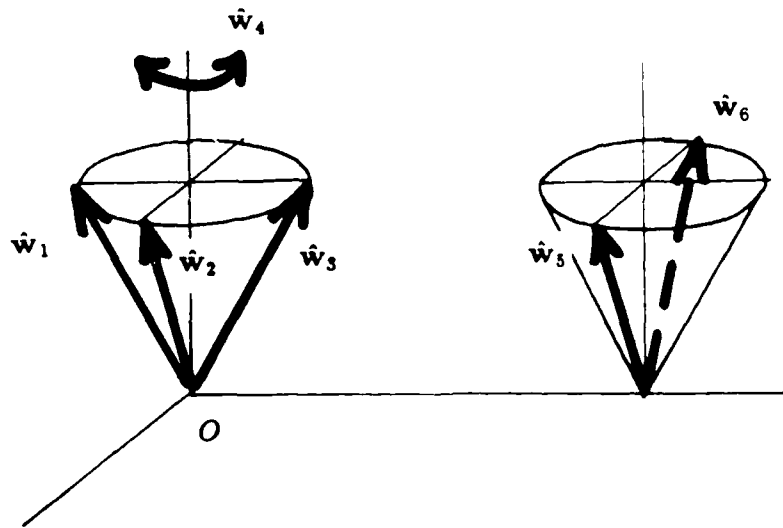


Figure 2.16: Two distinct soft-finger contacts give six independent wrenches.

Corollary 2.5 *A grasp with at least two distinct soft-finger contacts is force-closure if it is in equilibrium, with contact forces pointing strictly into the friction cones at the respective points of contact.*

Proof: Let's first prove that two distinct soft-finger contacts gives six independent contact wrenches. Let the origin of the reference frame be the first point of contact, Figure 2.16. The first friction cones gives three contact forces in three independent directions. All three contact forces have zero moment components. The first soft-finger contact has also a pure torque. So, we have four independent wrenches from the first soft-finger. Because the two point contacts are distinct, the moment of the second friction cone about the first point contact gives at least two different wrenches with different moment components than the first pure torque. So, in total, two distinct soft-finger contacts gives six independent contact wrenches.

A non-marginal equilibrium, in which all the contact forces are strictly within their respective friction cones, means a strictly positive sum of the contact wrenches is zero. Let's prove that we have a strictly positive sum of at least seven contact wrenches, in which six of them are independent. Each soft-finger contact can be approximated by a four-wrench convex (one pure torque and three forces), such that the force and torque at the point of contact is a strictly positive combination of the four wrenches. The grasp has at least two soft-finger contacts, i.e. has at least eight contact wrenches, in which at least six of them are independent. The contact forces and torques add to zero, so the strictly positive combination of at least eight contact wrenches is zero. From the vector closure theorem, Theorem 2.5, the grasp is definitively force closure. ■

2.4.3 Grasps with Three Hard-Finger Contacts

A real fingertip, although soft, has very limited resistance to rotations about its point of contact, and so behaves more like a hard-finger than a soft-finger. A hard-finger contact differs from a soft-finger contact by a torque about the contact normal. A grasp with two hard-finger contacts, instead of two soft-finger contacts, cannot generate or resist torques about the line joining the two points of contact. So, a force-closure grasp needs at least three hard-finger contacts with friction.

For polyhedra, the force-closure condition becomes a constraint on the relative configuration of the friction cones. The independent contact regions are constructed by cutting the two-sided cones and the faces of contact. The force-closure grasps with three hard-finger contacts can be split into four classes, Figure 2.17, depending on the number of friction cones that pairwise counter-overlap:

- The first grasp has no pair of counter-overlapping cones. An example is a three point grasp on a ball with very little friction. The three grasp points are symmetrically placed on a circle that has the same center as the ball. Note that the ball will slip away from the fingers if one of the three contact points is removed.
- The second grasp has one pair of counter-overlapping cones, from the top and bottom contacts. The third contact contributes a torque component about P_1P_2 . This contact can be removed without having the object slip from the fingers.
- The third grasp has two pairs of counter-overlapping cones. The second contact serves as a pivot when either the first or third contact is added or removed. An example is a three point grasp on two parallel faces, with two of the fingers on one same face.
- The fourth grasp has three pairs of counter-overlapping cones. All three contacts can be used as pivots, and any fingertip can be removed or added while the other two grasp the object. This grasp exists only if the coefficient of friction is greater than $\tan(\pi/6)$ degrees.

The above classification arises directly from the geometric construction of the independent contact regions. The classification highlights the similarity and difference between grasps with soft-fingers and grasps with hard-fingers. From the classification, we can change from one grasp to another by searching for a sequence of two-point and three-point grasps, Figure 2.18. The two-point grasps are force-closure if the fingertips are soft. We'll see in the next chapter, that the two-point and three-point grasps are also stable. In other words, one grasp is changed to another by a sequence of stable force-closure grasps. Only one finger is removed or added at a time, while the other two fingers maintain a stable force-closure grasp on the object.

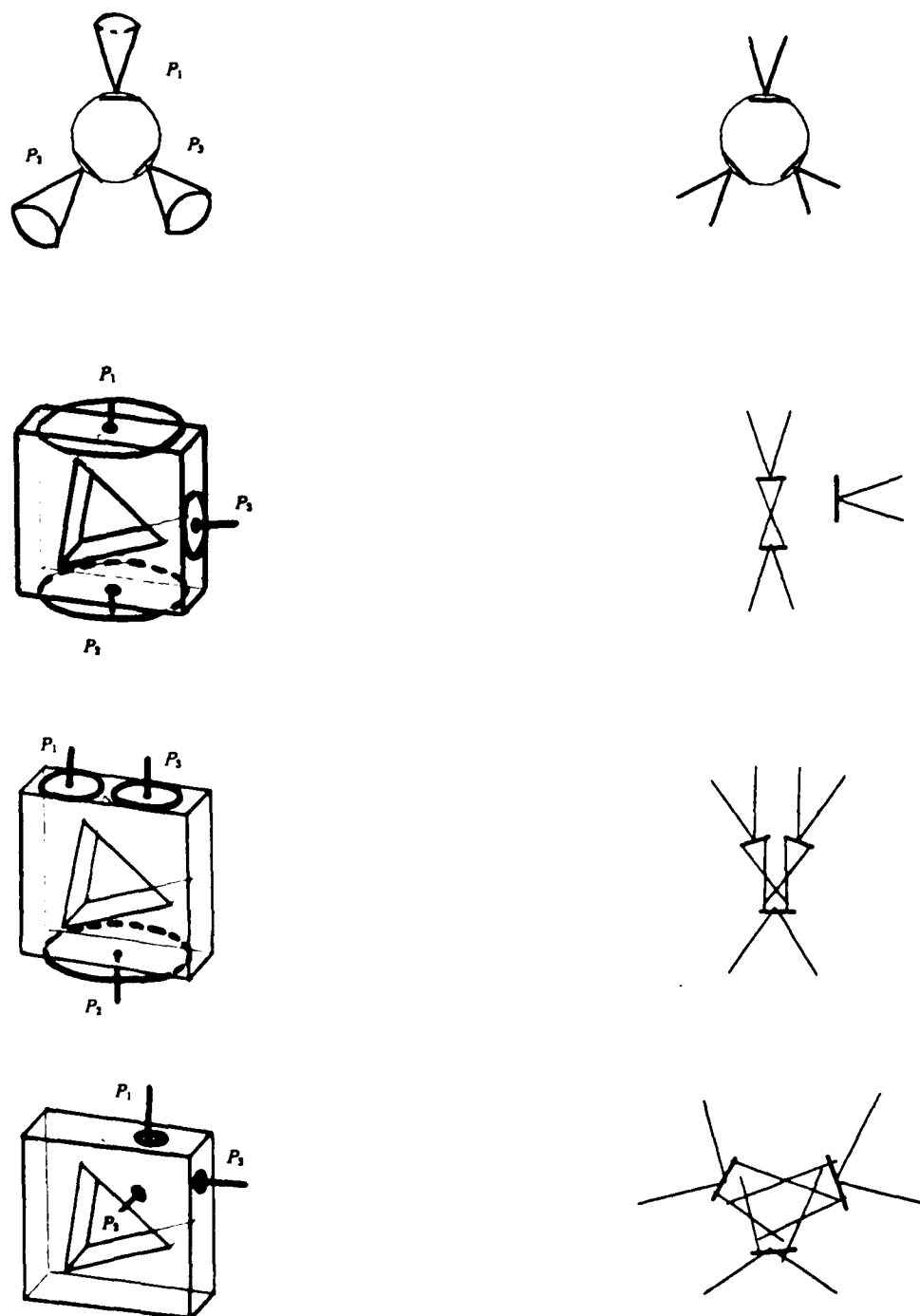


Figure 2.17: Force-closure grasps with three hard-finger contacts.

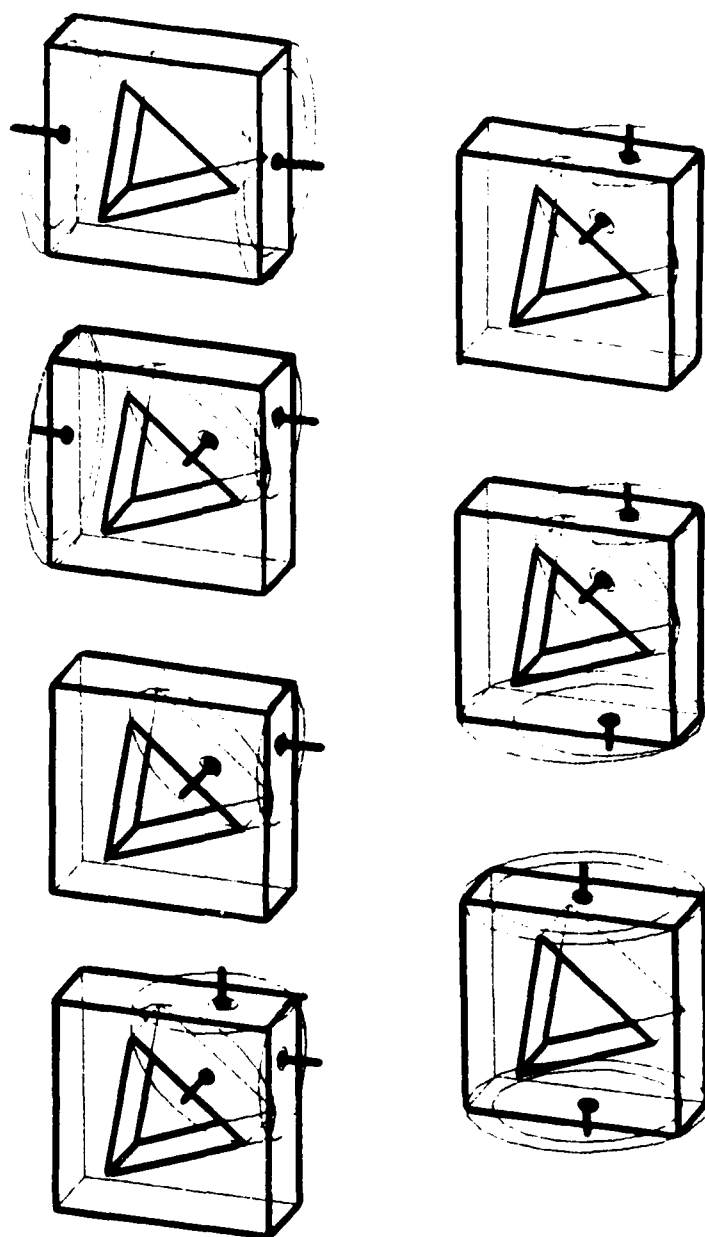


Figure 2.18: Sequence of two-point and three-point grasps.

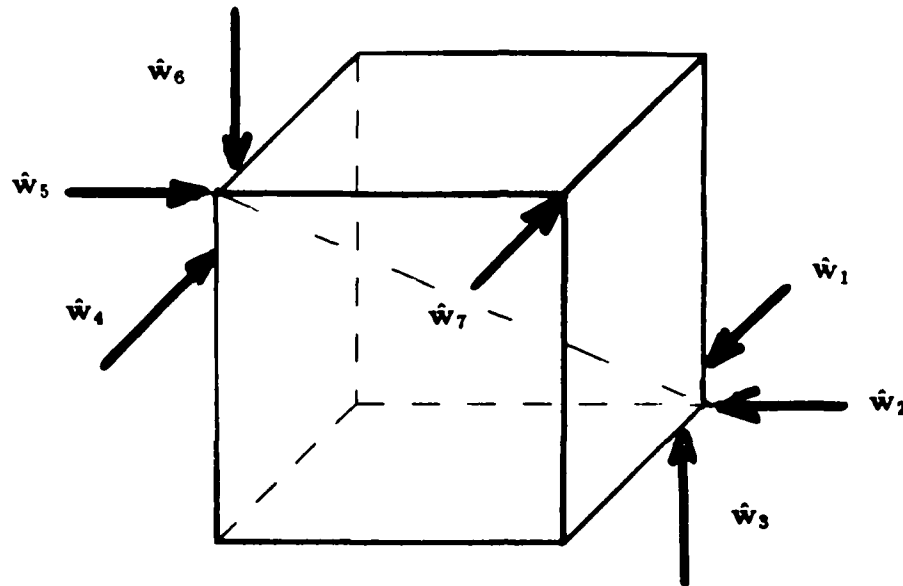


Figure 2.19: Force-closure grasps with seven frictionless contacts.

Like grasps with soft-finger contacts, non-marginal equilibrium grasps with at least three distinct hard contacts are also force-closure grasps:

Corollary 2.6 *A grasp with at least three distinct hard-finger contacts is force-closure if it is in equilibrium, with contact forces pointing strictly within the friction cones at the respective points of contact.*

2.4.4 Grasps with Seven Frictionless Point Contacts

Figure 2.19 shows a force-closure grasp on a cube, with seven frictionless point contacts. Without friction, we need at least seven frictionless point contacts instead of two soft-finger contacts, or three hard-finger contacts.

To have force-direction closure, a 3D grasp needs four frictionless contacts. Example is a grasp on a tetrahedron. For polyhedral objects, the force-direction closure problem reduces to a test of the n face normals. The test is formulated as deciding whether solutions exist for a system of n linear inequalities, $W^T \hat{\mathbf{t}}^S \geq \mathbf{0}$ in three unknowns (d_x, d_y, d_z) of the translational twist $\hat{\mathbf{t}} = (\mathbf{0}^T, \mathbf{d}^T)^T$. The force-direction closure problem does not depend on the location of the points of contact, because the normals are constant on the planar faces.

To have torque closure with unisense contacts, seven contacts are needed. Again, the test for torque closure is formulated as deciding whether solutions exist for a

system of n linear inequalities, $W^T \hat{\mathbf{t}}^S \geq \mathbf{0}$ in six unknowns: $(\delta_x, \delta_y, \delta_z, d_x, d_y, d_z)$ of the rotational twist $\hat{\mathbf{t}} = (\boldsymbol{\delta}^T, \mathbf{d}^T)^T$. From linear algebra, the six unknowns are all zero only if there are at least seven linear inequalities. In general, vector closure in n -dimensional space needs at least $n + 1$ vectors. For completeness, let's formulate the general vector-closure theorem:

Theorem 2.5 (Goldman and Tucker) *In an n -dimensional vector space, a set of vectors V is vector closure if and only if V has at least $n + 1$ vectors $(\mathbf{v}_1, \dots, \mathbf{v}_{n+1})$ such that:*

- n of the $n + 1$ vectors are linearly independent.
- A strictly positive combination of the $n + 1$ vectors is the zero vector.

$$\sum_{i=1}^{n+1} \alpha_i \mathbf{v}_i = \mathbf{0} \quad \alpha_i > 0 \quad (2.19)$$

The first statement expresses the necessary and sufficient condition for no homogeneous solutions to the system $V^T \mathbf{x} \geq \mathbf{0}$. V is the matrix with vectors \mathbf{v}_i as columns. The number of independent vectors must be equal to the dimension of the vector space. The second statement expresses the necessary and sufficient condition for no particular solutions. The above theorem is just a slightly different form of Lemma 6 proved by Goldman and Tucker. For proof, the reader is referred to (Goldman and Tucker 1956).

Analyzing whether a grasp with n point contacts is force-closure, is equivalent to deciding whether the system of linear inequalities $W^T \hat{\mathbf{t}}^S \geq \mathbf{0}$ has non-zero homogeneous or particular solutions. Typically, the system of linear inequalities is transformed into a system of linear equalities by introducing positive slack variables. Then Gauss-Jordan elimination is done on the augmented system of linear equalities. No homogeneous solution exists if the rank of the matrix is six. No particular solutions exists if the rank is six, and if the slack variables must be all zero. Deciding whether a system of n linear inequalities has solutions or not costs $O(n)$ time. However, solving for the solutions to a system of linear n inequalities costs $O(n^r)$ time, because there can be $\binom{n}{r-1}$ number of particular solutions, r is the rank of the system of linear inequalities.

Complexity 2.2 *Analyzing whether a grasp constrained by n contact wrenches is force-closure or not costs $O(n)$ time.*

Constructing the seven independent regions of contact is more expensive and harder. A convex region for a point of contact on a planar face corresponds to a wrench convex in the 6-dimensional wrench space. The problem is to find seven disjoint wrench convexes in this 6-dimensional space, such that any seven-tuple of wrenches from these seven convexes is torque closure. Due to the convexity of the

domain, the problem is reduced to a discrete test on all combinations of the seven convexes:

$$\begin{aligned} (C_1^<) \cap -(C_2^< \cup C_3^< \cup C_4^< C_5^< \cup C_6^< \cup C_7^<) &\neq \emptyset \\ (C_1^< \cup C_2^<) \cap -(C_3^< \cup C_4^< C_5^< \cup C_6^< \cup C_7^<) &\neq \emptyset \\ (C_1^< \cup C_2^< \cup C_3^<) \cap -(C_4^< C_5^< \cup C_6^< \cup C_7^<) &\neq \emptyset \end{aligned} \quad (2.20)$$

There are $\binom{7}{1}$, $\binom{7}{2}$, and $\binom{7}{3}$ equations respectively similar to the above three. They describe the necessary conditions of Equation (2.19). Note that two or three lines in space do not always intersect, so there is no geometric construction for the 3D case of seven frictionless point contacts like the 2D case of four frictionless point contacts.

The number of combinations is exponential in the required number of contacts c . This term makes the construction of independent regions of contact more expensive for frictionless grasps ($c = 7$) than for grasps with friction ($c = 2$ or 3). Computing the intersection and convex addition of the convexes also makes the construction harder.

If there are redundant fingers or faces, then we need to enumerate all possible minimal combinations of the fingers, or of the faces. Then for each minimal combination, we compute the independent regions of contact. Similar to the 2D case, the order of complexity is $O(\max(n, m)^c 2^c)$ time.³

The construction of the independent contact regions is transformed into the problem of finding disjoint convexes satisfying necessary conditions like (2.20). This transformation depends on the convexity property and on the correspondence between vectors in the convex and points of contact on the object. So any affine combination of two point contacts P_1 and P_2 inside a contact region must be a point contact P inside the same region:

$$\alpha \begin{bmatrix} \mathbf{s}_1 \\ \mathbf{s}_{10} \end{bmatrix} + (1 - \alpha) \begin{bmatrix} \mathbf{s}_2 \\ \mathbf{s}_{20} \end{bmatrix} = \begin{bmatrix} \mathbf{s} \\ \mathbf{s}_0 \end{bmatrix} \quad 0 \leq \alpha \leq 1 \quad (2.21)$$

A frictionless point contact is represented by a pure force going through the point of contact and normal to the surface. A pure force is a line vector, so the dot product of the upper and lower parts of the spatial vector must be zero:

$$\begin{aligned} \mathbf{s}_1 \cdot \mathbf{s}_{10} &= 0 \\ \mathbf{s}_2 \cdot \mathbf{s}_{20} &= 0 \\ \mathbf{s} \cdot \mathbf{s}_0 &= 0 \end{aligned} \quad (2.22)$$

Eliminating \mathbf{s} and \mathbf{s}_0 , we get:

$$\mathbf{s}_1 \cdot \mathbf{s}_{20} + \mathbf{s}_{10} \cdot \mathbf{s}_2 = 0 \quad (2.23)$$

³We assume here that the intersection of two convexes is done in constant time.

The equation expresses the condition that the two lines of force at points P_1 and P_2 must intersect or be parallel. Extrapolating this condition to other points of the contact region, the convexity property and the correspondence between vectors and contact points imply that the region of contact must: (1) be either flat or spherical, and (2) have a convex boundary. This explains why the construction of the contact regions is so simple for polyhedral objects. This also suggests that grasps on curved regions with constant center of curvature can be synthesized in the same way as grasps on planar faces.⁴

⁴Friction may help in relaxing the condition that the center of curvature must be constant for grasps on curved objects.

2.5 Conclusion

2.5.1 Main Results

The main results of this chapter are:

- The algorithms for constructing force closure grasps on polygons and polyhedra are direct, fast and simple. We find not only single grasps but the complete set of all force-closure grasps on a set of edges (resp. faces) in 2D (resp. 3D). We can also construct the independent regions of contact for the fingers. The construction is exponential in the minimum number of required fingers, and polynomial in the number of total fingers.
- We prove that non-marginal equilibrium grasps are also force-closure grasps if each grasp has at least two points contacts with friction in 2D, two soft-finger contacts or three hard-finger contacts in 3D. This proof supports a very simple heuristic for grasping objects: "Increase friction at the contact by covering the fingertips with soft rubber. Then grasp the object on two opposite sides."
- A grasp is described as the combination of individual contacts, which in turn are modeled as the combination of a few primitive contacts. In 2D, the primitive contacts are point contacts without and with friction. In 3D, they are frictionless point contacts, hard-finger and soft-finger contacts. A contact over a finite segment or surface has a very compact representation if its contact normal is constant. This explains why the synthesis of force-closure grasps is very simple for polygonal and polyhedral objects.
- Wrench convexes and twist convexes describe the constraints and freedoms of contacts and grasps. There are two dual view points: a constraint view point which captures the forces and moments exerted on the object, and a freedom view point which describes the motions of the object which are free or which break contact. The effect of the individual contacts are combined by taking the convex sum of the wrench convexes or the intersection of the twist convexes.
- A grasp is more likely to be force closure if there is friction, if the contacts are soft instead of hard, and especially if the soft fingers grasp the object at sharp vertices or edges.

2.5.2 Extensions

We have not explored the synthesis of independent regions of contact for the following types of grasps:

- 2D grasps with three point contacts with friction, where the three friction cones span all directions, but no two friction cones have counter-overlapping sectors.

- 3D grasps with three to six hard-finger contacts, where no two friction cones have counter-overlapping cones of direction.

These are minimal cases which arise when the coefficient of friction is small, or when the grasping edges or faces have almost the same normal.

For curved objects, the contact normal varies with the position of the point of contact, and so both force-direction closure and torque closure are position-dependent. The synthesis of independent regions of contact on curved objects becomes much harder. One obvious fix is to segment the boundary of the object into regions with low and high curvatures. Low curvature regions are approximated by straight edges (resp. planar faces) in 2D (resp. 3D), and high curvature regions by circular arcs (resp. ellipsoid surfaces) in 2D (resp. 3D). Grasps on low curvature regions are easily found. But, how about grasps on high curvature regions? How about grasps on both high and low curvature regions? How about grasps that have regions overlapping high and low curvature regions? The obvious fix very quickly becomes a nuisance, because the segmentation is not compatible with the force-closure constraint. We think the force-closure problem for curved objects needs more research, both for theoretical and practical purposes.

There is however a good heuristic, which captures the grasps on curved regions that are either convex or concave. We know that equilibrium grasps are also force-closure grasps if the 2D grasps has point contacts with friction, or the 3D grasps has soft-finger contacts. So, grasps at two curved regions which are back-to-back (Figure 4.7) or face-to-face are force-closure. The force-closure constraint becomes a constraint on the relative orientation of the curved regions.

Chapter 3

Constructing Stable Grasps

3.1 How Should the Fingers Be Servoed?

Chapter 2 answers the question: Where should the fingertips be placed? The fingers grasp the object at points inside the independent regions of contact, for which the grasp is always force closure. Force closure guarantees that arbitrary force and moment can be exerted on the object by pushing through the set of contacts. But, how much force should the fingers exert so as to have the grasped object in equilibrium? Then, how should the fingers resist the displacements of the object, such that this later is stable, and furthermore has a desired stiffness matrix?

Equilibrium is equivalent to having the sum of all contact forces equal to zero. Stability is equivalent to having a stiffness matrix on the grasped object. The stiffness at the grasped object comes from the active stiffness control of the fingers, or from the stiffness of the tendons and of the rubber at the fingertips.

We assume that the fingers are controlled independently from each other. We also assume that the linear and angular springs which model a fingertip are also independent of one another. The net effect of all the virtual springs is described by the potential function of the grasp, which is the the sum of the potentials from all the springs. The forward problem is to derive from the potential function of the grasp: 1) the analytical conditions for which the grasp is in stable equilibrium, and 2) the stiffness matrix and the center of compliance of the grasped object about its stable equilibrium. The reverse problem is to find the virtual springs at the fingers such that the grasp is stable and has a desired stiffness matrix. The link between this chapter and the previous one is:

“All force-closure grasps can be made stable.”

Stable grasps are analyzed and synthesized in both 2D and 3D. Grasped objects are arbitrary polygons in 2D, and arbitrary polyhedra in 3D. Curved objects and the effect of local curvature on the stability of the grasp will be explored in the next chapter. Figure 3.1 shows examples of stable grasps in 2D and 3D. The springs shown are controlled independently from each other.

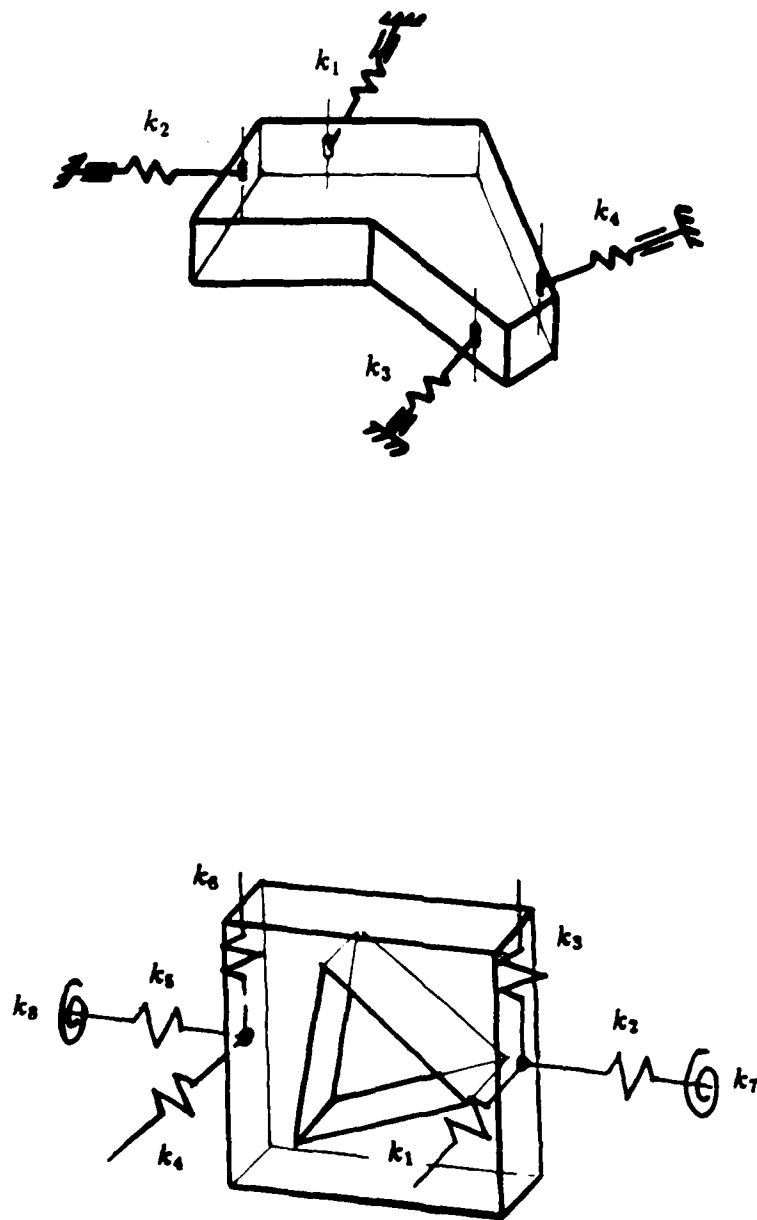


Figure 3.1: Examples of stable grasps in 2D and 3D.

3.2 Stable Grasps in 2D

3.2.1 Planar Grasps with Linear Springs

Potential Function of the Grasp

Figure 3.2 shows a finger F_i contacting without friction at point P_i . The softness of the fingertip, the stiffness of the tendons attached to the finger, and/or the active control of the finger joints are all modeled by a virtual spring with linear stiffness k_i . The linear spring k_i has fixed line of action, with direction normal to edge e_i , $\mathbf{k}_i = (\cos \alpha_i, \sin \alpha_i)^T$, and moment $^1 \mu_i = \mathbf{p}_i \times \mathbf{k}_i$, about the origin O .

When the object is displaced by (x, y, θ) , the edge e_i is translated by (x, y) and rotated by θ about the origin. The tip of spring k_i slides on edge e_i to its new position P'_i given by the intersection of the displaced edge e'_i and the line of action of spring k_i . The compression of linear spring k_i when the grasped object is moved away by (x, y, θ) from its equilibrium is $P_i P'_i$:

$$\sigma_i(x, y, \theta) = \sigma_{i0} + \frac{d_i(1 - \cos \theta) + \mu_i \sin \theta + x \cos(\alpha_i + \theta) + y \sin(\alpha_i + \theta)}{\cos \theta} \quad (3.1)$$

$d_i = \mathbf{p}_i \cdot \mathbf{k}_i$ is the algebraic distance from O to edge e_i .

The potential function of grasp G is equal to the sum of the potentials of all its springs:

$$U(x, y, \theta) = \sum_{i=1}^n \frac{1}{2} k_i \sigma_i^2(x, y, \theta) \quad (3.2)$$

The potential function of the grasped object is the sum of the potentials from the grasp and from the weight of the object (Hanafusa and Asada 1977, Asada 1979). For now, we look only at the effect of the grasping fingers on the equilibrium and stability of the object. We assume that the weight of the grasped object is negligible, or is perpendicular to the grasping plane of the object.

We assume that the potential energy of the grasp is conserved. We'll look only at grasps where the points of contact either slide without friction, or stick at the same points. There is no dissipation of the potential energy. The next chapter will look at dissipation of the potential energy of the grasp, due to slip at the fingertips in the presence of friction.

Grasp Equilibrium

The grasp G is in equilibrium if and only if the sum of all forces and moments in the grasping plane of G is zero. This is equivalent to the first partial derivatives of the potential function $U(x, y, \theta)$ being all zero:

The cross product of two 2-dimensional vectors is a scalar, which is the product of the two vector magnitudes and the sin of the angle between the two vectors.

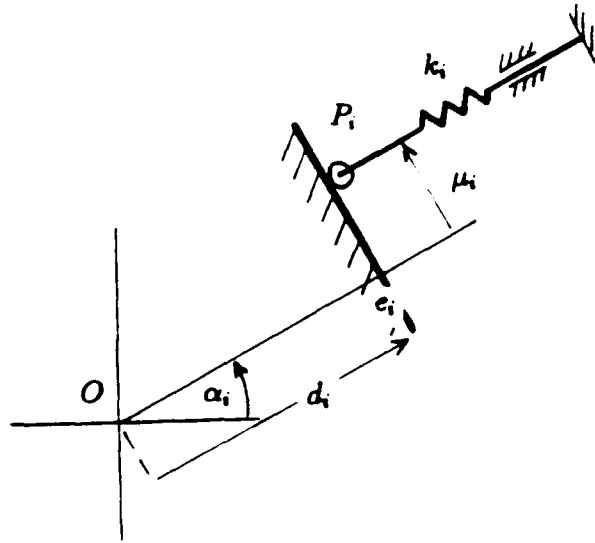


Figure 3.2: A frictionless fingertip modeled as a linear spring.

Theorem 3.1 *A grasp G composed of n virtual springs is in equilibrium if and only if:*

$$\begin{cases} \left. \frac{\partial U}{\partial x} \right|_{(0,0,0)} = \sum_{i=1}^n k_i \sigma_{i0} \cos \alpha_i = 0 \\ \left. \frac{\partial U}{\partial y} \right|_{(0,0,0)} = \sum_{i=1}^n k_i \sigma_{i0} \sin \alpha_i = 0 \\ \left. \frac{\partial U}{\partial \theta} \right|_{(0,0,0)} = \sum_{i=1}^n k_i \sigma_{i0} \mu_i = 0 \end{cases} \quad (3.3)$$

where the spring constants k_i , and the compressions σ_{i0} are all positive.

In the above columns, we recognize the spatial vectors $\hat{\mathbf{k}}_i = (\cos \alpha_i, \sin \alpha_i, \mu_i)^T$, describing the lines of action of the linear springs k_i , or as the unit wrenches describing the frictionless point contacts P_i . The above system of equations can be rewritten in a force-closure form:

$$\sum_{i=1}^n f_{i0} \hat{\mathbf{k}}_i = \hat{\mathbf{0}}, \quad f_{i0} \geq 0 \quad (3.4)$$

where $f_{i0} = k_i \sigma_{i0}$. Force equilibrium exists if and only if there exists a set of positive contact forces ² (f_{10}, \dots, f_{n0}) such that equation (3.4) holds, or if the grasp is force-closure. The force-closure condition is sufficient but not necessary for the existence of force equilibrium. For example, a grasp on two parallel edges can have force

²The contact force is positive (resp. negative) if the finger is pushing into (resp. pulling out of) the object.

equilibrium with two opposite wrenches instead of the minimum of four wrenches required for planar force-closure.

Corollary 3.1 *If grasp G is force-closure, then we can always find a set of positive contact forces at the points of contact, such that G is in equilibrium.*

Grasp Stability

The grasp G is stable if and only if the potential function $U(x, y, \theta)$ of G reaches a local minimum. We can write the Taylor expansion of the potential function $U(x, y, \theta)$ about the equilibrium as follows:

$$U(x, y, \theta) = \sum_{i=1}^n \frac{1}{2} k_i \sigma_{i0}^2 + \mathbf{x}^T \nabla U|_{(0,0,0)} + \frac{1}{2} \mathbf{x}^T H|_{(0,0,0)} \mathbf{x} + \dots \quad (3.5)$$

where $\mathbf{x} = (x, y, \theta)^T$, and $H|_{(0,0,0)}$ is the Hessian matrix of the potential function at the equilibrium grasp configuration. A multivariable function reaches a local minimum if 1) the first partial derivatives are all zero, and 2) the Hessian matrix of the second partial derivatives is positive definite. So:

Theorem 3.2 *A grasp G composed of n virtual springs is in stable equilibrium if both of the following hold:*

- The gradient $\nabla U|_{(0,0,0)}$ is zero.
- The Hessian matrix $H|_{(0,0,0)}$ of the potential function $U(x, y, \theta)$ is positive definite.

$$H_O = \begin{pmatrix} \frac{\partial^2 U}{\partial x^2} & \frac{\partial^2 U}{\partial x \partial y} & \frac{\partial^2 U}{\partial x \partial \theta} \\ \frac{\partial^2 U}{\partial y \partial x} & \frac{\partial^2 U}{\partial y^2} & \frac{\partial^2 U}{\partial y \partial \theta} \\ \frac{\partial^2 U}{\partial \theta \partial x} & \frac{\partial^2 U}{\partial \theta \partial y} & \frac{\partial^2 U}{\partial \theta^2} \end{pmatrix} \quad \text{at } (x, y, \theta) = (0, 0, 0) \quad (3.6)$$

$$= \begin{pmatrix} \sum k_i \cos^2 \alpha_i & \sum k_i \sin \alpha_i \cos \alpha_i & \sum k_i \mu_i \cos \alpha_i \\ \sum k_i \sin \alpha_i \cos \alpha_i & \sum k_i \sin^2 \alpha_i & \sum k_i \mu_i \sin \alpha_i \\ \sum k_i \mu_i \cos \alpha_i & \sum k_i \mu_i \sin \alpha_i & \sum k_i \mu_i^2 + \sum f_{i0} d_i \end{pmatrix}$$

$U(x, y, \theta)$ is the potential function of grasp G , where (x, y, θ) is the displacement of the object from its equilibrium configuration.

3.2.2 Compliance about Stable Equilibrium

The restoring wrench $\hat{\mathbf{w}}$ applied on the grasped object is equal to the negative of the gradient of $U(x, y, \theta)$. Assuming that the disturbances of the grasped object from

its stable equilibrium are small, we deduce from the Taylor expansion of $U(x, y, \theta)$ that:

$$\begin{aligned}\dot{\mathbf{w}} &= -\nabla U(x, y, \theta) \\ &= -\nabla U|_{(0,0,0)} - H|_{(0,0,0)} \mathbf{x} - \dots \\ &\approx -H|_{(0,0,0)} \begin{bmatrix} d_x \\ d_y \\ \delta_z \end{bmatrix}\end{aligned}\quad (3.7)$$

The compliance behavior of the grasped object about its stable equilibrium is described by a stiffness matrix which is equal to the Hessian matrix.

The above approximation is good for displacements in orientation δ_z less than 10 degrees, and for linear displacements (d_x, d_y) in the xy -plane less than one tenth of the size of the grasped object. The size of the object is defined as the diameter of the minimum circle that contains the object inside it. The twist displacement $\hat{\mathbf{t}}$ is written as $\hat{\mathbf{t}} = (\delta_z, d_x, d_y)^T$ instead of $\hat{\mathbf{t}} = (\theta, x, y)^T$ to remind us of the small displacement assumption.

The stiffness matrix of the grasp is more sensitive to errors in orientation than location. The reason is that the stiffness normal to the edge of contact varies drastically as we rotate the object close to 90 degrees. We might no longer have restoring wrench in the correct direction, and the grasp might no longer be force-closure. If there is no error in orientation, then the restoring force opposite to a linear displacement always exists regardless of the amount of displacement. The restoring force is nothing more than the non-null sum of the contact forces generated by the springs.

Stiffness Matrix of the Grasp

The stiffness matrix K of the grasp is equal to the Hessian matrix H_O about the stable equilibrium of the grasped object. The stiffness matrix K can be written as a sum of two matrices:

$$\begin{aligned}K &= K_S + K_P \\ K_S &= S \mathcal{K} S^T \\ &= \begin{pmatrix} C_1 & \cdots & C_n \\ S_1 & \cdots & S_n \\ \mu_1 & \cdots & \mu_n \end{pmatrix} \begin{pmatrix} k_1 & & \\ & \ddots & \\ & & k_n \end{pmatrix} \begin{pmatrix} C_1 & S_1 & \mu_1 \\ \vdots & \vdots & \vdots \\ C_n & S_n & \mu_n \end{pmatrix} \\ K_P &= \sum_{i=1}^n k_i \sigma_{i0} d_i \begin{pmatrix} 0 & 0 & 0 \\ 0 & 0 & 0 \\ 0 & 0 & 1 \end{pmatrix}\end{aligned}\quad (3.8)$$

The first matrix K_S is a product of three matrices $S \mathcal{K} S^T$. S is an $3 \times n$ rectangular matrix, whose columns are the spatial vectors of the linear springs. The matrix S is called the *spatial configuration matrix* of the linear springs. \mathcal{K} is

an $n \times n$ diagonal matrix with positive stiffnesses of the springs on its diagonal. The product SKS^T is positive definite if and only if S has full row, or equivalently, there are three linear springs with independent spatial vectors.

The second matrix K_P depends on the positions of the points of contact, and on the contact forces. K_P affects only the angular stiffness of the grasp. If the contact forces are small, or more concisely, if the compressions $\sigma_{i,0}$ are small relative to the size of the object, then $\sum k_i \sigma_{i,0} d_i$ is small compared to $\sum k_i \mu_i^2$. The stiffness matrix K of the grasp is approximatively equal to K_S , which comes from the spatial configuration of the linear springs acting on the grasped object.

A force closure grasp implies that the set of contact wrenches spans the whole wrench space. If each contact wrench is generated by a linear spring, then the set of linear springs has spatial vectors that span the whole vector space. The spatial configuration matrix of the linear springs S has full row, and K_S is positive definite. The compressions $\sigma_{i,0}$ can be chosen small compared to the size of the grasped object. The stiffness matrix K of the grasp is approximatively equal to K_S , and is therefore positive definite. In other words, a force-closure grasp implies a stable grasp exists.

Corollary 3.2 *If grasp G is force closure, then we can always synthesize a set of linear springs at the points of contact, such that G is in stable equilibrium.*

The stiffness matrix K is symmetric, and so has three perpendicular eigenvectors. If the stiffness matrix K is positive definite, then it has three strictly positive eigenvalues. The grasped object has three equivalent springs with spatial vectors equal to the eigenvectors, and stiffness constants equal to the eigenvalues.

The center of compliance of a planar grasp is the point about which a pure rotation of the object is resisted by a pure torque. More precisely, the center of compliance is the reference point, about which the stiffness matrix K is diagonalized into two blocks:

$$K = H|_{(0,0,0)} = \begin{pmatrix} \sum k_i \cos^2 \alpha_i & \sum k_i \sin \alpha_i \cos \alpha_i & 0 \\ \sum k_i \sin \alpha_i \cos \alpha_i & \sum k_i \sin^2 \alpha_i & 0 \\ 0 & 0 & \sum k_i (\mu_i^2 + \sigma_{i,0} d_i) \end{pmatrix} \quad (3.9)$$

Note that the angular displacement is decoupled from the two linear displacements of the object. The grasped object behaves as though there are three independent springs attached to it. Figure 3.3.

- Two linear springs with respective stiffness k_a , k_b , along two perpendicular axes in the grasping plane of the object. The stiffnesses and directions of these two linear springs are respectively the eigenvalues and the eigenvectors of the following 2×2 symmetric matrix:

$$K_{xy} = \begin{pmatrix} \sum k_i \cos^2 \alpha_i & \sum k_i \sin \alpha_i \cos \alpha_i \\ \sum k_i \sin \alpha_i \cos \alpha_i & \sum k_i \sin^2 \alpha_i \end{pmatrix} \quad (3.10)$$

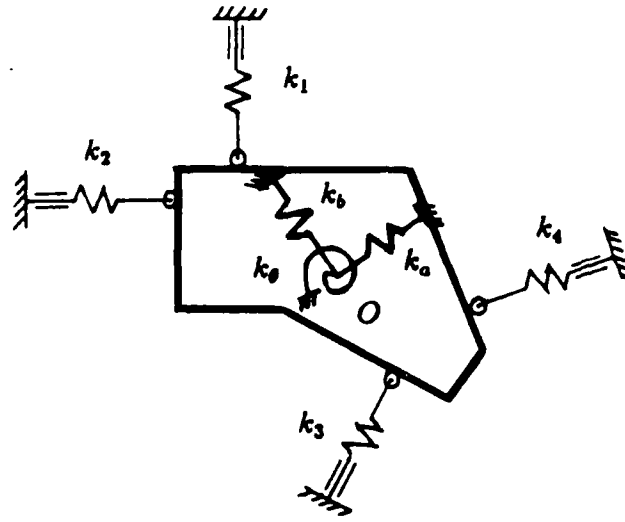


Figure 3.3: Compliance of the grasped object about its stable equilibrium.

- An angular spring with stiffness k_θ , and axis perpendicular to the grasping plane and going through the center of compliance O of the object.

$$k_\theta = \sum_{i=1}^n k_i (\mu_i^2 + \sigma_{i,o} d_i) \quad (3.11)$$

The matrix K_{zy} is nothing more than the sum of the linear stiffness matrices of the individual springs expressed in the global frame of the hand:

$$\begin{aligned} K_{zy} &= \begin{pmatrix} C_1 & \cdots & C_n \\ S_1 & \cdots & S_n \end{pmatrix} \begin{pmatrix} k_1 & & \\ & \ddots & \\ & & k_n \end{pmatrix} \begin{pmatrix} C_1 & S_1 \\ \vdots & \vdots \\ C_n & S_n \end{pmatrix} \\ &= \sum_{i=1}^n \text{Rot}(\alpha_i) \begin{pmatrix} k_i & 0 \\ 0 & 0 \end{pmatrix} \text{Rot}(-\alpha_i) \end{aligned}$$

where $\text{Rot}(\alpha_i)$ is the rotation from the base reference frame to the local frame at the fingertip.

The angular effects of these linear springs add up into the first sum of the angular stiffness k_θ :

$$k_\theta = \sum_{i=1}^n k_i \mu_i^2 + \sum_{i=1}^n f_{i,o} d_i$$

This angular effect depends on the moments of the lines of action of the springs about the center of rotation O .

The second sum comes from K_P . This sum comes from the second order variation of the compressions as the object rotates, $\partial^2 \sigma_i / \partial \theta^2$. A more general expression of the position-dependent stiffness matrix K_P is:

$$K_P = \pm \sum_{i=1}^n f_{i0} (\mathbf{p}_i \cdot \mathbf{k}_i) \begin{pmatrix} 0 & 0 & 0 \\ 0 & 0 & 0 \\ 0 & 0 & 1 \end{pmatrix} \quad (3.12)$$

The sign is + (resp. -) if the fingers slide (resp. stick) on the grasping edges. The reader is referred to Appendix A.3 for a similar derivation of the stiffness matrix, when the fingers stick on the grasping edges. The assumption is that the energy stored in the grasp is conserved. So, if there is friction, then the contact points must not move, so that there is no loss of potential energy. The next chapter will present a qualitative analysis of grasp stability when there is slip with friction.

Compliance Center of the Grasp

The stiffness matrix K is diagonalizable with independent linear and angular springs if and only if:

$$\sum_{i=1}^n \mu_i k_i \mathbf{k}_i = \sum_{i=1}^n |\mu_i k_i| (\text{sign}(\mu_i) \mathbf{k}_i) = \mathbf{0} \quad (3.13)$$

When can we find a set of positive spring constants (k_1, \dots, k_n) such that the above equation holds? The equation looks very much like the force-closure condition in the plane, except that we deal with only force directions. It can always be satisfied if the vectors $\{\text{sign}(\mu_i) \mathbf{k}_i\}$ span the space of all directions in the plane. The sign of the moment μ_i depends on the position of the compliance center with respect to the line of action of the virtual springs. This means that the compliance center must be inside some polygon delimited by the lines of action of the virtual springs. This polygon is called the *compliance polygon* of the grasp. Figure 3.4 shows the compliance polygon Ω_G within which the compliance center of grasp G must be. Note that the compliance polygon can cover the whole plane if there are more than four linear springs.

We now prove that if the grasp is force-closure then the compliance polygon always exists, and so equation (3.13) can be satisfied. Note that if grasp G is force-closure then the two cones generated by $(-\mathbf{k}_1, -\mathbf{k}_2)$ and $(-\mathbf{k}_3, -\mathbf{k}_4)$ counter-overlap in a non-zero convex polygon C_G , Figure 3.5. If we pick the compliance center O inside this convex polygon, then the springs k_1 and k_3 , resp. k_2 and k_4 , have negative, resp. positive, moments about O . One can check that there exists a positive linear combination of $\mathbf{k}_1, \mathbf{k}_2, \mathbf{k}_3, \mathbf{k}_4$ such that one walks counter-clockwise along the boundary of the convex polygon bounded by the lines of action of the springs. Equation (3.13) holds, and so the compliance polygon is always non null for force-closure grasps.

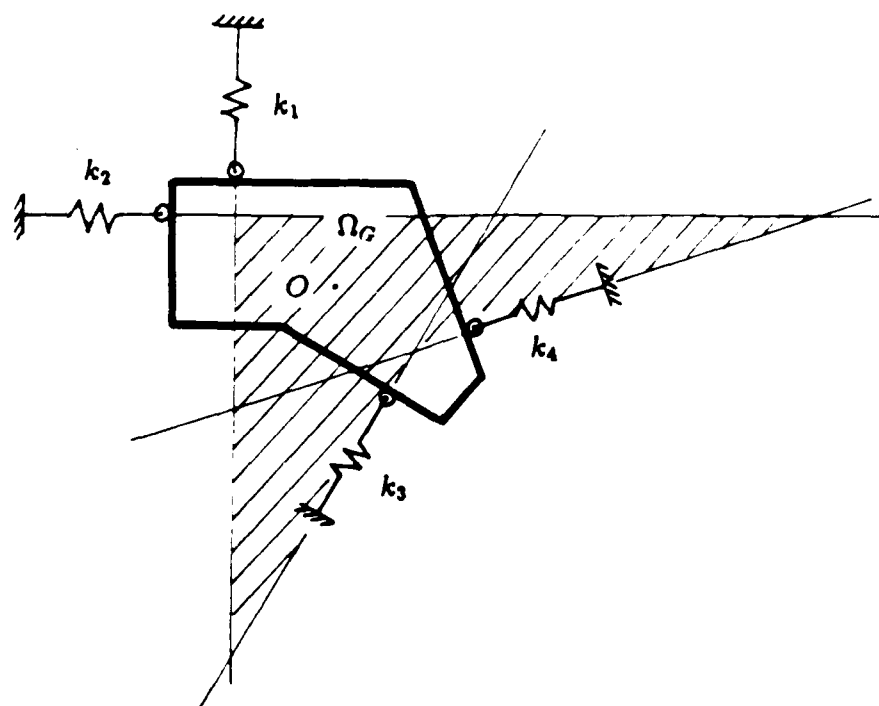


Figure 3.4: Compliance polygon of a grasp.

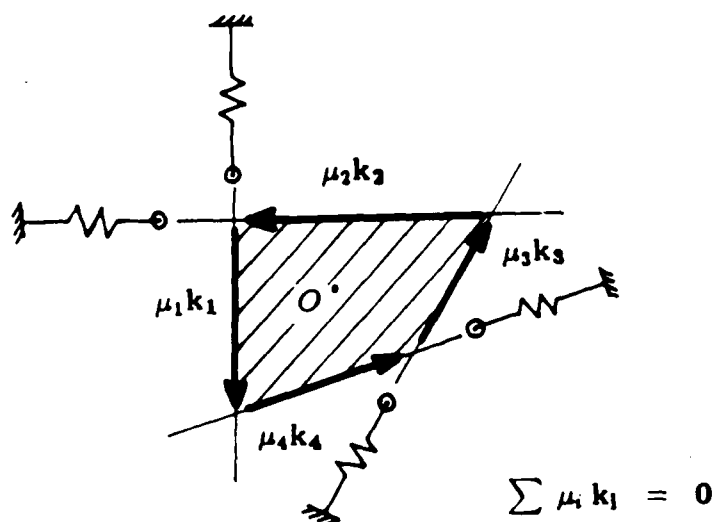


Figure 3.5: Compliance polygon always exists for force-closure grasps.

Corollary 3.3 *If grasp G is force-closure then:*

- *The compliance polygon of grasp G , denoted Ω_G , is non empty. The compliance polygon Ω_G has boundary supports the lines of action of the springs.*
- *The convex polygon C_G bounded by the lines of action of the springs is included in the compliance polygon Ω_G .*
- *If we pick the compliance center O of grasp G within the polygon Ω_G , then there always exists a set of spring constants k_1, \dots, k_n such that the stiffness matrix of grasp G is diagonalizable into linear and angular stiffness blocks.*

We prefer to pick the compliance center within the convex polygon C_G so that the spring constants are more or less equal. Within this polygon, the desired location of the compliance center O in the global frame depends on the task at hand. For example, to insert a peg into a hole, we ideally want to put the center of compliance at the mouth of the hole (Whitney 1982). Note that force-closure with frictionless contacts requires putting fingers on all four sides of the peg, which is infeasible! Luckily we can have force-closure with two point contacts with friction, and so we can grasp at the top of the peg and at the same time have a compliance center at the mouth of the hole, Figure 3.7. We achieve the same effect as the RCC gripper. But, with an active compliance hand, we have more flexibility in choosing the compliance center and the stiffness matrix of the grasp. We can achieve both a stable grasp and a desired compliant behavior of the grasped object during assembly.

Outside-in/Inside-out Grasps

To have restoring couples in the correct direction, the angular stiffness k_θ of grasp G must be strictly positive:

$$k_\theta = \sum_{i=1}^n k_i \mu_i^2 \pm \sum_{i=1}^n f_i d_i$$

The sign is + (resp. -) if the fingers slide (resp. stick) on the grasping edges. The first sum in the above expression depends on the placement of the compliance center inside the compliance polygon Ω_G . This sum is positive and increases as the compliance center moves to the boundary of Ω_G . The second sum is invariant with the location of the compliance center. It depends only on the contact forces and the relative configuration of the contacting edges.

How can we have positive angular stiffness k_θ ? First, if the distances d_i are all strictly positive, then the angular stiffness k_θ is also strictly positive. The line of support of an edge e_i divides the plane into two half-planes: interior or exterior respectively if the distance $d_i = \mathbf{p} \cdot \mathbf{n}_i$ is negative or positive. This observation leads to a classification of grasp configurations into three categories defined as follows:

- A grasp G is called an *outside-in* grasp if and only if the interior half planes of the contacting edges of G intersect.
- A grasp G is called an *inside-out* grasp if and only if the exterior half planes of the contacting edges of G intersect.

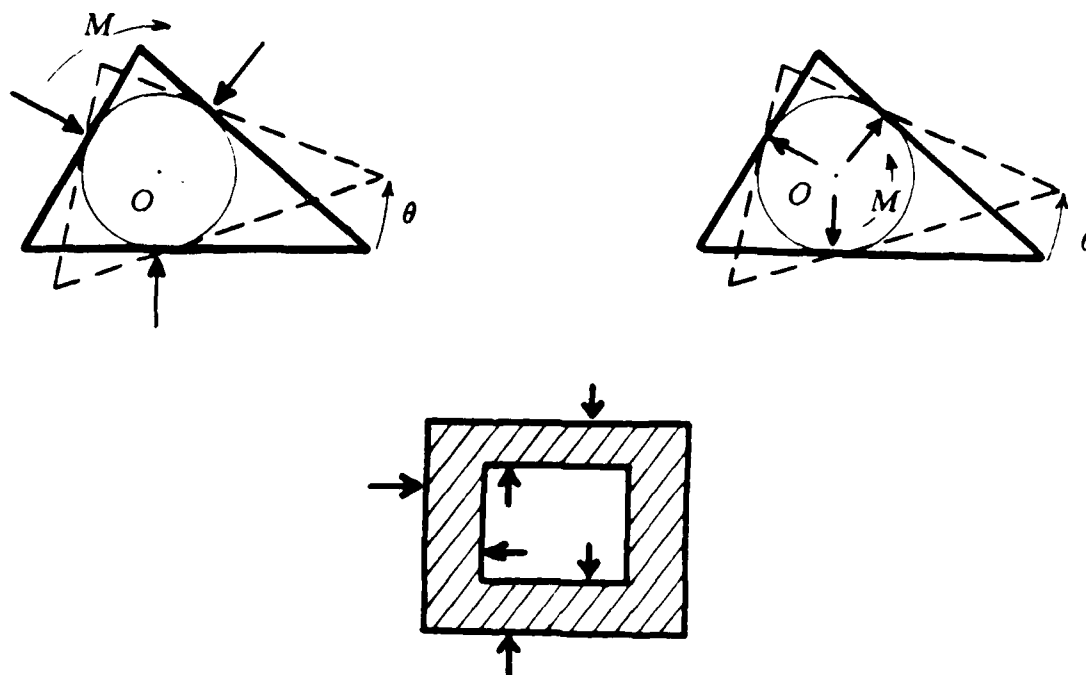


Figure 3.6: Outside-in / inside-out / mixed grasps.

- A grasp G is called a *mixed* grasp if and only if neither the interior half planes nor the exterior half planes intersect.

Grasps on the boundary of convex objects are examples of outside-in grasps. Grasps on the boundary of convex holes are examples of inside-out grasps. If a grasp G has exactly the minimum number of contacts required for force-closure, then grasp G is either outside-in or inside-out grasp. Mixed grasps come up only when there are more contacts than the minimum of two for point contacts with friction, and four for point contacts without friction, Figure 3.6.

From the expression of the angular stiffness k_θ , we see that it is always strictly positive for outside-in grasps. We can prove this by noting that the second sum is invariant to the position of the origin, so we can pick the origin to be in the intersection of the closed half planes, and have all the distances d_i positive. Baker, Fortune, and Grosse (1985) showed that outside-in grasps are stable if the springs contact at places where the inscribed circle is tangent to the grasping edges. No search is needed, the grasps are found in $O(n \log n)$ time by computing the Voronoi diagram of the polygonal object (Shamos 1978).

The angular stiffness k_θ may be negative for inside-out, and mixed grasps. Figure 3.6 shows two frictionless grasps on a same triangular ring. One would suspect that the two grasps on the triangular ring have the same behavior. But surprisingly, one finds that the outside-in grasp is stable, while the inside-out grasp is unstable relative to rotations.

Luckily, with force-closure grasps, we have another positive term in the expression of k_θ , which depends on the moments of the springs about the center of compliance. By scaling up the set of spring constants while keeping constant the set of contact forces, we can make the first sum greater than the second sum, and have k_θ strictly positive. This is possible only if the moments μ_i are not all zero, which means that the lines of action of the virtual springs do not all pass through the compliance center. A sufficient condition is again the force-closure condition.

Corollary 3.4 *A frictionless grasp G can be made stable relative to rotations if either of the following is true:*

- *Grasp G is an outside-in grasp.*
- *Grasp G is force closure.*

In conclusion, for the same set of grasp points, outside-in grasps are more stable for rotations than inside-out grasps, if there is no friction between the fingers and the object. The reverse holds if there is friction at the points of contact.

3.2.3 Finding Virtual Springs at the Fingertips

Synthesize a Compliant Grasp

We can not only make a force closure grasp stable, but also synthesize a compliance center for the grasp:

Corollary 3.5 *Let G be a planar grasp with n fingers, each is a linear spring with arbitrary finite stiffness k_i and compression σ_{i0} . If grasp G is force-closure then we can always synthesize a set of n linear springs such that grasp G is stable and has a compliance center O inside the compliance polygon Ω_G .*

The compliance center O must be inside the compliance polygon Ω_G , defined by the lines of action of the linear springs, or the normals and points of contact in a frictionless grasp. So, without friction, a choice of a compliance center implies a choice of the placement of the points of contact. Pin and hole insertion cannot be done without friction, because the four points of contact must be on all four sides of the pin.

For point contacts with friction, Figure 3.7 shows an interesting comparison between compliant fingertips that have passive and active stiffness. Examples of passive stiffness are real physical springs, like fingertips covered with rubber, or the Remote Center Compliance. With two fingers covered with rubber, the compliance center is not only fixed, but can only be inside a compliance rectangle with two diagonal corners at the two points of contact. The rectangle comes from the normal and tangential springs which model the rubber at the points of contact. The Remote Center of Compliance is a wrist built with fixed passive springs. The springs are designed such that the center of compliance is at the tip of the pin.

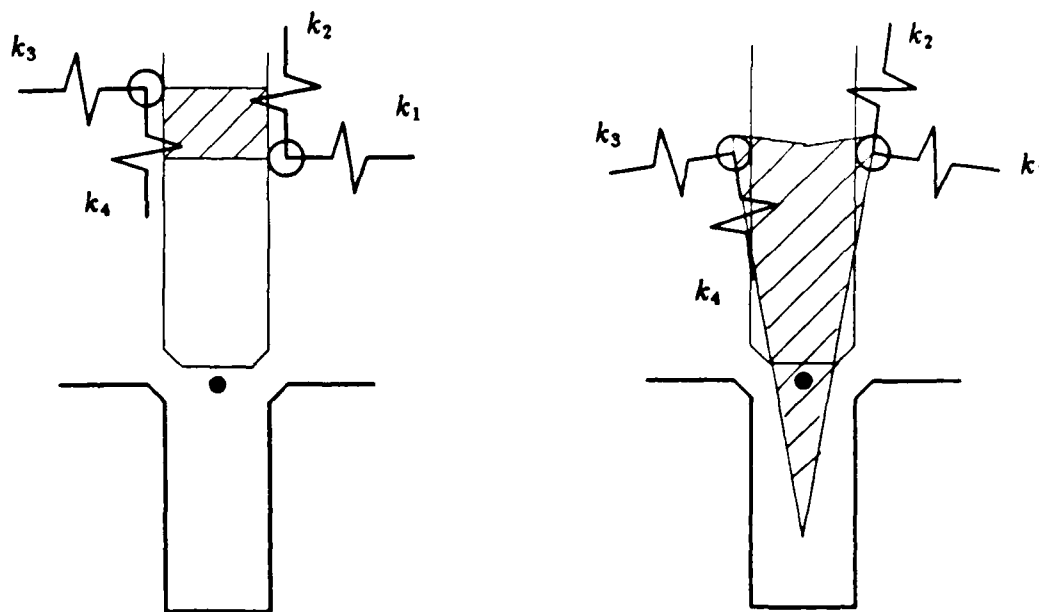


Figure 3.7: Pin and hole insertion with passive and active stiffness.

Active stiffness comes from stiffness control at the fingertips or at the joints. If the fingers have active compliance, then the virtual springs at the fingertips can be oriented such that the compliance polygon overlaps the desired compliance center. So, with friction, a choice of a compliance center implies a choice of the orientation of the virtual springs at the given points of contact.

Algorithm 3.1 *Let G be a force-closure grasp with a desired compliance center O inside the compliance polygon Ω_G , defined by the lines of action of the n virtual springs. The n virtual springs at the points of contact can be synthesized so that G is stable as follows:*

1. *Find a set of contact forces (f_{1o}, \dots, f_{no}) such that force equilibrium is achieved. This is equivalent to solving a system of six equations with n unknowns.*
2. *From the desired compliance center O , find a set of positive spring constants (k_1, \dots, k_n) such that:*

$$\sum_{i=1}^n \mu_i k_i \mathbf{k}_i = \mathbf{0}$$

where \mathbf{k}_i and μ_i are respectively the direction and moment of the virtual spring k_i about the compliance center O . This is solving a system of two equations in n unknowns.

3. Check that the angular stiffness k_θ of grasp G is strictly positive:

$$k_\theta = \sum_{i=1}^n k_i (\mu_i^2 + \sigma_{i0} d_i)$$

If not scale up the set of spring constants (k_1, \dots, k_n) and reduce the set of compressions $(\sigma_{10}, \dots, \sigma_{n0})$, keeping the set of contact forces (f_{10}, \dots, f_{n0}) unchanged, until k_θ is greater than zero.

4. Find the virtual compressions at equilibrium:

$$\sigma_{i0} = \frac{1}{k_i} f_{i0}$$

5. Output the set of spring constants (k_1, \dots, k_n) , and the respective set of compressions $(\sigma_{10}, \dots, \sigma_{n0})$ such that each finger F_i behaves as a virtual spring as follows:

$$\mathbf{f}_i = \begin{bmatrix} f_{in} \\ f_{it} \end{bmatrix} = \begin{pmatrix} k_i & 0 \\ 0 & 0 \end{pmatrix} \begin{bmatrix} \sigma_{i0} - \sigma_i \\ 0 - \tau_i \end{bmatrix}$$

where \mathbf{f}_i is the force applied by the fingertip F_i on the grasped object, and $(\sigma_i, \tau_i)^T$ is the displacement of the finger normal and tangential to the i th contacting edge.

Using Gauss row elimination, a system of m equations in n unknowns can be solved in $(\min(n, m) \times n \times m)$ time. So, steps 1 and 2 can be solved in $O(n)$ time, where n is the number of linear springs. The other steps cost $O(n)$ time each.

Complexity 3.1 A force-closure grasp G with a desired compliance center O inside the compliance polygon Ω_G can be made stable in $O(n)$ time.

The four virtual springs of a 2D grasp are typically computed in about 0.2 seconds on a Symbolics machine.

Controlling a Compliant Grasp

Figure 3.8 shows the relationships between force and instantaneous displacement at three different levels:

- At the grasped object, we want to choose a compliance center and a stiffness matrix for grasp G such that the grasped object is stable and have restoring wrenches as follows

$$\mathcal{F} = -K_G d\lambda$$

- From the desired compliance at the grasped object, we would like to deduce the corresponding set of spring constants and compressions at the fingertips:

$$F = -K_f dx$$

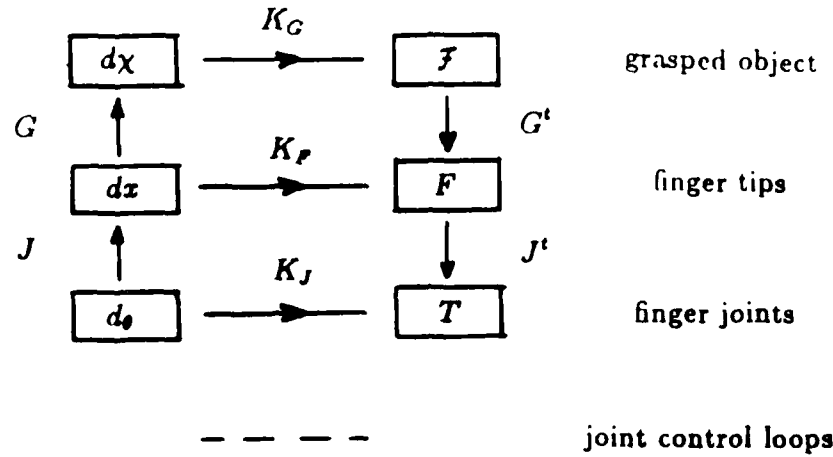


Figure 3.8: Linked chains and their loop equations.

- From the virtual springs at the fingertips, we then would like to derive the stiffness at all of its joints:

$$T = K_J d\theta$$

We can go further and derive the gains in the control loop of each joint, such that the above joint compliance is enforced. Or we can assume that each joint has a stiffness control loop with programmable stiffness.

From the kinematics of the grasp, the external and internal forces applied at the grasped object relate with the fingertip forces by the grasp matrix G^{-T} (Salisbury 1980, Salisbury and Craig 1981, Salisbury 1982). Similarly, from the kinematics of the linked fingers, the force and velocity at each fingertip relate with its corresponding joint torques and velocities by the Jacobian matrices J^{-T} and J . We get loops from which we can derive easily the stiffness matrix of one level in terms of the stiffness matrix of another level. For example, given the desired compliance K_G at the grasped object, we deduce:

$$\begin{aligned} K_F &= G^T K_G G \\ K_J &= J^T G^T K_G G J \end{aligned} \quad (3.14)$$

The mapping between the object forces and fingertip forces can be done as a matrix multiplication, as a solution to a system of equations, or as a vector decomposition along independent vectors (Hollerbach and Narasimhan 1986). Similarly, for the mapping between the fingertip forces and the joint torques

The execution of frictionless grasps is greatly simplified and a lot less sensitive to errors, because of the existence of stable configurations. Knowing that a stable grasp exists on a set of edges, we can just grasp near the desired stable grasp points with the computed virtual springs, and let the fingers adjust themselves on these edges until they end up on the planned grasp points. Each finger can be servoed independently, and so the execution of a grasp is fast. Any oscillation will hopefully be damped by the mechanical damping in the fingers and some nominal damping in the joint control loops.

The planning and execution of assembly operations is also greatly simplified and a lot less sensitive to errors, because we can choose the center of compliance and the stiffness matrix. Instead of planning for explicit force and trajectory, we plan for a compliant behavior of the parts respective to each other. For example, to do peg and hole insertion, we need to stably grasp the peg, put the compliance center at the mouth of the hole, and push the peg into the hole. The values of the virtual springs can be automatically computed from the shape of the peg and hole. A dextrous hand with active compliance is therefore more flexible than the RCC gripper, (Whitney 1982).

Comparison with Grip Matrix

The grip matrix G^{-T} is an $n \times n$ matrix which relates the n external and internal forces applied at the grasped object to the n fingertip forces. K_G is an $n \times n$ generalized stiffness matrix at the grasped object which has the 6 linear and angular stiffnesses plus $n - 6$ internal stiffnesses. K_F is an $n \times n$ matrix which describes the springs at the fingertips, expressed in frames local to the points of contact. From the conservation of equivalent work at the object and at the fingertips, Salisbury and Craig deduced:

$$K_G = G^{-T} K_F G^{-1} \quad (3.15)$$

The grip matrix G^{-T} has a $6 \times n$ block which is nothing more than the configuration matrix S . Note that S relates only the 6 external forces and moments at the grasped object to the n fingertip forces at the n springs. G^{-T} and S both capture the spatial configuration of the finger tip springs. The 6×6 stiffness matrix at the grasped object K , is a block of the generalized stiffness matrix K_G . The stiffness matrix K describes only the 6 linear and angular stiffnesses of the grasped object. We have shown that the stiffness matrix K of the grasped object is the sum of two matrices K_s and K_p :

$$\begin{aligned} K &= K_s + K_p \\ K_s &= S K S^T \end{aligned} \quad (3.16)$$

$K_s = K$ if the local frames at the points of contact are oriented with the linear springs at the fingertips. So the grip matrix G^{-T} and the configuration matrix S both are only a first order approximation of the linkages between the grasped object and the fingertips. S is first order because its columns are spatial vectors \mathbf{k}_i which come from $\nabla \sigma$.

The second order approximation of the linkages between the grasped object and fingertips shows up as a position-dependent stiffness matrix K_P , which comes from the terms $\partial^2 \sigma_i / \partial \theta^2$. Our derivation of the stiffness matrix, Equations (3.8) and (3.12) is more accurate. The stiffnesses at the grasped object and at the fingertips are related not only by the conservation of total energy in the system, but also by the geometry about the grasp points. The geometry here is the point contacts which either stick or slide without friction on straight edges.

3.3 Stable Grasps in 3D

The 3D contacts between the fingertips and the grasped object are modeled as frictionless point contacts, hard-finger contacts, or soft-finger contacts with friction. Each contact is modeled as a virtual spring, which in turn is a set of independent linear and angular springs. The stiffness of the grasp comes from the combination of all these independent springs.

A frictionless point contact has one linear spring, having direction the normal to the surface of contact, and going through the point of contact. A hard-finger contact has three linear springs, all going through the point of contact, and oriented along the normal and the two tangential directions of the surface of contact. A soft-finger contact has in addition an angular spring, with axis going through the point of contact, and oriented along the normal of the surface of contact.

The framework of stable grasps with independent linear springs in 2D generalizes to 3D. To a first order approximation, linear and angular springs can be described by their stiffness constants and spatial vectors. The spatial vector of a spring describes the line of action of the wrench exerted by this spring on the object. It is a line vector for a linear spring, and a free vector for an angular spring.

I will first derive the change in compression at the linear and angular springs, when the object is moved away from its equilibrium. The potential function of the grasp is the sum of the potential functions at all the linear and angular springs. From the potential function of the grasp, I deduce the conditions for equilibrium and stability, and the compliant behavior of the grasped object. In the 2D analysis, I have assumed that the fingers slip without friction on the object. For variety, the 3D analysis assumes that the fingers stick at their points of contact. As before, we'll see that the two cases, with the fingers sticking or slipping without friction, differ only by a sign in the position-dependent stiffness matrix K_P .

3.3.1 Ideal Independent Springs

Linear Spring Model

A linear spring k_i is characterized by its stiffness constant k_i , its direction \mathbf{k}_i , oriented with the normal of the surface of contact, and its tips P_i . Figure 3.9. As the grasped object is displaced by an infinitesimal twist $\hat{\mathbf{t}} = (\delta^T, \mathbf{d}^T)^T$, the point of contact P_i is moved to its new location P'_i given by:

$$\mathbf{p}'_i = \text{Rot}(\delta_x, \delta_y, \delta_z) \mathbf{p}_i + \mathbf{d} \quad (3.17)$$

The rotation $\text{Rot}(\delta_x, \delta_y, \delta_z)$ cannot be described as a Roll-Pitch-Yaw rotation matrix, because Roll-Pitch-Yaw matrices have different high order terms with different orderings of the three rotations: $\text{Roll}(z, \delta_x)$, $\text{Pitch}(y, \delta_y)$, and $\text{Yaw}(x, \delta_z)$. To get a rotation matrix that is order independent, I compute the equivalent angle and axis of rotation, and from these, deduce the rotation matrix (Paul 1981). The equivalent angle of rotation is the magnitude of the rotation vector δ . The equivalent axis of

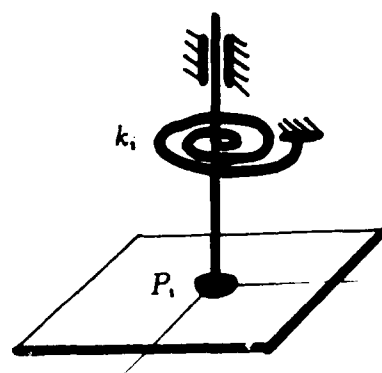
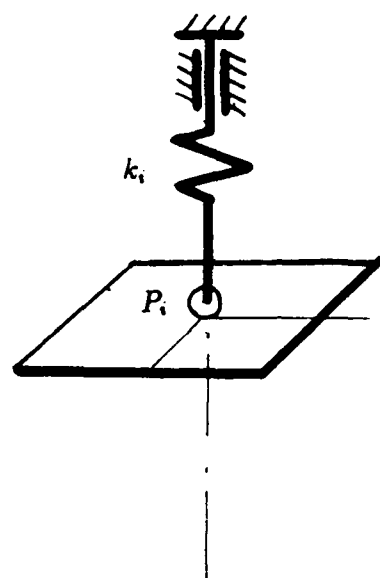


Figure 3.9: Models for linear and angular springs in 3D.

rotation is the normalized vector from δ . The angular stiffness matrix of the grasp has second order partial derivatives in the angles $\delta_x, \delta_y, \delta_z$. So, the rotation matrix must be at least expanded to second order terms. Assuming infinitesimal rotations, the Taylor expansion up to second order terms of the rotation matrix is:

$$\begin{aligned} Rot(\delta_x, \delta_y, \delta_z) &\approx \begin{pmatrix} 1 & 0 & 0 \\ 0 & 1 & 0 \\ 0 & 0 & 1 \end{pmatrix} + \begin{pmatrix} 0 & -\delta_z & \delta_y \\ \delta_z & 0 & -\delta_x \\ -\delta_y & \delta_x & 0 \end{pmatrix} \\ &\quad + \frac{1}{2} \begin{pmatrix} -(\delta_y^2 + \delta_z^2) & \delta_x \delta_y & \delta_x \delta_z \\ \delta_x \delta_y & -(\delta_x^2 + \delta_z^2) & \delta_y \delta_z \\ \delta_x \delta_z & \delta_y \delta_z & -(\delta_x^2 + \delta_y^2) \end{pmatrix} \quad (3.18) \\ &\approx I + [\delta \times] + \frac{1}{2} ((\delta \delta^T) - (\delta \cdot \delta) I) \end{aligned}$$

The matrix of first order terms is an anti-symmetric matrix $[\delta \times]$, describing the cross-product with the rotation vector δ . The matrix of second order terms can be written as a difference of two matrices. The first matrix is the dyadic product, or outer product, of the rotation vector δ with itself, $(\delta \delta^T)$. The dyadic product³ of two vectors is the matrix obtained from multiplying the first vector with the transpose of the second vector. The second matrix is a diagonal matrix with the dot-product of the rotation vector with itself, $(\delta \cdot \delta)$, on the diagonal.

A linear spring k_i exerts a pure force on the object, if and only if its tip P_i is displaced along the direction \mathbf{k}_i . Displacements perpendicular to \mathbf{k}_i , and rotations about point P_i have no effect on the spring k_i . So the effective compression σ_i at a linear spring k_i due to a twist $\hat{\mathbf{t}} = (\delta^T, \mathbf{d}^T)^T$ of the object is:

$$\begin{aligned} \sigma_i &= \sigma_{i0} + \mathbf{k}_i \cdot (\mathbf{p}_i' - \mathbf{p}_i) \\ &\approx \sigma_{i0} + \mathbf{k}_i \cdot (\delta \times \mathbf{p}_i) + \mathbf{k}_i \cdot \mathbf{d} + \frac{1}{2} \mathbf{k}_i \cdot [(\delta \delta^T) - (\delta \cdot \delta) I] \mathbf{p}_i \\ &\approx \sigma_{i0} + \begin{bmatrix} \mathbf{k}_i \\ \mathbf{p}_i \times \mathbf{k}_i \end{bmatrix} : \begin{bmatrix} \delta \\ \mathbf{d} \end{bmatrix} \\ &\quad + \frac{1}{2} \begin{bmatrix} k_{ix} & k_{iy} & k_{iz} \end{bmatrix} ((\delta \delta^T) - (\delta \cdot \delta) I) \begin{bmatrix} p_{ix} \\ p_{iy} \\ p_{iz} \end{bmatrix} \quad (3.19) \end{aligned}$$

The first order term is the spatial dot product of the line vector $\hat{\mathbf{k}}_i$, representing the line of action of spring k_i , and the twist displacement $\hat{\mathbf{t}}$ of the object. So, to a first order approximation, the spatial vector $\hat{\mathbf{k}}_i = (\mathbf{k}_i^T, (\mathbf{p}_i \times \mathbf{k}_i)^T)^T$ describes the configuration of the linear spring k_i . The second order term depends on the position of the finger tip P_i , which by assumption, does not slip during the rotation. We'll

³The dyadic product is different from its dot-product analogue, whose result is a scalar, not a matrix. The dot-product of two vectors is the matrix multiplication of the transpose of the first vector with the second vector.

see that this term leads to a position-dependent term in the angular stiffness matrix of the grasp.

The linear spring k_i resists a twist displacement of the object with a pure force along the line of action of the spring, or with a wrench along the spatial vector $\hat{\mathbf{k}}_i$:

$$\hat{\mathbf{w}}_i = -k_i \sigma_i \hat{\mathbf{k}}_i \quad (3.20)$$

We'll see next that angular springs are described by free vectors, and they obey the same framework as linear springs.

Lemma 3.1 *To a first order approximation, a linear spring is represented by its stiffness k_i and its spatial vector $\hat{\mathbf{k}}_i$. The spatial vector $\hat{\mathbf{k}}_i$ describes the line of force of the linear spring:*

$$\hat{\mathbf{k}}_i = \begin{bmatrix} \mathbf{k}_i \\ \mathbf{p}_i \times \mathbf{k}_i \end{bmatrix} \quad (3.21)$$

\mathbf{p}_i is the position of the point of contact, and \mathbf{k}_i is the direction of the linear spring.

Angular Spring Model

A soft-finger contact can also resist rotations of the object about the axis passing through the point of contact, and oriented with the normal at the surface of contact. This resistance to rotations is captured with an angular spring having stiffness k_i , axis direction \mathbf{k}_i , and point of contact P_i . The axis direction \mathbf{k}_i is oriented with the normal to the surface of contact.

Let twist $\hat{\mathbf{t}} = (\delta^T, \mathbf{d}^T)^T$ be the small displacement of the object computed relative to a fixed origin O . When computed relative to the point of contact P_i , a twist has the same angular part, but a different linear part:

$$\begin{aligned} \hat{\mathbf{t}}_{P_i} &= \hat{\mathbf{t}}_O + \begin{bmatrix} \mathbf{0} \\ (\mathbf{p}_O - \mathbf{p}_i) \times \delta \end{bmatrix} \\ &= \begin{bmatrix} \delta \\ \mathbf{d} - (\mathbf{p}_i \times \delta) \end{bmatrix} \end{aligned} \quad (3.22)$$

So the twist seen at the point of contact P_i has rotation vector δ and translation vector $\mathbf{d} - (\mathbf{p}_i \times \delta)$.

The translation of the point of contact P_i has no effect on the angular spring, which counteracts only rotations along direction \mathbf{k}_i . The effective rotation seen by the angular spring k_i is the dot product of the rotation vector δ and the axis direction \mathbf{k}_i :

$$\begin{aligned} \sigma_i &= \mathbf{k}_i \cdot \delta \\ &= \begin{bmatrix} \mathbf{0} \\ \mathbf{k}_i \end{bmatrix} \cdot \begin{bmatrix} \mathbf{d} - (\mathbf{p}_i \times \delta) \\ \delta \end{bmatrix} \\ &= \hat{\mathbf{k}}_i \cdot \hat{\mathbf{t}} \end{aligned} \quad (3.23)$$

where $\hat{\mathbf{k}}_i = (\mathbf{0}^T, \mathbf{k}_i^T)^T$ is a free vector representing the angular spring k_i .

The resisting effect will be a pure torque with direction along the axis of the angular spring, or a wrench along the free vector $\hat{\mathbf{k}}_i$:

$$\hat{\mathbf{w}}_i = -k_i \sigma_i \hat{\mathbf{k}}_i \quad (3.24)$$

Lemma 3.2 *To a first order approximation, an angular spring is represented by its stiffness k_i and its spatial vector $\hat{\mathbf{k}}_i$. The spatial vector $\hat{\mathbf{k}}_i$ describes the direction of torque of the angular spring:*

$$\hat{\mathbf{k}}_i = \begin{bmatrix} \mathbf{0} \\ \mathbf{k}_i \end{bmatrix} \quad (3.25)$$

\mathbf{k}_i is the direction of the angular spring.

In a real finger, the stiffness of the angular spring varies as a function of the normal pressure at the finger contact. But for sake of simplicity, the angular stiffness is assumed constant. I also assume there is no slipping at the point of contact, and there is no coupling between the linear and angular springs. However, we'll see that nothing much is lost because of the simplifying assumptions. On the contrary, we obtain a simple and general framework that provides both a qualitative and a quantitative explanation to why and when grasps are stable.

3.3.2 Equilibrium and Stability Conditions

Potential Function of the Grasp

The potential function of the grasp is the sum of the potential functions from all the n linear and angular springs:

$$\begin{aligned} U &= \sum_{i=1}^n \frac{1}{2} k_i \sigma_i^2 \\ &= \frac{1}{2} [\sigma_1 \cdots \sigma_n] \begin{pmatrix} k_1 & & \\ & \ddots & \\ & & k_n \end{pmatrix} \begin{bmatrix} \sigma_1 \\ \vdots \\ \sigma_n \end{bmatrix} \end{aligned} \quad (3.26)$$

The Taylor expansion of the potential function U of the grasp about its equilibrium configuration can be written in a matrix form as follows:

$$U \approx \sum_{i=1}^n \frac{1}{2} k_i \sigma_{i0}^2 + \mathbf{x}^T \nabla U|_{\mathbf{x}=0} + \frac{1}{2} \mathbf{x}^T H|_{\mathbf{x}=0} \mathbf{x} \quad (3.27)$$

where $\mathbf{x} = \hat{\mathbf{t}}^S$ is the 6×1 spatial transpose of the displacement twist $\hat{\mathbf{t}}$. H is the Hessian matrix of second order partial derivatives.

Equilibrium and Force-Closure

A grasp is in equilibrium, if and only if the gradient of its potential function U is zero. From equations (3.19) and (3.26), the equilibrium condition can be written in a matrix form as follows:

$$\begin{aligned} \nabla U|_{\mathbf{x}=\mathbf{0}} &= \sum_{i=1}^n k_i \sigma_{i0} \hat{\mathbf{k}}_i = \hat{\mathbf{0}} \\ &= [\hat{\mathbf{k}}_1 \quad \cdots \quad \hat{\mathbf{k}}_n] \begin{pmatrix} k_1 & & \\ & \ddots & \\ & & k_n \end{pmatrix} \begin{bmatrix} \sigma_{10} \\ \vdots \\ \sigma_{n0} \end{bmatrix} \end{aligned} \quad (3.28)$$

The first matrix is the configuration matrix S of the linear and angular springs. We recognize the negative of the gradient as the sum of the contact wrenches acting on the grasped object. They are the contact forces and torques from the linear and angular springs.

If the grasp is force-closure, then the wrench convexes at the contacts span the total space of wrenches. In other words, we can generate an arbitrary wrench on the object from non-negative combination of the contact wrenches. So, we can generate a zero wrench, or have an equilibrium grasp. Force-closure is a sufficient but not a necessary condition for equilibrium. To have an equilibrium grasp we just need the zero wrench to be in the subspace generated by the contact wrenches, and this subspace does not have to be total.

Finding the set of n contact wrenches is equivalent to solving a system of six equations in n compressions, $\sigma_{10}, \dots, \sigma_{n0}$, or in n contact forces and torques, f_{10}, \dots, f_{n0} , $f_{i0} = k_i \sigma_{i0}$. There is at least one free variable, which is the internal force of the grasp. For good numerical accuracy, Gaussian elimination with both row and column pivotings is used (Strang 1976, 1986). Generalized inverses, along with some optimizations are used when there are redundant contacts (Ben-Israel and Greville 1974, Rao 1980). The time complexity is $O(n)$, because the number of equations is fixed.

Corollary 3.6 *If a grasp G , defined the set of n contacts at P_1, \dots, P_n , is force-closure, then the set of contact forces and torques for which grasp G is in equilibrium, always exists and can be computed in $O(n)$ time.*

In general, the weight $m\hat{\mathbf{g}}$ of the object is not negligible, and so must be balanced by the contact wrenches. In this case, to have an equilibrium grasp, we need the opposite of the weight to be in the subspace generated by the contact wrenches. The weight $m\hat{\mathbf{g}}$ adds a gravity term $-m\hat{\mathbf{g}} \cdot \hat{\mathbf{t}}$ to the potential U of the grasp, and the result is the potential function of the grasped object. The first derivative of the gravity term, with respect to the twist displacement $\hat{\mathbf{t}}$, gives $-m\hat{\mathbf{g}}$, the opposite of the weight. The second derivative is zero. So, the weight of the object only add a bias force to the grasp, and does not affect the stability of the grasp.

Stability and Six Independent Springs

The stiffness matrix K is the Hessian matrix $H_{\mathbf{x} \ 0}$ of the potential function U of the grasp about the equilibrium configuration. The stiffness matrix of the grasp comes from the stiffness contributions of the l linear springs and of the $n - l$ angular springs. For clarity, the stiffness matrix K is rewritten as the sum of two matrices:

$$K = K_S + K_P \quad (3.29)$$

The first matrix, denoted by K_S , depends only on the spatial vectors of the l linear and $n - l$ angular springs:

$$\begin{aligned} K_S &= \begin{bmatrix} \hat{\mathbf{k}}_1 & \cdots & \hat{\mathbf{k}}_n \end{bmatrix} \begin{pmatrix} k_1 & & \\ & \ddots & \\ & & k_n \end{pmatrix} \begin{bmatrix} \hat{\mathbf{k}}_1^T \\ \vdots \\ \hat{\mathbf{k}}_n^T \end{bmatrix} \\ &= \begin{bmatrix} \mathbf{k}_1 & \cdots & \mathbf{k}_l \\ (\mathbf{p}_1 \times \mathbf{k}_1) & \cdots & (\mathbf{p}_l \times \mathbf{k}_l) \end{bmatrix} \begin{pmatrix} k_1 & & \\ & \ddots & \\ & & k_l \end{pmatrix} \begin{bmatrix} \mathbf{k}_1^T & (\mathbf{p}_1 \times \mathbf{k}_1)^T \\ \vdots & \vdots \\ \mathbf{k}_l^T & (\mathbf{p}_l \times \mathbf{k}_l)^T \end{bmatrix} \\ &\quad + \begin{bmatrix} \mathbf{0} & \cdots & \mathbf{0} \\ \mathbf{k}_{l+1} & \cdots & \mathbf{k}_n \end{bmatrix} \begin{pmatrix} k_{l+1} & & \\ & \ddots & \\ & & k_n \end{pmatrix} \begin{bmatrix} \mathbf{0}^T & \mathbf{k}_{l+1}^T \\ \vdots & \vdots \\ \mathbf{0}^T & \mathbf{k}_n^T \end{bmatrix} \end{aligned} \quad (3.30)$$

The second matrix K_P has four 3×3 block matrices that are all zeros, except the lower-right block, denoted by $K_{P\delta}$, which corresponds to the position of the angular stiffness matrix:

$$K_P = \pm \begin{pmatrix} \begin{bmatrix} 0 \\ 0 \end{bmatrix} & \begin{bmatrix} 0 \\ 0 \end{bmatrix} \\ \begin{bmatrix} 0 \\ 0 \end{bmatrix} & K_{P\delta} \end{pmatrix} \quad (3.31)$$

The sign is $+$ for contacts without friction, and $-$ for contacts with friction. The potential of the grasp is conserved only if there is no slip in the presence of friction. So, the assumptions are that the fingertips either slide on the faces when there is no friction, or stick when there is friction. Slip in the presence of friction is discussed qualitatively in the next chapter.

The matrix $K_{P\delta}$ comes from the second order effect of the l linear springs, when the object is rotated. $K_{P\delta}$ is a 3×3 angular stiffness matrix which depends on the tip positions and the contact forces of the l linear springs:

$$K_{P\delta} = \left(\sum_{i=1}^l f_{i0} (\mathbf{p}_i \cdot \mathbf{k}_i) \right) I - [\mathbf{p}_1 \ \cdots \ \mathbf{p}_l] \begin{pmatrix} f_{10} & & \\ & \ddots & \\ & & f_{l0} \end{pmatrix} \begin{bmatrix} \mathbf{k}_1^T \\ \vdots \\ \mathbf{k}_l^T \end{bmatrix} \quad (3.32)$$

The grasp is stable if the stiffness matrix K is positive definite. The matrix K_S is a product of three matrices. The first matrix, denoted by S , is a $6 \times n$ matrix, whose

columns are the spatial vectors of the n linear and angular springs. The matrix S describes the spatial configurations of the springs in the grasp, and so is called the *configuration matrix* of the virtual springs. The third matrix is S^T , the transpose of the configuration matrix S . The matrix in the middle is an $n \times n$ diagonal matrix K , with the n stiffness constants on its diagonal. Multiplying the matrix S^T with the displacement $\mathbf{x} = \hat{\mathbf{t}}^S$ gives an $n \times 1$ column of the n effective displacements at the n linear and angular springs: $S^T \mathbf{x}$. When multiplying SKS^T on the left with \mathbf{x}^T , and on the right with \mathbf{x} , we get a quadratic, $(S^T \mathbf{x})^T K (S^T \mathbf{x})$, which is either zero or positive, because the matrix K has only positive values on its diagonal. In particular, this product is zero if and only if the displacement $\mathbf{x} = \mathbf{0}$, or the matrix S has dependent rows (Strang 1976, 1986). In other words, the stiffness matrix SKS^T from the configurations of the springs is positive definite, if and only if the set of n linear and angular springs has at least six springs whose spatial vectors are independent of each other.

If the grasp is force-closure, then the set of contact wrenches span the whole 6-dimensional space of wrenches. If these contact wrenches are generated by springs, either virtual ⁴ or real ⁵, then the spatial vectors of these springs also span the whole 6-dimensional space. This means that we have six springs with independent spatial vectors.

There is another term, $K_{P\delta}$, which is subtracted from, or added to the angular stiffness matrix of the grasp, depending on whether there is friction at the point contacts or not. However, if the contact forces of the l linear springs are small, then $K_{P\delta}$ will be small compared to the angular stiffness matrix block in K_S . We can make the contact forces small by scaling down ⁶ the set of compressions found from equilibrium. This scaling factor can be computed in $O(n)$ time.

In other words, with stiffness at the contacts, and with the compressions at the springs small compared to the size of the object, a force-closure grasp implies a positive definite stiffness matrix K , or a stable grasp. The set of n contact forces and torques are found from solving for an equilibrium grasp, with a desired internal grasp force. Equation (3.28). The n stiffness constants can be set to some positive default stiffness value. The compressions at the springs are then deduced, and they can be scaled down if necessary. The algorithm is similar to Algorithm 3.1. So, a force-closure grasp with n virtual springs can be made stable in $O(n)$ time.

Corollary 3.7 *If a grasp G , defined the set of n contacts at P_1, \dots, P_n , is force-closure, then the set of n virtual springs for which grasp G is stable, always exists and can be computed in $O(n)$ time.*

As in the planar case, the matrix $K_{P\delta}$ can make the angular stiffness matrix of an outside-in grasp negative definite when there is friction, and more positive

⁴The stiffness at the fingertip can come from the stiffness control loops at the finger joints

⁵An example is a soft rubber tip, modeled as three orthogonal linear springs, and one angular spring.

⁶A rule of thumb is to choose the compressions at the linear springs to be one-tenth of the size of the object. By size, I mean average size, or diameter of the circumscribed sphere.

negative, otherwise. For example, let's pick an outside-in grasp on a convex object. The dot products $\mathbf{p}_i \cdot \mathbf{k}_i$ are positive,⁷ and they add up to a dominant diagonal that is positive, or to large positive eigenvalues. The matrix K_{P_i} will dominate the lower-right 3×3 angular stiffness matrix from SKS^T , if the linear compressions σ_i are much larger than the size of the object. Subtracting (resp. adding) this dominating K_{P_i} very likely will result in an angular stiffness block that is negative definite (resp. more positive definite). The reverse is true for inside-out grasps.⁸

We conclude that friction makes an outside-in (resp. inside-out) grasp less (resp. more) stable respective to rotations. The reverse is true for grasps without friction. The "in-between" stability comes from the configurations and the stiffness constants of the springs, and has stiffness matrix $K_S = SKS^T$.

Two Hard-Finger Contacts Versus Two Soft-Finger Contacts

Figure 3.10 shows two grasps G_1, G_2 , on a pair of parallel faces, that are identical except that the first grasp has hard-finger contacts, and the second, soft-finger contacts.

Grasp G_1 has six linear springs, but only five are independent. In Section 2.4.3, we have seen that a grasp with 2 hard-finger contacts cannot generate torques parallel to the segment joining the two points of contact. So, the free vector which has direction parallel to the segment P_1P_2 , joining the two points of contact is not inside the subspace generated by the spatial vectors of the six linear springs. The matrix $K_S = SKS^T$ is positive semi-definite, and the grasp will not resist rotations of the object about segment P_1P_2 . The stiffness K_S of the grasp shown is:

$$\begin{aligned}
 K_S &= \begin{pmatrix} 1 & 0 & 0 & 1 & 0 & 0 \\ 0 & 1 & 0 & 0 & -1 & 0 \\ 0 & 0 & 1 & 0 & 0 & 1 \\ 0 & 0 & d & 0 & 0 & -d \\ 0 & 0 & 0 & 0 & 0 & 0 \\ d & 0 & 0 & d & 0 & 0 \end{pmatrix} \begin{pmatrix} k_1 & & & & & \\ & k_2 & & & & \\ & & k_3 & & & \\ & & & k_4 & & \\ & & & & k_5 & \\ & & & & & k_6 \end{pmatrix} \begin{pmatrix} 1 & 0 & 0 & 0 & 0 & -d \\ 0 & 1 & 0 & 0 & 0 & 0 \\ 0 & 0 & 1 & d & 0 & 0 \\ 1 & 0 & 0 & 0 & 0 & d \\ 0 & -1 & 0 & 0 & 0 & 0 \\ 0 & 0 & 1 & -d & 0 & 0 \end{pmatrix} \\
 &= \begin{pmatrix} k_1 + k_4 & & & & & \\ & k_2 + k_5 & & & & \\ & & k_3 + k_6 & & & \\ & & & (k_3 + k_6) d^2 & & \\ & & & & 0 & \\ & & & & & (k_1 + k_4) d^2 \end{pmatrix}
 \end{aligned} \tag{3.33}$$

The stiffness matrix of the grasp K has another submatrix, K_{P_i} , which is subtracted from its angular stiffness block. For the outside-in grasp in Figure 3.10, K_{P_i}

⁷The origin is taken to be inside the object

⁸This observation is only qualitative and approximate. There is no theorem which says about the positive definiteness of a difference of two positive definite matrices.

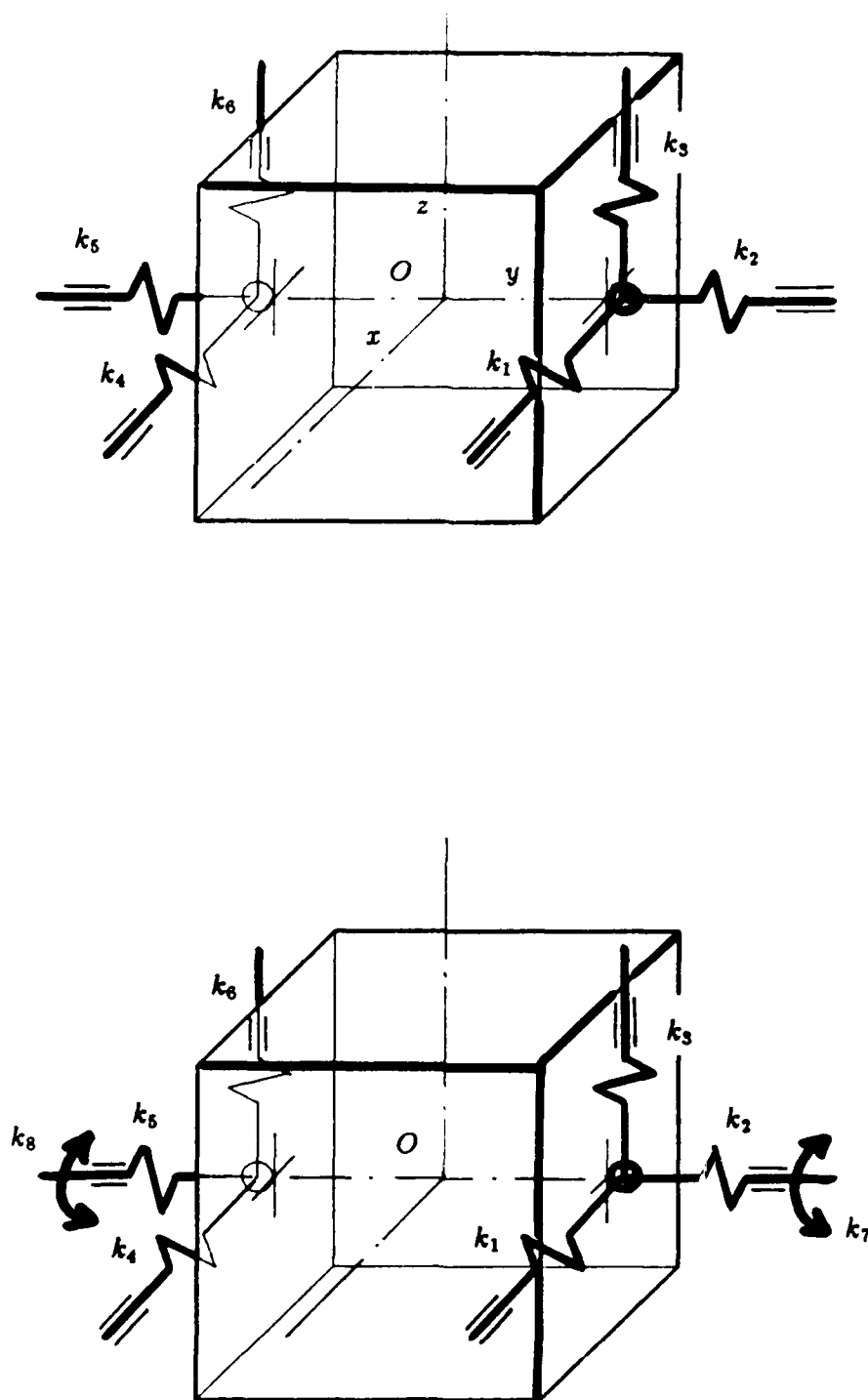


Figure 3.10: Two hard-finger contacts versus two soft-finger contacts.

is a diagonal matrix with positive values, except a zero at the slot which corresponds to rotations about segment P_1P_2 :

$$\begin{aligned}
 K_{P\delta} &= 2 f_o d \begin{pmatrix} 1 & 0 & 0 \\ 0 & 1 & 0 \\ 0 & 0 & 1 \end{pmatrix} \\
 &\quad - \begin{pmatrix} 0 & 0 & 0 & 0 & 0 & 0 \\ d & d & d & -d & -d & -d \\ 0 & 0 & 0 & 0 & 0 & 0 \end{pmatrix} \begin{pmatrix} 0 & & & & & \\ & f_o & & & & \\ & & 0 & & & \\ & & & 0 & & \\ & & & & f_o & \\ & & & & & 0 \end{pmatrix} \begin{pmatrix} 1 & 0 & 0 \\ 0 & 1 & 0 \\ 0 & 0 & 1 \\ 1 & 0 & 0 \\ 0 & -1 & 0 \\ 0 & 0 & 1 \end{pmatrix} \\
 &= 2 f_o d \begin{pmatrix} 1 & 0 & 0 \\ 0 & 0 & 0 \\ 0 & 0 & 1 \end{pmatrix}
 \end{aligned} \tag{3.34}$$

So, the grasp G_1 cannot resist rotations about segment P_1P_2 . The stiffness matrix K has negative eigenvalues for the two rotations perpendicular to P_1P_2 , if the virtual compressions, or the contact forces, at the fingertips are large. The object is unstable, and tends to flip over. This flipping behavior has been reported by Cutkosky (1984, 1985).

A soft-finger contact has in addition an angular spring in the direction of the linear spring normal to the surface of contact. Grasp G_2 has six linear springs and two angular springs. The angular springs have free vectors with projections in the direction P_1P_2 , and so are independent from the six linear springs. The configuration matrix S of the springs has full rank, and the stiffness matrix K_S is positive definite.

If the compressions at the linear springs are small compared to the length of segment P_1P_2 , then $K_{P\delta}$ is small compared to the angular stiffness block from K_S . then grasp G_2 is stable. The larger the virtual compressions at the fingertips, the larger is $K_{P\delta}$, and the less stable grasp G_2 is, with respect to rotations perpendicular to P_1P_2 . The rotation about segment P_1P_2 is unaffected, and is due only to the presence of the two angular springs.⁹

3.3.3 Compliance about Stable Equilibrium

The compliant behavior of the grasped object about its stable equilibrium is described by the stiffness matrix of the grasp. We have seen that this stiffness matrix is composed of two terms. The first term depends on the spatial configurations of the springs, and the second term depends on whether the fingertips stick or slide without friction on the faces of the grasped object. This section will explore the properties of the stiffness matrices K , K_S , and $K_{P\delta}$. K_S is a good approximation

⁹In reality, as the normal pressure at the points of contact is increased, we get larger angular stiffness, but this variation is not captured by our simple model of angular spring.

to the real stiffness matrix K when the compressions of the linear springs are small compared to the size of the object.

Stiffness Matrix of the Object

The matrix $K_S = S K S^T$ is symmetric. To see that $K_{P\delta}$ is also symmetric, let's rewrite it as:

$$K_{P\delta} = \left(\sum_{i=1}^l f_{i0} (\mathbf{p}_i \cdot \mathbf{k}_i) \right) I - \sum_{i=1}^l f_{i0} (\mathbf{p}_i \mathbf{k}_i^T) \quad (3.35)$$

The first term is a diagonal matrix. The second term is a symmetric matrix if the contact forces have zero total moment about the origin:

$$\sum_{i=1}^l f_{i0} (\mathbf{p}_i \mathbf{k}_i^T) = \begin{pmatrix} \sum p_{ix} f_{ix} & \sum p_{ix} f_{iy} & \sum p_{ix} f_{iz} \\ \sum p_{iy} f_{ix} & \sum p_{iy} f_{iy} & \sum p_{iy} f_{iz} \\ \sum p_{iz} f_{ix} & \sum p_{iz} f_{iy} & \sum p_{iz} f_{iz} \end{pmatrix}$$

The off-diagonal terms $M[i, j]$ in the above matrix are equal to their respective transposed terms $M[j, i]$. Their pairwise differences are equal to the moments of the contact forces about the axes of the reference frame, which are all zero if the grasp is in equilibrium with the l linear springs. For example, $(M[x, y] - M[y, x])$ is the moment of the contact forces of the l linear springs about the z -axis.

The stiffness matrix K of the grasp is the sum of two symmetric matrices, and therefore is symmetric, Equation (3.29). This means that K has perpendicular eigenvectors. If the grasp is stable, then the stiffness matrix K is positive definite, and so the eigenvalues are all strictly positive.

The eigenvectors describe the spatial directions for which the restoring wrenches $\hat{\mathbf{w}}$, applied on the object by the fingers, are proportional to the displacement \mathbf{x} , which is the spatial transpose of the twist $\hat{\mathbf{t}}$ of the object. The corresponding eigenvalues describe the stiffness of the grasp along these spatial directions. The grasped object will behave as though it has six independent springs attached to it. The configuration of these springs is described by the eigenvectors, and the stiffness by the corresponding eigenvalues:

$$\begin{aligned} \hat{\mathbf{w}} &= K \hat{\mathbf{t}}^S \\ \begin{bmatrix} \mathbf{f} \\ \mathbf{m} \end{bmatrix} &= \begin{pmatrix} K_d & K_\times \\ K_\times^T & K_\delta \end{pmatrix} \begin{bmatrix} \mathbf{d} \\ \delta \end{bmatrix} \end{aligned} \quad (3.36)$$

K_d , K_\times , K_δ are the 3×3 block matrices of the grasp stiffness matrix K . I will refer to these block matrices as linear, angular, and cross matrices respectively.

One important special case is when the eigenvectors have only translational or rotational parts. This case corresponds to a stiffness matrix K which is split into two linear and angular 3×3 block matrices, K_d and K_δ . The grasped object has the origin O as compliance center, and translations and rotations of the object about origin O are resisted respectively by pure forces and pure torques from the grasp.

In other words, the object behaves as though it has three linear springs and three angular springs, attached at its compliance center O . This case will be explored further in the next section.

From the springs at the n contacts, we get a stiffness matrix of the grasp, and analyze it to find the eigenvalues and eigenvectors, that is, the springs attached to the grasped object. This is the analysis, or forward problem, which is straightforward, and costs $O(n)$ time. In robotics, we most often need to solve the reverse problem, which is: from a desired stiffness matrix at the grasped object, find the virtual springs at the contacts. First, let's do a counting argument to find the minimum number of fingers that are needed. Then, we'll explore the reverse problem, and its complexity. In solving the reverse problem, I assume the stiffness matrix of the grasp is approximated by K_S , which describes the first-order effect of the linear and angular springs.

A stiffness matrix is specified by its six eigenvalues, and its six eigenvectors. Each eigenvector has six coordinates, so the six eigenvectors has thirty-six variables to specify. However, not all thirty-six variables are independent. An eigenvector must have unit magnitude, and must be perpendicular to the other eigenvectors. There are six constraint equations from the six norms, and fifteen others from the dot-product of pairs of eigenvectors. So, a stiffness matrix has twenty-one free variables, six from the eigenvalues, and fifteen from the eigenvectors.

Given a desired stiffness matrix K at the grasped object, the springs at the contacts are approximatively computed from:

$$\begin{aligned} K &= S K_S S^T \\ &= \sum_{i=1}^n k_i (\hat{\mathbf{k}}_i \hat{\mathbf{k}}_i^T) \end{aligned} \quad (3.37)$$

If the points of contact are fixed, for example, by a given force-closure grasp, then the configurations of the springs are fixed. Then, the unknowns can only be the stiffness constants k_i . To solve for an arbitrary stiffness matrix K , there must be at least twenty-one independent springs, that is, six soft-finger contacts, or seven hard-finger contacts, or twenty-one frictionless point contacts.

Equation (3.37) can be rewritten as a system of twenty-one equations,¹⁰ with the stiffnesses k_i as unknowns. The stiffness constants of the n virtual springs can be solved, using Gaussian elimination, or least square error methods in $O(n)$ time. There is one constraint however: the stiffness values must be strictly positive. Optimization with constraints must be used. (Rao 1980, Strang 1986).

To reduce the number of necessary fingers, we must choose the spatial configurations of the springs, or the points of contact and the contact normals. For example, from the desired stiffness K , we compute the eigenvalues and eigenvectors. The grasping faces are chosen such that they have normals most closely oriented with

¹⁰ Six equations for the diagonal term, and fifteen others for the off-diagonal term.

the eigenvectors that have large eigenvalues. This alignment scheme also makes the stiffness matrix of the grasp less dependent on friction.

A line vector has six coordinates, but only four are free variables. So a frictionless point contact, modeled as a linear spring, has five free variables, four from the spatial vector, and one from the stiffness constant. A hard-finger contact, modeled as three perpendicular linear springs going through the same contact point, has eight free variables, three from the common point of contact, two from the orientations of the the three linear springs, and three from the three stiffness constants. A soft-finger contact, modeled as a hard-finger contact plus an angular spring about the normal at the point contact, has nine free variables, one more than a hard-finger contact for the angular stiffness constant. So, to solve for an arbitrary stiffness matrix K , we need at least five frictionless point contacts, or three hard-finger contacts, or three soft-finger contacts. This assumes that we can choose both the grasp configuration and the stiffness constants of the springs.

Center of Compliance of the Object

In general, the eigenvectors of the stiffness matrix K have both linear or angular parts, and the cross matrix K_\times is non zero. From Equation (3.30), the matrix K describes the weighted dyadic product of the Plücker vectors of the springs, where the weights are the stiffness constants. Since angular springs have one of the Plücker vectors zero, the cross matrix K_\times depends only on the linear springs:

$$\begin{aligned}
 K &= \sum_{i=1}^l k_i (\mathbf{k}_i (\mathbf{p}_i \times \mathbf{k}_i)^T) \\
 &= \sum_{i=1}^l k_i \begin{pmatrix} k_{iz} (\mathbf{p}_i \times \mathbf{k}_i)_x & k_{iz} (\mathbf{p}_i \times \mathbf{k}_i)_y & k_{iz} (\mathbf{p}_i \times \mathbf{k}_i)_z \\ k_{iy} (\mathbf{p}_i \times \mathbf{k}_i)_x & k_{iy} (\mathbf{p}_i \times \mathbf{k}_i)_y & k_{iy} (\mathbf{p}_i \times \mathbf{k}_i)_z \\ k_{ix} (\mathbf{p}_i \times \mathbf{k}_i)_x & k_{ix} (\mathbf{p}_i \times \mathbf{k}_i)_y & k_{ix} (\mathbf{p}_i \times \mathbf{k}_i)_z \end{pmatrix} \quad (3.38)
 \end{aligned}$$

The moment of the linear springs depends on the location of the origin. So, by changing the origin of the reference frame, we can get K_\times to be smallest. If K becomes the zero matrix, the new origin is the center of compliance of the grasp.

The matrix K has nine elements, of which eight are independent. The three diagonal elements of K adds up to a weighted sum of the dot products between the Plücker vectors of the springs, which is always zero because line vectors have perpendicular Plücker vectors. We have eight equations in the three coordinates of the center of compliance. So, a stable grasp with n independent springs does not generally have a center of compliance. I typically solve for the least square error compliance center, and this costs $O(n)$ time.

Not all positions of the compliance center are feasible. Similar to the planar case, the compliance center must be inside a region, called the compliance polyhedron, for which there exist non-negative stiffness constants such that K is a zero matrix. The 3×3 matrix of the dyadic product can be written as a 9-element column vector.

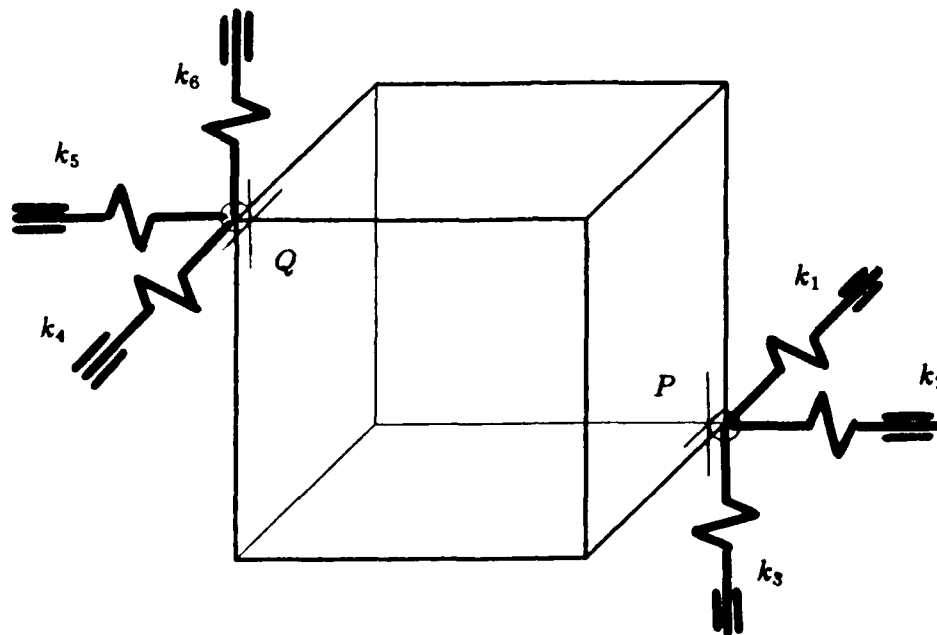


Figure 3.11: Compliance polyhedron in a grasp with 2 hard-finger contacts.

and the analytic condition for the existence of a compliance center is a system of nine homogeneous equations:

$$\sum_{i=1}^n k_i \begin{bmatrix} (\mathbf{p}_i \times \mathbf{k}_i)_x & \mathbf{k}_i \\ (\mathbf{p}_i \times \mathbf{k}_i)_y & \mathbf{k}_i \\ (\mathbf{p}_i \times \mathbf{k}_i)_z & \mathbf{k}_i \end{bmatrix} = \begin{bmatrix} 0 \\ 0 \\ 0 \end{bmatrix}$$

in which eight equations are independent. The stiffness constants k_i are negative. The above equation depends on the moments $\mathbf{p}_i = \mathbf{k}_i \times \mathbf{O}$, the placement of the compliance center \mathbf{O} relative to the contact springs.

A compliance center exists if and only if the set of all \mathbf{O} is a convex which includes the zero element. We will assume that the 9 element load matrix is nonsingular, that the condition implies at each contact point that the hard-finger contact is active.

Figure 3.12 shows the compliance

AD-A106 419

THE SYNTHESIS OF STABLE FORCE-CLOSURE GRASPS(U)
MASSACHUSETTS INST OF TECH CAMBRIDGE ARTIFICIAL
INTELLIGENCE LAB V NGUYEN JUL 86 AI-TR-905

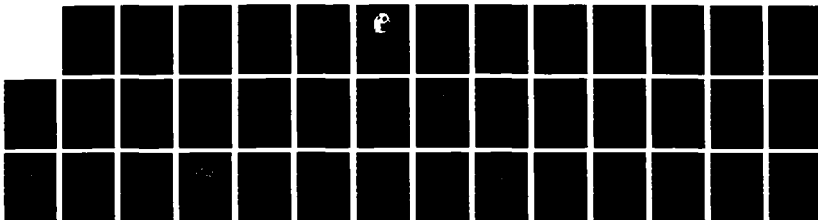
2/2

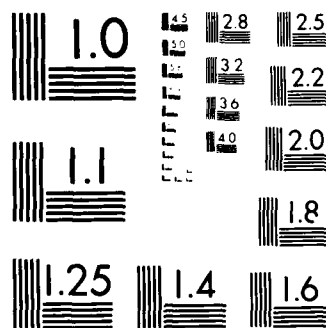
UNCLASSIFIED

NO0014-85-K-0124

F/G 23/1

NL





MICROCOPY RESOLUTION TEST CHART
NATIONAL BUREAU OF STANDARDS 1963-A

the two points of contact is always a valid locus for the compliance center. This segment corresponds to two points of contact having proportional sets of springs. The compliance polyhedron is in between the two points of contact for fingertips covered by rubber. For two fingers with active stiffness control, we can orient the lines of action of the linear springs at the two points of contact such that the compliance polyhedron includes the desired compliance center. So, choosing a compliance center is equivalent to orienting the compliance frames and choosing the stiffnesses at the fingertips.

Not all positive definite or positive semi-definite stiffness matrices are feasible, even with arbitrarily many fingers. We have seen that a stiffness matrix has twenty-one free variables. We can count differently as follows: six free variables for the diagonal, and fifteen others for the off-diagonal elements. However, the upper-right block K_x has eight independent elements instead of nine. So, a feasible stiffness matrix has only twenty free variables instead of twenty-one. The range of feasible stiffness matrices is strictly included in the domain of positive stiffness matrices, because the physical contacts can not have arbitrary spatial vectors for their springs.

Corollary 3.8 *The stiffness constants of the n virtual springs can be computed in $O(n)$ time, such that the grasp has approximatively the desired stiffness matrix and compliance center.*

The linear springs of a two-point or three-point grasp are typically computed in about 0.4 seconds on a Symbolics machine.

3.4 Conclusion

3.4.1 Main Results

- We prove that all force-closure grasps can be made stable (Corollary 3.5, and Corollary 3.7). The algorithm for constructing stable grasps is both simple and efficient (Algorithm 3.1). It costs $O(n)$ time to synthesize a set of n virtual springs such that a given force-closure grasp is stable, and has approximatively some desired stiffness matrix.
- We show that the stiffness matrix K of the grasp has a matrix K_S which depends on the spatial configuration of the virtual springs. The geometric relation is simple, $K_S = SKS^T$, where the columns of S are the spatial vectors describing the lines of action of the springs. K_S is positive definite if and only if there are at least three (resp. six) virtual springs with independent spatial vectors for 2D (resp. 3D) grasps.

The stiffness matrix K_S is positive definite if the grasp has at least two soft finger contacts. This explains why we get stable grasps so easily, most of the times by just closing two soft fingers onto the grasped object.

- We show that the stiffness matrix has also a position-dependent matrix K_P which depends on whether the finger stick or slide on the straight edges (resp. flat faces) of the object. K_P makes outside-in grasps more stable than inside-out grasps if the fingers slide without friction on the object. The reverse holds if there is friction and the fingers stick.
- We show that the compliance center of the grasp must be inside a region delimited by the lines of action of the linear springs. So a placement of the compliance center implies either a relative orientation of the linear springs, or a placement of the points of contact, or both.
- We can choose the compliance center and the stiffness matrix of the grasp, or in other words, choose the behavior of the grasped object about its stable equilibrium. The object behaves as though it is attached to independent linear and angular springs at its compliance center (Figure 3.3). The grasp is robust to disturbances. If the object is accidentally displaced, there will be restoring wrenches that will pull it back to its stable equilibrium. All this is done automatically, fast, and without any extra effort from planning or execution.

3.4.2 Experiments

The synthesis of stable force-closure grasps proceeds in two steps:

- Given a set of grasping edges or faces, construct the independent regions of contact, for which the grasp is always force closure.

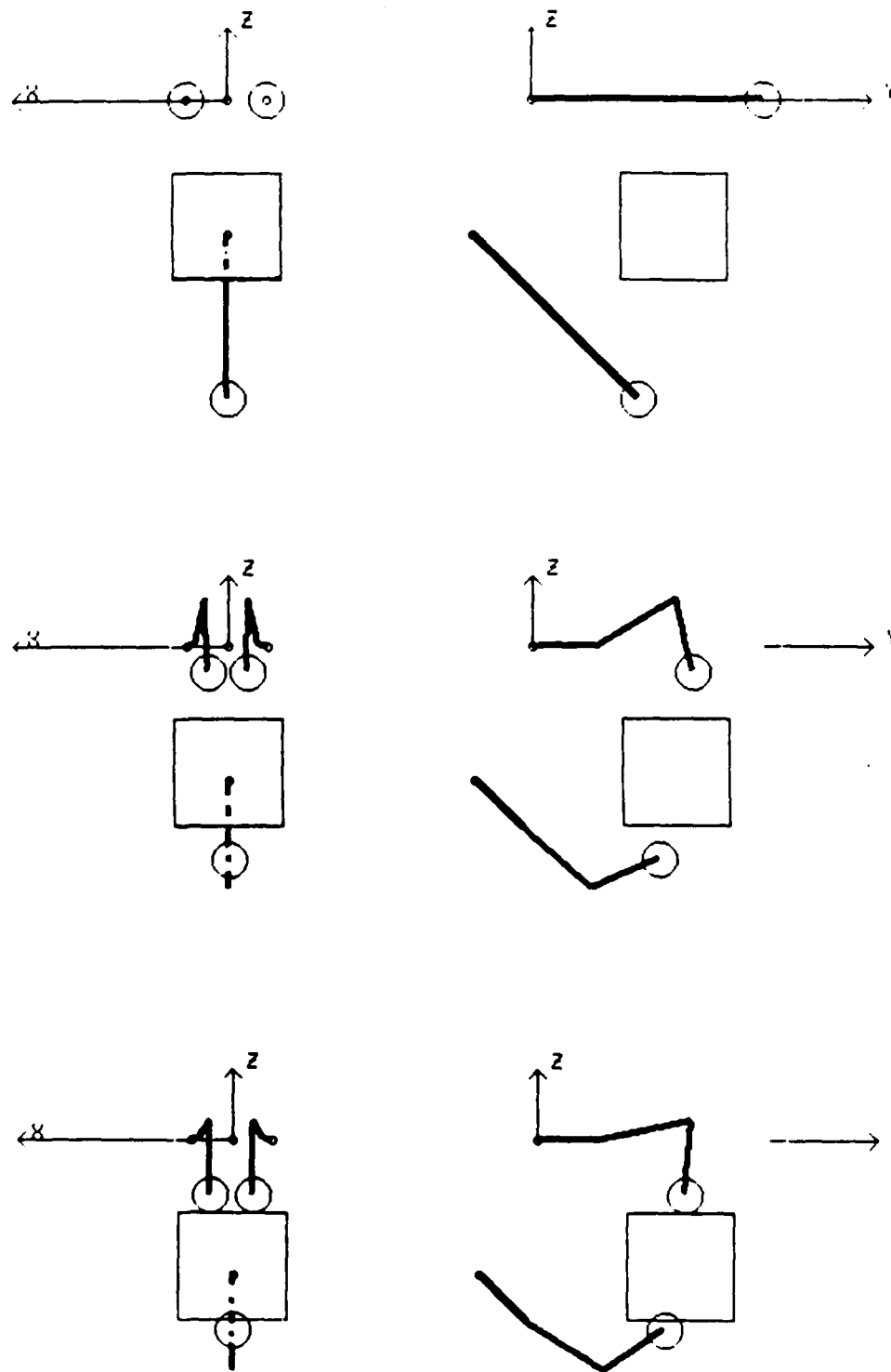


Figure 3.12: A sequence of commands which executes a grasp.

- Pick the mid points of the independent regions as the desired grasp points. Synthesize the virtual springs at the desired grasp points such that the grasp is stable, and has some desired stiffness matrix or compliance center. Least square error optimization is used when the stiffness matrix can not be achieved exactly with the finite number of springs.

The grasp synthesis has been implemented for both 2D and 3D grasps. The code is written in Zeta Lisp, compiled and run on Symbolics Lisp machines. It takes about 1/10 seconds to construct a force closure grasp, and about 1/5 seconds to construct the virtual springs.

The grasp configuration and the contact regions are then given to a path planner which finds collision-free paths for the fingers. We assume that the fingers do not have intersecting paths, so their paths can be planned independently from each other. Each finger is a revolute arm, with configuration represented by its joint angles. Using the Configuration Space method (Lozano-Pérez 1983, Donald 1984), the finger is shrunk to a configuration point in joint space, while the grasped object is grown into a configuration obstacle. A collision-free path for the finger becomes a path for the configuration point which does not intersect the configuration obstacle. The find-path problem is transformed into a search for a path between two initial and final configurations.

The output of the high level planning is a sequence of commands such as (move-fingers-to ...), (grasp-at ...), all in joint space. For good accuracy, the fingers are position controlled during move-fingers-to commands, and the trajectory is generated by a simple joint interpolation between collision-free via points. The fingers must be stiffness controlled to have the fingers comply between themselves during the grasping operation, and to get the desired stiffness matrix at the grasped object. We insert approach points just before the grasp points. The approach points are places where the fingers switch from position control to stiffness control. Figure 3.12.

Experiments have been performed with the Stanford/JPL hand. The hand has three identical fingers; each finger has three joints pulled by a set of four tendons (Salisbury 1982). The fingers are position controlled at their innermost loop. Force and stiffness control are added at the outer loop, (Salisbury 1980, Salisbury and Craig 1981, Chiu 1985), Figure 3.13.

First, grasps are executed with the fingers in position control mode. The stiffness at the grasp points comes from the rubber covers of the fingertips, and from the tendons. The grasps are very stable. Then the grasped object is pushed until the fingers slip on the grasping faces. We verified that after the fingers slip, the grasped object remain stable. We also verified that the impulses or short disturbance forces tend to make marginally stable grasps more stable.

Next, the fingers are stiffness controlled during the closing of the fingers onto the grasp points. We observe:

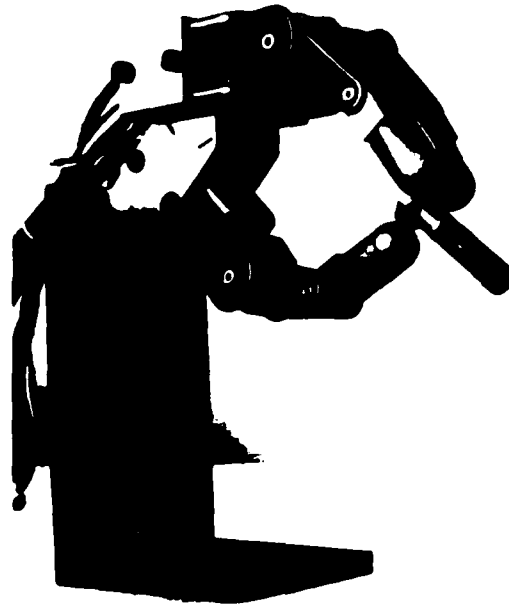


Figure 3.13: The Stanford/JPL hand.

- Very slow motions of the fingertips, due to the large friction in the tendons. Note that the stiffness loop controls the forces that are exerted by the motors at the ends of the tendons. These forces although correct, are too small to overcome the high frictional forces in the tendons and pulleys. A fix will be to add a feed-forward term to compensate for the frictional forces, and also to compensate the gravity and inertia forces. However, feed-forward control is sensitive to errors in modeling.
- The control loop becomes unstable at about two thirds of the physical stiffness of the tendons. We have seen that the virtual compressions must be small compared to the size of the grasped object. With low stiffness at the virtual springs, small virtual compressions imply small contact forces, and so the weight of the object must be small!

High stiffness requires faster servo rates (about 300 hz), and having force and position sensors as close to the fingers as possible. Currently, due to slow servo rates (currently 50 Hz), we are forced to rely on the friction and stiffness in the tendons to provide a compliant interface between the joint motors and the end effectors.

The above observations are expected. After all, the real fingers have their own physical limitations, such as the maximum stiffness is the stiffness of the tendons. Since the fingers are stiffness-controlled, their stiffnesses are further limited by the servo rate. Active stiffness gives us flexibility in choosing the stiffness values at the

fingers. More importantly, active stiffness allows us to abstract the complicated behavior of the fingers by a set of idealized springs, then focus on the problem of synthesizing grasps, not just analyzing grasps.

With the current three-finger hand, grasps are done best with a simple position control of the fingers, (servo rate is 1000 hz). The stiffness that makes the grasp stable and very compliant, does not come from active stiffness, but comes from the stiffness in the tendons and in the fingertips. It may be that this is also why human hands have passive stiffness built into the soft fingertips, into the tendons and the muscles.

Chapter 4

Grasping With Slip

4.1 How to Deal with Slip?

How should one deal with slip in grasping an object? Should one avoid slip, and plan the grasp and the motion of the fingers such that no slip will occur? Although difficult, such a plan is not impossible to find and execute. The contact forces must always point into the friction cones at the points of contact. The fingers must be position-controlled with high accuracy to the desired grasp points. Then, the fingers must make contact with the object at the same time.

Many previous papers have shown that slip can be used as a flexible transducer, which results in an automatic compliance of the object to the physical constraints of its environment. Fine motions of the object can be planned with slip and active compliance models such as springs or dampers (Lozano-Pérez, Mason and Taylor 1983, Erdmann 1984, Buckley 1986). Pushing operations with slip reorient the grasped object between the grippers (Mason 1982, Brost 1986). An analysis of how the fingers slide on the object during grasping is used to plan a twirling motion of a bar between three fingers (Fearing 1984, 1986).

This chapter takes the view-point that slip is beneficial, as a compliant interface between the desired grasp and the actual grasp. Slip is allowed during and after the initial grasp. By looking at when slip occurs, it is possible to compute bounds on the allowed displacement of the object, and so deduce the stiffness required for the grasp. By looking at where the fingers slip to, it is possible to plan grasps where the fingers are guaranteed to be inside the grasping edges. Next, we'll look at how slip affects the force closure and stability properties of the grasp. It is easy to plan grasps that are force-closure and stable as long as the fingers do not slip beyond the grasping edges. Last, we explore the effect of curvature and slip on the stability of the object. The fingers slide not on straight edges, but on curved segments approximated by circular arcs.

4.2 Analysis of Slip in 2D

4.2.1 When Do the Fingers Slip?

Figure 4.1 shows a compliant finger contacting a vertical edge. The contact is modeled as a point contact with friction, and has two independent linear springs attached to it. Each spring has a fixed line of action, and only counteracts displacements along its line of action. The compression at the tip P of a linear spring k is given by:

$$\sigma = \sigma_i + (\text{Rot}(z, \theta) \mathbf{p} - \mathbf{p}) \cdot \mathbf{k} + \mathbf{d} \cdot \mathbf{k} \quad (4.1)$$

in which θ is the rotation, and $\mathbf{d} = (x, y)^T$ is the translation of the object.

The angle ψ between the contact normal and contact force at point P is given by:

$$\tan \psi = \frac{k_t \sigma_t}{k_n \sigma_n} \quad (4.2)$$

where σ_n , and σ_t are the normal and tangential compressions, found from the above equation by replacing \mathbf{k} , respectively by the normal and tangential directions at P .

The fingertip sticks if the angle ψ is between $-\phi$ and ϕ , where $\tan \phi$ is the coefficient of friction at the contact. We can find the variation of angle ψ as the object is rotated about a point on the contact normal, or translated along the normal and tangential directions of the contact. For the simple case where the normal and tangential stiffness constants are equal, the angle ψ varies as follows:

$$\begin{aligned} \tan \psi(x) &= \frac{\sigma_{to}}{\sigma_{no} + x} \\ \tan \psi(y) &= \tan \psi_o + \frac{1}{\sigma_{no}} y \\ \tan \psi(\theta) &= \frac{\sigma_{to} + |\mathbf{p}| \sin \theta}{\sigma_{no} + |\mathbf{p}| (\cos \theta - 1)} \end{aligned} \quad (4.3)$$

Figure 4.2 plots the graphs of $\tan \psi$, and shows the places where slip occurs as the object is translated or rotated. The three graphs have respectively the shape of a hyperbola, a straight line, and a tan curve.

The forward problem is to find when the fingers slip, which directly relates to how much the grasped object is displaced. The reverse problem is to find conditions for which the fingers do not slip. For example, given a grasp configuration, we compute bounds on the maximum displacement of the object for which no slip will occur. From the bounds on the disturbance forces, and from the allowed displacement of the object, we deduce the order of magnitude of the stiffness matrix of the grasp, and use it to scale the stiffness constants of all the virtual springs.

Corollary 4.1 *Given a grasp and bounds on the disturbance force, the necessary stiffness scale of the n virtual springs, for which the fingers will not slip, can be computed in $O(n)$ time.*

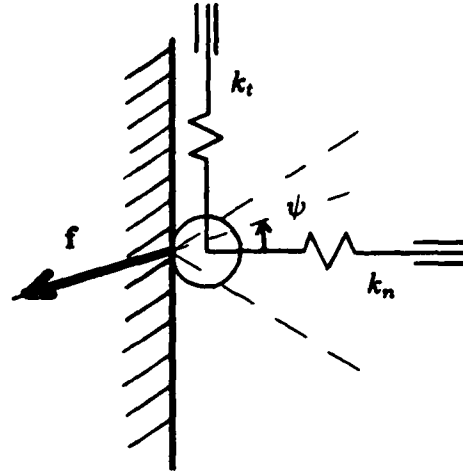


Figure 4.1: A fingertip modeled as two independent springs.

4.2.2 Where Will The Fingers Slip To?

We also need to find the direction towards which the fingers will slip, and calculate bounds on the places where the fingers will stick at, after slipping. A fingertip can be seen as being pulled by a virtual spring with the following stiffness behavior:

$$\mathbf{f} = K(\mathbf{p}_o - \mathbf{p})$$

$$\begin{bmatrix} f_n \\ f_t \end{bmatrix} = \begin{pmatrix} k_n & 0 \\ 0 & k_t \end{pmatrix} \begin{bmatrix} \sigma_n \\ \sigma_t \end{bmatrix} \quad (4.4)$$

Figure 4.3 shows the regions where the fingertip will slip, stick, or loose contact. The stick region is a cone with angle $2\phi \frac{k_n}{k_t}$. It is defined as the region of the fingertip P where the contact force \mathbf{f} , generated by the virtual spring, points into the friction cone at the point of contact. The finger will slip towards the stick cone, and is pulled towards its bias position \mathbf{p}_o , which is fixed not relative to the grasped object, but relative to the base of the hand. When the object is displaced in the hand, the finger will stick and move with the point of contact, until it reaches one of the edges of the stick cone, then it slips.

The finger is guaranteed to stick inside the edge of contact, if the stick cone cuts in the interior of the edge of contact. This condition can be satisfied by a proper positioning of the bias position \mathbf{p}_o , and a proper ratio between the normal and tangential stiffnesses. The finger will not loose contact with the object, if the

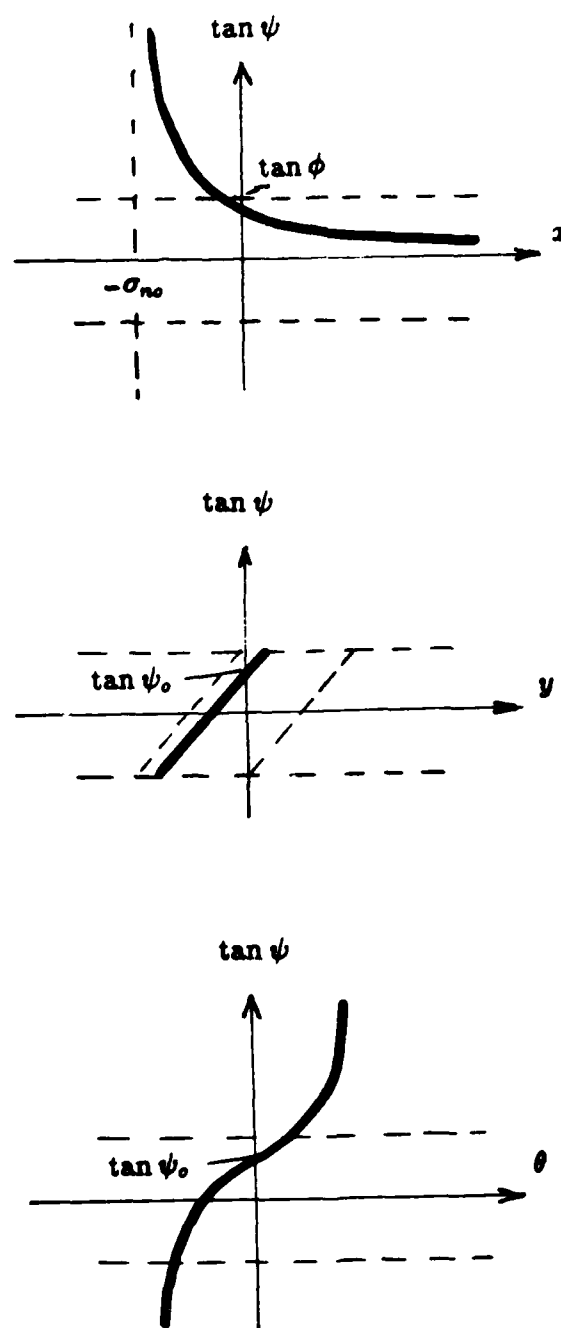


Figure 4.2: Places where slip occurs as the object is displaced.

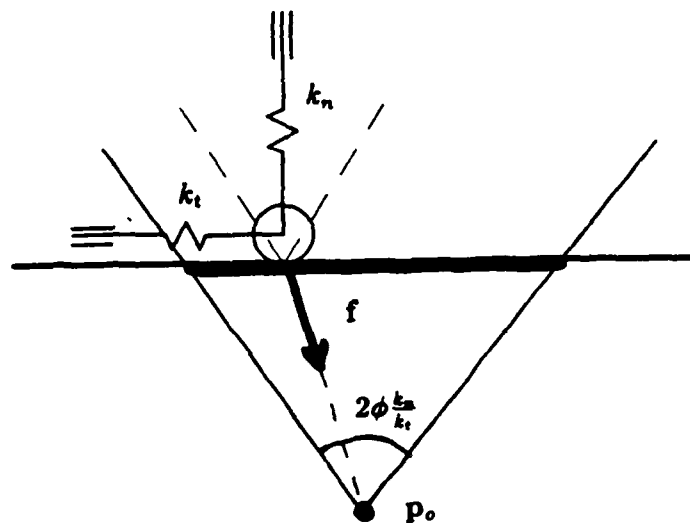


Figure 4.3: Stick and slip regions for the fingertip.

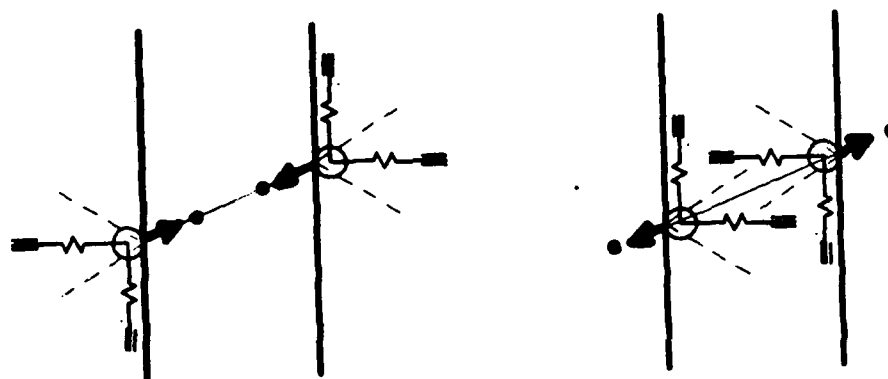


Figure 4.4: Places where the fingers will slip to.

normal compression σ_{nc} is always greater than the translational displacement of the object along this normal direction. We assume that the displacement of the object is finite, and small compared to the normal compression, and the length of the contact edges.

Figure 4.4 shows two point contacts on a pair of parallel edges. Each point contact is pulled by a virtual spring towards its own bias position. As long as the stick cones intersect in the interior of the edges of contact, the fingers are guaranteed to stick on the contact edges. Better yet, the virtual springs can be synthesized such that the fingertips will stick inside the independent regions of contact. The bias positions of the virtual springs are constrained by the equilibrium grasp condition, and so can only be scaled.

Corollary 4.2 *Given a desired grasp, the scale of the n virtual compressions $\sigma_{i,0}$, for which the fingers will stick inside the independent regions of contact, can be computed in $O(n)$ time.*

4.3 Effect of Slip on Force-Closure and Stability

We have modeled the physics of many fingers grasping an object as many virtual springs pressing on the object. In this idealized model, the slip between the fingertips and the object comes from two primary sources:

- The spatial configurations of the virtual springs change and the object is fixed. An example is Figure 4.4.a, where the two fingertips slip towards each other. The lines of action the virtual springs change relative to each other.
- The object translates and rotates in between the fingers, while the virtual springs have fixed spatial configurations. An example is a grasp without friction. The virtual springs at the fingertips have fixed lines of action. The object slips between the fingers, as it is displaced from its stable equilibrium.

Let's assume that the initial grasp is force-closure and stable. We assume the fingertips will not slip outside of the edges of contact. The final grasp is defined by the set of grasp points where the fingers stick after they slip. The problem is to find when the final grasp is force-closure and stable.

4.3.1 Grasps without Friction

Slip is always present in a frictionless grasp. If the finger tips slip relative to each other, we have in effect a grasp with a completely different set of grasp points. This new grasp is *force-closure* if the grasp points are still inside the independent contact regions. A conservative bound on the slip, allowed at the fingers, can be computed based on the lengths of the independent contact regions.

In a grasp without friction, the fingertips are controlled so that they behave as linear springs with fixed lines of action. To a good approximation, we can assume that the lines of action of these virtual springs are fixed. So, the major source of slip comes from the translation and rotation of the object in between the fingers.

A pure translation of the object moves the points of contact, but leaves the contact normals unchanged, Figure 4.5. The points of contact moves along the lines of action of the linear springs, and these lines of action are unchanged. Force-closure depends on the relative configuration of these lines of action, and so is unchanged by a pure translation of the object. The grasp remains force-closure after arbitrary translations of the grasped object, as long as the fingertips do not leave the grasping edges, of course. An upper bound on the translation that preserves force-closure can be found from the positions of the fingertips, and the lengths of the grasping edges.

A pure rotation of the object not only moves the points of contact, but also rotates the contact normals, Figure 4.5. Each fingertip has a different effective spring on the object, because its contact normal has changed. The effective spring has stiffness scaled by $\cos \delta_z$, and line of action going through the new contact point.

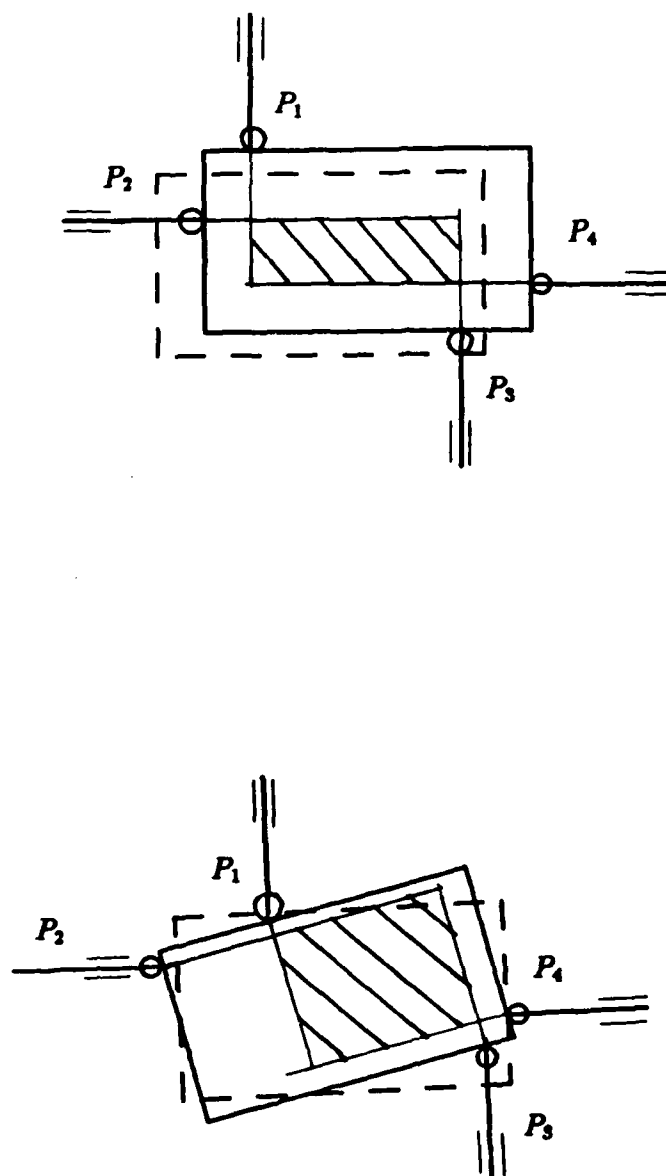


Figure 1.5: Effect of large displacements on a frictionless grasp.

and oriented with the new contact normal. The new grasp has a new set of grasp points, and a new set of linear springs. The relative configuration of the linear springs is no longer preserved. We deduce whether the new grasp is force-closure or not, by looking at the new grasp points. A conservative bound on the rotation is the maximum rotation such that the new grasp points are always inside the independent contact regions.

With stiffness at the contacts, a force-closure grasp implies a stable grasp. The compressions at the linear springs are assumed small compared to the size of the object, therefore, the stiffness matrix $K \approx K_S$. The matrix K_S depends only on the spatial configurations of the virtual springs. It is invariant with respect to arbitrary translations, but changes drastically with large rotations of the object. Since the stiffness matrix K_S is positive definite, an force-closure grasp is also a stable grasp, Corollary 3.3. The potential function of the grasp has a local minimum at the equilibrium grasp configuration. This local minimum is also a global minimum for all translations of the object, due to the invariance of K_S respective to translations. This means that the equilibrium grasp configuration is globally stable for the set of contact edges, if we allow only translational errors, and very small rotational errors (typically less than 10 degrees) of the grasped object.

Since there is no friction, the potential energy that is stored in the springs is constant, and conserved. Gravity and other external wrenches displace the grasped object. This displacement can be found from force and torque balance equations, or from the external work which is added to the potential function of the grasp. As the external wrenches are removed, the grasped object returns to its old stable equilibrium.

We see that translations of the object preserve the force-closure and stability properties of the grasp, whereas rotations quickly destroy them. In the worst case, we have to rely on the independent contact regions to guarantee that force-closure and stability are preserved:

Corollary 4.3 *Without friction, a force-closure grasp with n linear springs is globally stable for arbitrary translations of the object, as long as the fingertips are still inside their respective grasping edges. The grasp is stable only for small rotations of the object.*

4.3.2 Grasps with Friction

We've seen that we can synthesize the virtual springs at the point contacts with friction, such that the fingers, if they slip, will always stick within the edges of contact. These fingers are pulled, independently from each other, towards their own bias positions. As the fingertip slips, the point of contact changes, and so either or both the spatial configurations of the normal and tangential springs change. We have shown that an equilibrium grasp with at least two point contacts with friction is also a force-closure grasp, if the contact forces point strictly inside the friction

cones. In other words, if the fingers stick and the equilibrium is not marginal, then the grasp with friction is a force-closure grasp.

With stiffness at the contacts, a force-closure grasp implies a stable grasp, Corollary 3.2. So, after the fingers slip, the grasp at the points where the fingers stick is both force-closure and stable. To guarantee stability for rotations, the compressions at the linear springs must be small compared to the size of the object.

Corollary 4.4 *A planar grasp with friction is both force-closure and stable, as long as the grasped object is in equilibrium, with contact forces from the virtual springs pointing strictly inside their respective friction cones.*

As the object slips, friction dissipates potential energy in the form of heat, and the total potential energy of the object is less. The potential energy of the object is the sum of the potential energy of the grasp, which is stored in the springs, and the gravity potential from the height of the object in the gravity field. In Figure 4.4.a, suppose the weight is perpendicular to the contact plane, and the fingers slip on the object, due to some impulse force with negligible work. There is no external work added into the system, and friction dissipates potential energy, so the new grasp configuration must have a lower potential, and so is more stable. Disturbances which are zero-integral impulses always slide the grasped object into a more stable grasp. So, as long as the contact edges are long enough, slip and disturbances make marginally stable grasp more stable. For the case of Figure 4.4.a, the two fingers will slide towards each other, and the grasp has a lower potential.

4.4 Slip on Circular Arcs

Up to now, the grasped object has been modeled as a polygon, and slip and stability are studied with virtual springs contacting on straight edges. When the boundary of the grasped object is curved instead of polygonal, the stability of the object is greatly enhanced if the contacts slides inside concave arcs of the boundary (Hanafusa and Asada 1977, Asada 1979). We'll see that the local curvature at the grasp points does not affect the equilibrium of the grasp. But local curvature has a major effect on the stability of the grasp. It adds another term K_C to the stiffness matrix K_S , which comes from the spatial configurations of the virtual springs.

4.4.1 Model Local Curvatures with Wide Circular Arcs

Arcs with low curvature are approximated as straight edges. Arcs with high curvature are approximated as vertices. Arcs with medium curvature¹ are approximated as circular arcs, with radius equal to the radius of curvature r at the point of contact.

Depending on whether friction is significant or not, the stiffness at the 2D contact can be modeled as one or two independent linear springs, Figure 4.6. A finger contacting without friction at a convex corner is an extremely unstable contact, and should be avoided. A frictionless contact at a concave corner is a very stable contact respective to lateral translations and rotations. The more interesting cases are when the fingers slip without friction on circular arcs with radii of curvature comparable to the size of the grasped object.

Figure 4.7 shows a linear spring k_i contacting a convex arc with radius r_i . For simplicity, the line of action of the spring k_i originally goes through the center C_i of the convex arc. Let's also assume that the displacement of the object is small, so that the point of contact P_i remains on its circular arc.

As the object is displaced by twist $\hat{t} = (\delta_x, d_x, d_y)^T$, the point of contact P_i moves to its new position P'_i , defined as the intersection of the displaced convex arc (C'_i, r_i) and the fixed line of action of the linear spring k_i . The compression at the linear spring k_i is:

$$\begin{aligned} \sigma_i &= \sigma'_i + (\mathbf{c}'_i - \mathbf{c}_i) \cdot \mathbf{k}_i \pm \frac{1}{2r_i} [(\mathbf{c}'_i - \mathbf{c}_i) - ((\mathbf{c}'_i - \mathbf{c}_i) \cdot \mathbf{k}_i) \mathbf{k}_i]^2 \\ &\approx \sigma'_i + \hat{\mathbf{k}}_i \cdot \hat{t} - \frac{1}{2} (\mathbf{c}_i \cdot \mathbf{k}_i) \delta_x^2 \\ &\quad \pm \frac{1}{2r_i} \left[(1 - C_i^2) d_x^2 - (1 - S_i^2) d_y^2 + (c_{ix}^2 + c_{iy}^2 - \mu_i^2) \delta_x^2 \right. \\ &\quad \left. - 2C_i S_i d_x d_y - 2(c_{iy} + \mu_i C_i) d_x \delta_x - 2(c_{ix} - \mu_i S_i) d_y \delta_x \right] \end{aligned} \quad (4.5)$$

where $\hat{\mathbf{k}}_i = (C_i, S_i, \mu_i)^T$ is the spatial vector describing the line of action of the linear spring k_i . The sign is + (resp. -) for concave (resp. convex) arcs.

¹ A medium curvature is around $1/R$, where R is the radius of the minimum circle containing the grasped object. The diameter $2R$ has been referred as the size of the object.

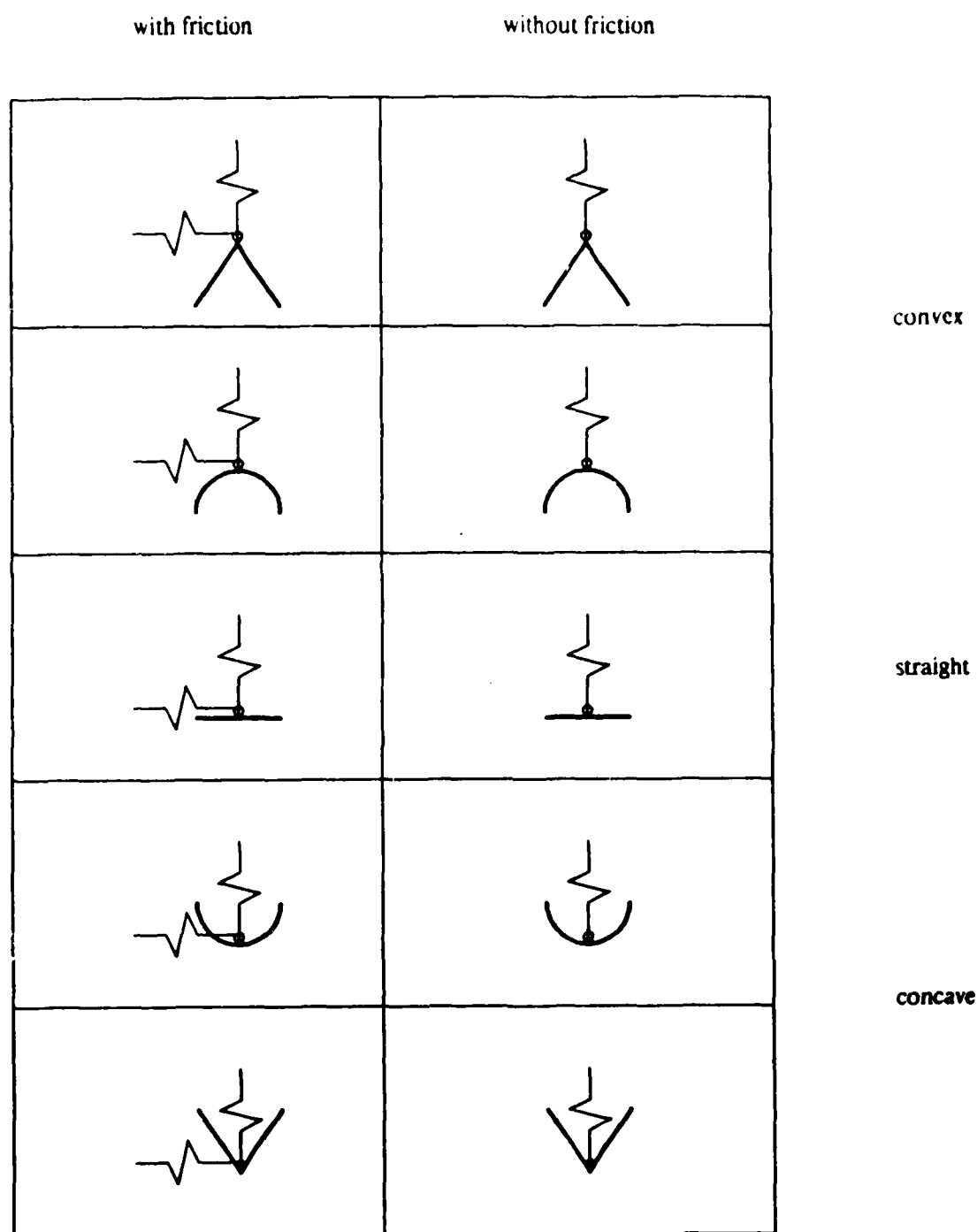


Figure 4.6: Point contacts slipping on curved segments.

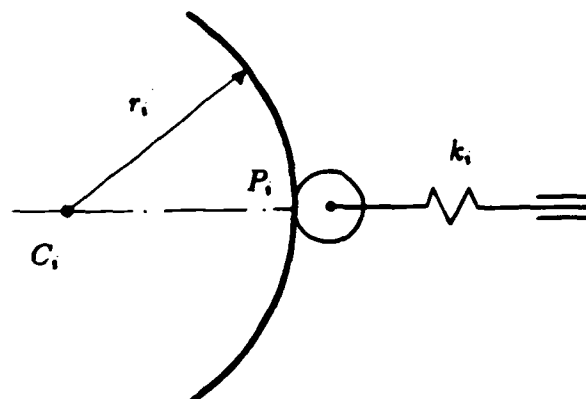


Figure 4.7: Model local curvature with a wide circular arc.

The above equation has first order term, a dot product between the spatial vector of the spring $\hat{\mathbf{k}}_i$, and the twist displacement of the object $\hat{\mathbf{t}}$. The gradient of potential function U of the grasp gives again the sum of the contact wrenches exerted on the object. The second order term gives the stiffness matrix of the grasp about the equilibrium configuration.

4.4.2 Effect of Local Curvature on Stability

The stiffness matrix of the grasp, and of the object, can be written as a sum of two matrices:

$$\mathbf{K} = \mathbf{K}_S + \mathbf{K}_C$$

$$\mathbf{K}_S = \sum_{i=1}^n k_i (\hat{\mathbf{k}}_i \hat{\mathbf{k}}_i^T)$$

$$\begin{aligned} \mathbf{K}_C = & - \sum_{i=1}^n f_{io} \begin{pmatrix} 0 & 0 & 0 \\ 0 & 0 & 0 \\ 0 & 0 & \mathbf{c}_i \cdot \hat{\mathbf{k}}_i \end{pmatrix} \\ & \pm \sum_{i=1}^n \frac{f_{io}}{r_i} \begin{pmatrix} 1 - C_i^2 & -C_i S_i & -c_{iy} - \mu_i C_i \\ -C_i S_i & 1 - S_i^2 & c_{ix} - \mu_i S_i \\ -c_{iy} - \mu_i C_i & c_{ix} - \mu_i S_i & c_{ix}^2 + c_{iy}^2 - \mu_i^2 \end{pmatrix} \end{aligned} \quad (4.6)$$

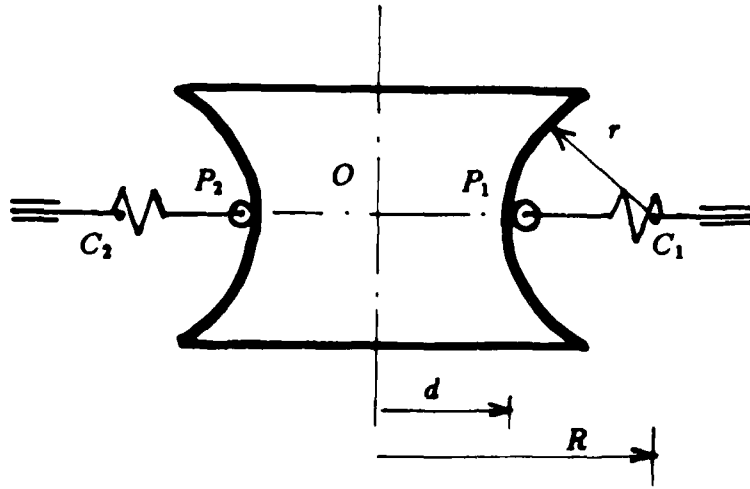


Figure 4.8: Two frictionless point contacts pressing at two concave half-circles.

K_S , also written as SKS^T , is the stiffness matrix from the spatial configuration of the virtual springs only. K_C is a sum of the stiffness contributions from the circular arcs (C_i, r_i) . The sign is + (resp. -) for concave (resp. convex) arcs.

Figure 4.8 shows a frictionless grasp at two concavities. The finger contacts are modeled as two linear springs with same stiffness constant k , and contact force f_o . The stiffness matrix from the spatial configurations of these two linear springs has only the stiffness component along the common line of action of these springs:

$$\begin{aligned}
 K_S &= \begin{bmatrix} 1 & -1 \\ 0 & 0 \\ 0 & 0 \end{bmatrix} \begin{pmatrix} k & 0 \\ 0 & k \end{pmatrix} \begin{bmatrix} 1 & 0 & 0 \\ -1 & 0 & 0 \end{bmatrix} \\
 &= 2k \begin{pmatrix} 1 & 0 & 0 \\ 0 & 0 & 0 \\ 0 & 0 & 0 \end{pmatrix}
 \end{aligned} \tag{4.7}$$

The stiffness matrix K_C from frictionless slip within the two concavities of radius r , and with two centers at $(R, 0)$ and $(-R, 0)$ is:

$$K_C = -2f_o \begin{pmatrix} 0 & 0 & 0 \\ 0 & 0 & 0 \\ 0 & 0 & R \end{pmatrix} \pm 2f_o \frac{R}{r} \begin{pmatrix} 0 & 0 & 0 \\ 0 & \frac{1}{R} & 0 \\ 0 & 0 & R \end{pmatrix} \tag{4.8}$$

Slipping inside the two concavities generates linear stiffness in the y -direction, and angular stiffness about the z -direction. As expected, these stiffnesses are positive for concave arcs and negative for convex arcs. The first term of K_C depends on the location of the centers of curvature. The second term of K_C is inversely proportional to the radius of curvature.

- As $r \rightarrow \infty$, the circular arcs become straight edges. A straight edge is the limit of either a concave arc or a convex arc. Unfortunately, the limit of K_C blows up to $+\infty$ and $-\infty$ respectively for concave and convex arcs. The center of curvature is not well defined for a straight edge. By taking the average of the two limits, the terms in r and R drop out. After some reduction, the stiffness K_C has only a positive angular stiffness equal to $2f_0 d$, where d is the distance from the origin to the right vertical edge. We recognize this stiffness as equal to the angular stiffness from the two frictionless points of contact: $\sum f_{i0}(\mathbf{p}_i \cdot \mathbf{k}_i)$. As expected, the limiting contacts are two point contacts without friction sliding on straight edges.

- As $r \rightarrow 0$, the circular arcs become corners. The second term in K_C becomes very large, and gives large negative (resp. positive) linear stiffness in the y -direction, and angular stiffness about the z -direction, for convex (resp. concave) corners. The grasp is therefore very stable for concave corners, and very unstable for convex corners.

For small radius of curvature, the points of contact coincide with the centers of curvatures. We can view a point of contact which does not slip as the limiting case of either a convex or a concave arc with very small radius of curvature. The average of the two limits is the first term of K_C , which is a negative angular stiffness $-2f_0 R$. We recognize this stiffness as equal to the angular stiffness from two point contacts with friction: $-\sum f_{i0}(\mathbf{p}_i \cdot \mathbf{k}_i)$. So, a point contact with friction is the limiting case of an arc with zero radius of curvature.

- Now, let's look at the case of wide circular arcs, whose radius of curvature is comparable to the size of the object. The stiffness matrix K_C in equation 4.8 can be rewritten as:

$$K_C = \pm 2 \frac{R}{r} f_0 \begin{pmatrix} 0 & 0 & 0 \\ 0 & \frac{1}{R} & 0 \\ 0 & 0 & \mathbf{p} \cdot \mathbf{k} \end{pmatrix} \quad (4.9)$$

The grasp is stable (resp. unstable) for concave (resp. convex) arcs, for y -translations and z -rotations. The linear stiffness in the y -direction is:

$$k_y = \sum k_i \frac{\sigma_i}{r_i} \quad (4.10)$$

which is very small because $\sigma_i \ll r_i$.

The angular stiffness is similar to point contacts with (resp. without) friction, except there is a multiplying factor of R/r_i when the segment of contact is curved instead of straight:

$$k_z = \sum \frac{R}{r_i} f_{i0}(\mathbf{p}_i \cdot \mathbf{k}_i) \quad (4.11)$$

Due to this factor R/r , local curvatures have a major impact on the stability of grasps respective to rotations. The two models of point contacts with and without friction turn out to be a very close approximation to slip on convex and concave arcs. The difference between outside-in grasps and inside-out grasps is the sign of the dot-product $(\mathbf{p}_i \cdot \mathbf{k}_i)$. Grasps without friction on concave (resp. convex) arcs more (resp. less) stable if the fingers grasp outside-in. The reverse holds for inside-out grasps.

4.5 Conclusion

The main results of this chapter are:

- Virtual springs at the contacts can be synthesized such that the fingertips are guaranteed to stick inside their respective grasping edges, after they slip. Typically, given the lengths of the grasping edges, and the expected disturbance force, we compute the scales for the stiffness constants and the compressions of the virtual springs. These scales are computable in linear time in the number of contacts.
- Frictionless grasps remain force-closure and stable for arbitrarily large translations and for small rotations of the grasped object. Qualitatively, the object will be pulled back to its stable equilibrium if it does not rotate drastically due to the slipping between the fingers and the object.
- Grasps with friction remains force closure and stable, as long as the grasped object is in equilibrium, with the contact forces pointing strictly inside their respective friction cones. Qualitatively, if the fingers stick again on their grasping edges, after they slip, then the new grasp is force closure and stable.
- Slip on circular arcs affects the stability of the object. The stiffness matrix of the grasp is the sum of K_S and K_C . The stiffness matrix K_S comes from the spatial configuration of the springs. The matrix K_C plays the role of the position-dependent matrix K_P . It describes the effect of the fingers slipping on the circular arcs. It is negative (resp. positive) for convex (resp. concave) arcs.
- Point contacts which stick or slide without friction on straight edges are good approximations to fingertips slipping respectively on convex and concave arcs.

The above results extend from 2D to 3D. Future problems can be a full analysis of slip on curved surfaces. It is interesting to enumerate all the simple cases where a globally stable grasp exists. Then using these cases, one can address, at least in part, the reverse problem of constructing grasps on curved objects.

Chapter 5

Conclusion

5.1 A Review

After all the equations and proofs, I want to conclude this thesis with the following remark:

"Grasp synthesis is a simple geometric problem."

Constructing grasps is definitely a geometric problem, and one which is very simple for two point contacts with friction in 2D, or two soft-finger contacts in 3D:

- Chapter 2 shows how to construct the independent regions of contact for the two finger tips. These two independent regions are either back-to-back or face-to-face with each other. Force-closure is just a constraint on the relative placement and orientation of these two contact regions. Remember that we can only push on the object, not pull on it. This is basically why we need two opposing fingers.
- Chapter 3 shows how to synthesize the virtual springs at the finger tips, so that the grasp is stable and has a desired stiffness matrix. The key result here is a simple geometric relation between stability and stiffness on the grasped object and the spatial configurations of the virtual springs at the contacts. Basically, the virtual springs must be along the stiffness directions of the grasped object.
- Chapter 4 looks at how slip and curvature affect the force-closure and stability of the grasps. It turns out that we have good reasons not to be afraid of slip, even accidental slip in grasps where we rely on friction between the fingers and the grasped object. This supports another approach to planning grasps, which is to find places where the fingers will stick.

However, one should not be content with simple working cases, guided by either heuristics or intuitions based on what people do. The most important lesson from this research is the value of a general and formal framework which results in

insights, not discovered or proved by intuitions or heuristics. A lot of the results and explanations reported in this thesis come directly from the formal framework, not the other way around.

5.2 Open Problems

There are still a lot of open problems for future research:

- Grasps on curved objects. — We have discussed why the independent regions of contact are harder to construct, when the surface normal is not constant. We have analyzed the effect of curvature on the stability of grasps in 2D. More research is needed, especially on finding the independent regions of contact, where the fingers stick and the grasp is force-closure. It is interesting to show that such independent regions of contact can be constructed directly from the shape of the object, and search as in (Hanafusa and Asada 1977, Asada 1979) is not needed.
- Form-closure grasps. — Examples of form-closure grasps we have looked at are: four frictionless point contact in 2D, and seven frictionless point contacts in 3D. We have mainly looked at grasps which use the finger tip. How about grasps with frictionless edge and face contacts, or structural restraint from many contacts on different links of a same finger? These grasps are called form-closure grasps (Lakshminarayana 1978). Form-closure is a stronger constraint than force-closure. It might explain the power grasps found in humans, (Cutkosky and Wright 1986). A general framework is needed to explain how humans grasp objects.
- Reorienting the object within the fingers. — We have showed that grasps can be changed by a sequence of stable force-closure grasps. Large manipulations can be done by devising a sequence of stable force-closure grasps which rotates the object into the desired configuration. Fearing (1984, 1986) shows the twirling of a bar between three fingers. This twirling is an example of a sequence of stable force-closure grasps. Small manipulations are currently done best by treating the object grasped by the fingers as a linked mechanism, assuming no slipping at the contacts (Chiu 1985). These two forms of manipulations can generate a wide range of motions for the grasped object.

Appendix A

A.1 Force-Direction Closure With Planar Forces

The necessary and sufficient condition for a set of wrenches W to generate force with arbitrary direction is:

Theorem A.1 *A set of wrenches W can generate force in any direction if and only if there exists a three-tuple of wrenches $(\hat{w}_1, \hat{w}_2, \hat{w}_3)$ whose respective force directions f_1, f_2, f_3 satisfy:*

- Two of the three directions f_1, f_2, f_3 are independent.
- There exist α, β, γ all greater than zero, such that:

$$\alpha f_1 + \beta f_2 + \gamma f_3 = 0$$

That is, a strictly positive combination of the three directions is zero.

Proof: No reciprocal or repelling translational twist means the system of linear inequalities described by:

$$W^T \hat{t}^S \geq 0 \quad (A.1)$$

has no non-zero solution $\hat{t} = (0, d_x, d_y)^T$.

Since a translational twist is a free vector with zero angular displacement, we get a reduced system of homogeneous linear inequalities in only two unknowns d_x, d_y . For such system to have no solution, we must need at least three inequalities, or W must have at least three wrenches (Kuhn and Tucker 1956, Strang 1976).

Without loss of generality, let's assume that W contains exactly one such three-tuple $(\hat{w}_1, \hat{w}_2, \hat{w}_3)$. After dropping out the angular terms, system (A.1) reduces to:

$$\begin{pmatrix} f_{1x} & f_{1y} \\ f_{2x} & f_{2y} \\ f_{3x} & f_{3y} \end{pmatrix} \begin{bmatrix} d_x \\ d_y \end{bmatrix} \geq \begin{bmatrix} 0 \\ 0 \\ 0 \end{bmatrix} \quad (A.2)$$

There is no homogeneous solution if and only if the 3×2 matrix W^T is of rank 2, or if and only if two of the three force directions are non-parallel, Figure A.1.

Assuming that there is no homogeneous solution, the rank of W^T is $r = 2$. Any particular solution must be a 1-face (Goldman and Tucker 1956) with a zero

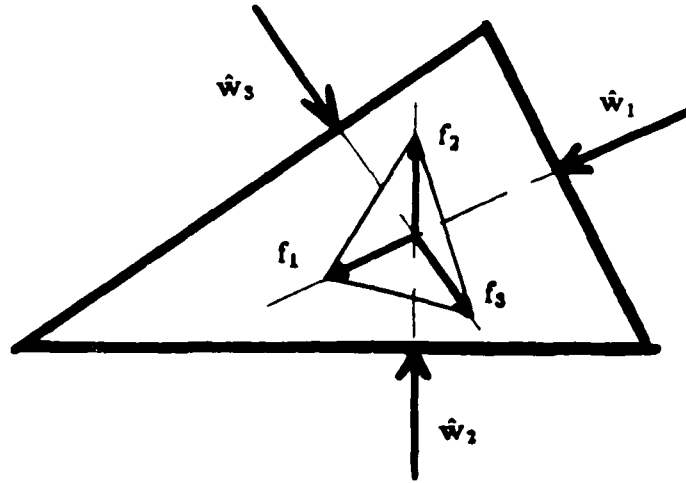


Figure A.1: A geometrical view of force-direction closure.

product with one row of W^T and strictly positive products with the remaining rows of W^T . In other words, the necessary and sufficient condition for the existence of a particular solution is that the solution has a zero product with one row of W^T , and two non-zero products having the same sign with the two remaining rows of W^T .¹

Conversely, there is no particular solution if and only if all 1-face vectors perpendicular to one row of W^T have products of different signs with the remaining rows of W^T . Concretely, let's solve for the nonexistence of repelling translational displacement d reciprocal to the force direction f_1 :

$$\begin{pmatrix} f_{1z} & f_{1y} \\ f_{2z} & f_{2y} \\ f_{3z} & f_{3y} \end{pmatrix} \begin{bmatrix} d_x \\ d_y \end{bmatrix} = \begin{bmatrix} 0 \\ \beta_1 \\ -\gamma_1 \end{bmatrix} \quad (\text{A.3})$$

β_1, γ_1 are both of the same sign and non-zero.

From the first equation of system (A.3), we solve for d_x, d_y in terms of f_{1z}, f_{1y} , and replace them in the second and third equations to get an equation in terms of the three force directions f_1, f_2, f_3 . After simplifications, we get:

$$(f_2 \times f_3) f_1 + \beta_1 f_2 + \gamma_1 f_3 = 0 \quad (\text{A.4})$$

The cross product of two 2-dimensional vectors is a scalar, which is the product of the magnitudes of the two vectors, and the sin of the angle between these two

¹In the case the two non-zero products are both negative, we can always negate the solution to make the non-zero products positive.

vectors.

By rotating the subscripts and coefficients, we get two other equations for the non-existence of repelling translational twist which is respectively reciprocal to the force direction \mathbf{f}_2 , and \mathbf{f}_3 .

$$\alpha_2 \mathbf{f}_1 + (\mathbf{f}_3 \times \mathbf{f}_1) \mathbf{f}_2 + \gamma_2 \mathbf{f}_3 = \mathbf{0} \quad (\text{A.5})$$

$$\alpha_3 \mathbf{f}_1 + \beta_3 \mathbf{f}_2 + (\mathbf{f}_1 \times \mathbf{f}_2) \mathbf{f}_3 = \mathbf{0} \quad (\text{A.6})$$

In the above equations, (A.4) (A.5) (A.6), the coefficients α_i, β_i must have the same sign within each equation.

Without loss of generality, let's assume that the force directions $\mathbf{f}_1, \mathbf{f}_2, \mathbf{f}_3$ are ordered counter-clockwise, so that all the pairwise cross products are strictly greater than zero. Since we have assumed that two of the three force directions are independent, the third force direction can be uniquely expressed as a linear combination of the first two. This implies that the three equations (A.4), (A.5), and (A.6) all express one unique linear combination, describing the constraint that the positive combination of the three force directions is null. We conclude that: assuming two force directions are non parallel, there is no repelling translational twist if and only if there exist α, β, γ all greater than zero, such that:

$$\alpha \mathbf{f}_1 + \beta \mathbf{f}_2 + \gamma \mathbf{f}_3 = \mathbf{0} \quad (\text{A.7})$$

■

A.2 Torque Closure With Planar Forces

The following theorem states the analytical necessary and sufficient condition for a set of contact forces to generate clockwise and counter-clockwise torques.

Theorem A.2 *A set of planar forces W can generate clockwise and counter-clockwise torques if and only if there exists a four-tuple of forces $(\hat{\mathbf{w}}_1, \hat{\mathbf{w}}_2, \hat{\mathbf{w}}_3, \hat{\mathbf{w}}_4)$ such that:*

- *Three of the four forces have lines of action that do not intersect at a common point or at infinity.*
- *Let $\mathbf{f}_1, \dots, \mathbf{f}_4$ be the force directions of $\hat{\mathbf{w}}_1, \dots, \hat{\mathbf{w}}_4$. Let \mathbf{p}_{12} (resp. \mathbf{p}_{34}) be the point where the lines of action of $\hat{\mathbf{w}}_1$ and $\hat{\mathbf{w}}_2$ (resp. $\hat{\mathbf{w}}_3$ and $\hat{\mathbf{w}}_4$) intersect. There exist $\alpha, \beta, \gamma, \delta$ all greater than zero, such that:*

$$\begin{aligned} \mathbf{p}_{34} - \mathbf{p}_{12} &= \pm (\alpha \mathbf{f}_1 + \beta \mathbf{f}_2) \\ &= \mp (\gamma \mathbf{f}_3 + \delta \mathbf{f}_4) \end{aligned}$$

Proof: (The proof is quite long and has the same flavor as the proof of Theorem A.1. On first reading, the reader is advised to skip this proof and return to it later.)

No rotational twist reciprocal or repelling to W means the system of linear inequations described by:

$$W^T \hat{\mathbf{t}}^S \geq 0 \quad (\text{A.8})$$

has neither homogeneous nor particular solution. $\hat{\mathbf{t}} = (\delta_z, \delta_z r_y, -\delta_z r_x)^T$ is the infinitesimal rotation.

We get a system of homogeneous linear inequations in three unknowns. For such a system to have no solution, we need at least four inequations, or four wrenches. Without loss of generality, we assume that W is exactly one such four-tuple of wrenches.

There is no homogeneous solution if and only if the 4×3 matrix W^T is of rank 3, or if and only if there is a 3×3 block from W^T that has non zero determinant. Assume that the first three rows form such block. The determinant is:

$$\det(\hat{\mathbf{w}}_1, \hat{\mathbf{w}}_2, \hat{\mathbf{w}}_3) = \begin{vmatrix} f_{1x} & f_{1y} & \mathbf{p}_1 \times \mathbf{f}_1 \\ f_{2x} & f_{2y} & \mathbf{p}_2 \times \mathbf{f}_2 \\ f_{3x} & f_{3y} & \mathbf{p}_3 \times \mathbf{f}_3 \end{vmatrix} \quad (\text{A.9})$$

By expanding the determinant along the third column, we get:

$$\begin{aligned} \det(\hat{\mathbf{w}}_1, \hat{\mathbf{w}}_2, \hat{\mathbf{w}}_3) &= (\mathbf{p}_1 \times \mathbf{f}_1)(\mathbf{f}_2 \times \mathbf{f}_3) \\ &+ (\mathbf{p}_2 \times \mathbf{f}_2)(\mathbf{f}_3 \times \mathbf{f}_1) \\ &+ (\mathbf{p}_3 \times \mathbf{f}_3)(\mathbf{f}_1 \times \mathbf{f}_2) \end{aligned} \quad (\text{A.10})$$

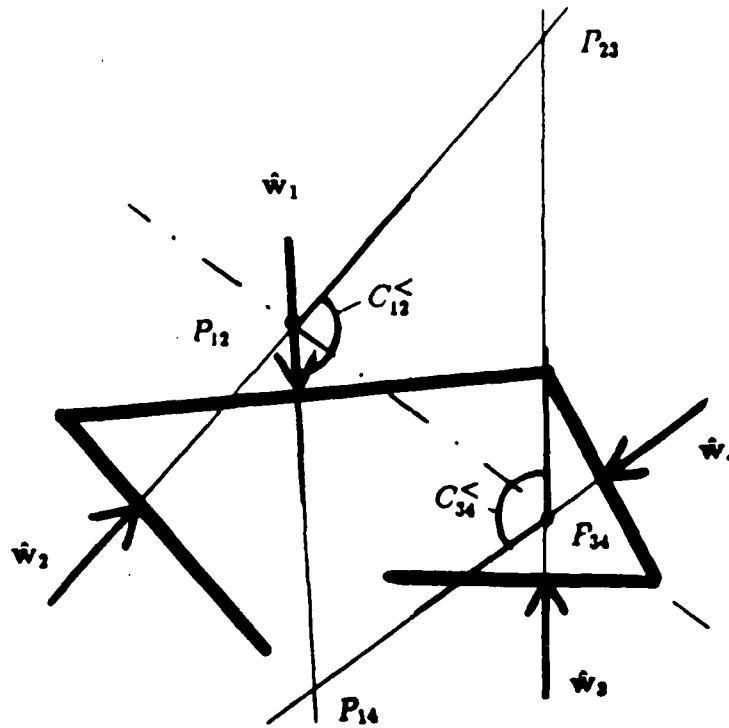


Figure A.2: A geometrical view of torque closure.

From the above equation, if the three lines of force are parallel with each other, then the three cross products of the force directions are zero, and so is the determinant. Let's assume that they are not all three parallel, and that the lines of action of \hat{w}_1, \hat{w}_2 intersect at p_{12} . We can choose p_{12} as the origin of our reference frame. With this choice of origin, the moment components of the wrenches \hat{w}_1, \hat{w}_2 become zero, and so the first two terms in right hand side of equation (A.10) drop out. The determinant reduces to:

$$\det(\hat{w}_1, \hat{w}_2, \hat{w}_3) = ((p_3 - p_{12}) \times f_3)(f_1 \times f_2) \quad (A.11)$$

The determinant can be zero if and only if the first cross-product in equation (A.11) is zero, or if and only if the line of force of \hat{w}_3 also goes through p_{12} . We conclude that there is no free rotation if and only if both the followings do not hold:

- The three lines of force intersect at a common point. In this case, the object B can freely rotate about the z -axis going through this common point.
- The three lines of force are all parallel. This case corresponds to a free translation perpendicular to the direction of the three forces. We can think of this translation as a rotation with point of rotation at infinity.

Assuming that the 4×3 matrix W^T is of rank 3, there is no particular solution to system (A.8) if and only if any 2-face vector orthogonal to two rows of W^T

has products of different signs with the remaining rows of W^T . Let's solve for the non-existence of rotational twist, reciprocal to the first two wrenches $\hat{\mathbf{w}}_1, \hat{\mathbf{w}}_2$, and repelling to the two last wrenches $\hat{\mathbf{w}}_3, \hat{\mathbf{w}}_4$:

$$\begin{pmatrix} f_{1x} & f_{1y} & \mathbf{p}_1 \times \mathbf{f}_1 \\ f_{2x} & f_{2y} & \mathbf{p}_2 \times \mathbf{f}_2 \\ f_{3x} & f_{3y} & \mathbf{p}_3 \times \mathbf{f}_3 \\ f_{4x} & f_{4y} & \mathbf{p}_4 \times \mathbf{f}_4 \end{pmatrix} \begin{bmatrix} \delta_z r_y \\ -\delta_z r_x \\ \delta_z \end{bmatrix} = \begin{bmatrix} 0 \\ 0 \\ \gamma_0 \\ -\delta_0 \end{bmatrix} \quad (\text{A.12})$$

γ_0, δ_0 are both of the same sign and non zero.

Without loss of generality, let's factor out δ_z . Let P_{12} , (resp. P_{34}) be the point where the lines of force of $\hat{\mathbf{w}}_1, \hat{\mathbf{w}}_2$ (resp. $\hat{\mathbf{w}}_3, \hat{\mathbf{w}}_4$) intersect. From the first two equations, we solve for the point of rotation \mathbf{p} :

$$\begin{aligned} \mathbf{p} &= \frac{1}{\mathbf{f}_1 \times \mathbf{f}_2} ((\mathbf{p}_2 \times \mathbf{f}_2) \mathbf{f}_1 - (\mathbf{p}_1 \times \mathbf{f}_1) \mathbf{f}_2) \\ &= \mathbf{p}_{12} \end{aligned} \quad (\text{A.13})$$

The above equation makes sense: the point of free rotation is the point where the two lines of force intersect. Similarly, from the third and fourth equations of system (A.12), we solve for the instantaneous center of rotation \mathbf{p} :

$$\begin{aligned} \mathbf{p} &= \frac{1}{\mathbf{f}_3 \times \mathbf{f}_4} ((\mathbf{p}_4 \times \mathbf{f}_4) \mathbf{f}_3 - (\mathbf{p}_3 \times \mathbf{f}_3) \mathbf{f}_4) \\ &\quad + \frac{1}{\mathbf{f}_3 \times \mathbf{f}_4} (\gamma_0 \mathbf{f}_3 - \delta_0 \mathbf{f}_4) \\ &= \mathbf{p}_{34} + \frac{1}{\mathbf{f}_3 \times \mathbf{f}_4} (\gamma_0 \mathbf{f}_3 + \delta_0 \mathbf{f}_4) \end{aligned} \quad (\text{A.14})$$

Eliminating \mathbf{p} from the two equations (A.13) (A.14), we find a constraint equation with the following form:

$$\mathbf{p}_{12} - \mathbf{p}_{34} = (\gamma_1 \mathbf{f}_3 + \delta_1 \mathbf{f}_4) \quad (\text{A.15})$$

where γ_1, δ_1 have both the same sign and non zero.

By rotating the numbers 1, ..., 4 and the coefficients α, \dots, δ , we get the equation expressing the nonexistence of repelling rotational twist $\hat{\mathbf{t}}^S$ which is reciprocal to the wrenches $\hat{\mathbf{w}}_3, \hat{\mathbf{w}}_4$:

$$\mathbf{p}_{34} - \mathbf{p}_{12} = (\alpha_1 \mathbf{f}_1 + \beta_1 \mathbf{f}_2) \quad (\text{A.16})$$

We also get four other equations for the other two pairings $((\hat{\mathbf{w}}_1, \hat{\mathbf{w}}_3), (\hat{\mathbf{w}}_2, \hat{\mathbf{w}}_4))$ and $((\hat{\mathbf{w}}_1, \hat{\mathbf{w}}_4), (\hat{\mathbf{w}}_2, \hat{\mathbf{w}}_3))$:

$$\mathbf{p}_{13} - \mathbf{p}_{24} = (\beta_2 \mathbf{f}_2 + \delta_2 \mathbf{f}_4) \quad (\text{A.17})$$

$$\mathbf{p}_{24} - \mathbf{p}_{13} = (\alpha_2 \mathbf{f}_1 + \gamma_2 \mathbf{f}_3) \quad (\text{A.18})$$

$$\mathbf{p}_{14} - \mathbf{p}_{23} = (\beta_3 \mathbf{f}_2 + \gamma_3 \mathbf{f}_3) \quad (\text{A.19})$$

$$\mathbf{p}_{23} - \mathbf{p}_{14} = (\alpha_3 \mathbf{f}_1 - \delta_3 \mathbf{f}_4) \quad (\text{A.20})$$

We use the fact that the points P_{12}, P_{13}, P_{14} are on the same line of action of wrench $\hat{\mathbf{w}}_1$, etc. ... to prove that the above six equations (A.15) – (A.20) are satisfied if and only if all the coefficients $\alpha_i, \dots, \delta_i$ are of the same sign. We are able to prove a stronger result which states that if one pair of equations like (A.15, A.16) holds, with coefficients $\alpha_1, \dots, \delta_1$ all of the same sign, then the other two pairs (A.17, A.18) and (A.19, A.20) hold, and vice versa. See Lemma A.1.

With Lemma A.1, we conclude that there is no rotational twist repelling to W if and only if any of the 3 pairs of equations (A.15, A.16), (A.17, A.18), (A.19, A.20) hold. Namely, if and only if there exists a pairing such as $(\hat{\mathbf{w}}_1, \hat{\mathbf{w}}_2), (\hat{\mathbf{w}}_3, \hat{\mathbf{w}}_4)$ with $\alpha, \beta, \gamma, \delta$ all greater than zero, such that:

$$\begin{aligned} \mathbf{p}_{34} - \mathbf{p}_{12} &= \pm (\alpha \mathbf{f}_1 + \beta \mathbf{f}_2) \\ &= \mp (\gamma \mathbf{f}_3 + \delta \mathbf{f}_4) \end{aligned} \quad (\text{A.21})$$

Particular cases arise when the pairing $((\hat{\mathbf{w}}_1, \hat{\mathbf{w}}_2), (\hat{\mathbf{w}}_3, \hat{\mathbf{w}}_4))$ has $\hat{\mathbf{w}}_1$ parallel to $\hat{\mathbf{w}}_2$, or $\hat{\mathbf{w}}_3$ parallel to $\hat{\mathbf{w}}_4$. We can avoid handling these particular cases by considering another pairing like $((\hat{\mathbf{w}}_1, \hat{\mathbf{w}}_3), (\hat{\mathbf{w}}_2, \hat{\mathbf{w}}_4))$, or $((\hat{\mathbf{w}}_1, \hat{\mathbf{w}}_4), (\hat{\mathbf{w}}_2, \hat{\mathbf{w}}_3))$. If we assume that the four forces in W span the space of all force directions, then we never get three forces that are parallel with each other. So there is always at least two pairings that work to prove the nonexistence of rotational twists repelling to W if the grasp has torque closure. ■

To complete the discussion of this section, we state and prove Lemma A.1 which allows us to consider only one pairing instead of all three possible pairings:

Lemma A.1 *Let four lines with directions $\mathbf{f}_1, \mathbf{f}_2, \mathbf{f}_3, \mathbf{f}_4$ intersect pairwise at six points P_{12}, \dots, P_{34} .*

$$\begin{aligned} \mathbf{p}_{34} - \mathbf{p}_{12} &= (\alpha_1 \mathbf{f}_1 - \beta_1 \mathbf{f}_2) \\ &= -(\gamma_1 \mathbf{f}_3 + \delta_1 \mathbf{f}_4) \\ \mathbf{p}_{24} - \mathbf{p}_{13} &= (\alpha_2 \mathbf{f}_1 + \gamma_2 \mathbf{f}_3) \\ &= -(\beta_2 \mathbf{f}_2 - \delta_2 \mathbf{f}_4) \\ \mathbf{p}_{23} - \mathbf{p}_{14} &= (\alpha_3 \mathbf{f}_1 - \delta_3 \mathbf{f}_4) \\ &= (\beta_3 \mathbf{f}_2 + \gamma_3 \mathbf{f}_3) \end{aligned} \quad (\text{A.22})$$

The above 6 equations all have Greek coefficients with the same sign within each equation (not necessarily across all six equations) if and only if $\alpha_i, \beta_i, \gamma_i, \delta_i$ all have the same sign for either $i = 1$, or 2, or 3.

Proof: Let's assume that we have the first two equations:

$$\begin{aligned} \mathbf{p}_{34} - \mathbf{p}_{12} &= (\alpha_1 \mathbf{f}_1 - \beta_1 \mathbf{f}_2) \\ &= -(\gamma_1 \mathbf{f}_3 + \delta_1 \mathbf{f}_4) \end{aligned} \quad (\text{A.23})$$

with $\alpha_1 > 0$, $\beta_1 > 0$, and $\gamma_1 \delta_1 > 0$. We'll prove that the four coefficients $\alpha_1, \beta_1, \gamma_1, \delta_1$ are all greater than zero, that is, we have the scenario illustrated in Figure 7. We compute the intersection points \mathbf{p}_{23} and \mathbf{p}_{14} :

$$\begin{aligned} \mathbf{p}_{23} &= \mathbf{p}_{12} + \frac{\mathbf{1} \times \mathbf{f}_3}{\mathbf{f}_2 \times \mathbf{f}_3} \mathbf{f}_2 \\ &= \mathbf{p}_{34} + \frac{\mathbf{1} \times \mathbf{f}_2}{\mathbf{f}_2 \times \mathbf{f}_3} \mathbf{f}_3 \\ \mathbf{p}_{14} &= \mathbf{p}_{12} + \frac{\mathbf{1} \times \mathbf{f}_4}{\mathbf{f}_1 \times \mathbf{f}_4} \mathbf{f}_1 \\ &= \mathbf{p}_{34} + \frac{\mathbf{1} \times \mathbf{f}_1}{\mathbf{f}_1 \times \mathbf{f}_4} \mathbf{f}_4 \end{aligned} \quad (\text{A.24})$$

where $\mathbf{1} = \mathbf{p}_{34} - \mathbf{p}_{12}$. Next, we compute the expression for $\mathbf{p}_{23} - \mathbf{p}_{14}$:

$$\begin{aligned} \mathbf{p}_{23} - \mathbf{p}_{14} &= -\gamma_1 \frac{\mathbf{f}_3 \times \mathbf{f}_4}{\mathbf{f}_4 \times \mathbf{f}_1} \mathbf{f}_1 + \delta_1 \frac{\mathbf{f}_3 \times \mathbf{f}_4}{\mathbf{f}_2 \times \mathbf{f}_3} \mathbf{f}_2 \\ &= \alpha_1 \frac{\mathbf{f}_1 \times \mathbf{f}_2}{\mathbf{f}_2 \times \mathbf{f}_3} \mathbf{f}_3 - \beta_1 \frac{\mathbf{f}_1 \times \mathbf{f}_2}{\mathbf{f}_4 \times \mathbf{f}_1} \mathbf{f}_4 \end{aligned} \quad (\text{A.25})$$

Expressing $\mathbf{p}_{23} - \mathbf{p}_{14}$ in terms of linear combination of $(\mathbf{f}_2, \mathbf{f}_3)$ is difficult. Instead of proving that there exist β_3, γ_3 non zero and of the same sign such that:

$$\mathbf{p}_{23} - \mathbf{p}_{14} = \beta_3 \mathbf{f}_2 + \gamma_3 \mathbf{f}_3$$

we prove the equivalent: the vector $\mathbf{p}_{23} - \mathbf{p}_{14}$ has opposite sign cross-products with the vectors $\mathbf{f}_2, \mathbf{f}_3$, i.e:

$$((\mathbf{p}_{23} - \mathbf{p}_{14}) \times \mathbf{f}_2) ((\mathbf{p}_{23} - \mathbf{p}_{14}) \times \mathbf{f}_3) < 0$$

From equations (A.25), we get:

$$((\mathbf{p}_{23} - \mathbf{p}_{14}) \times \mathbf{f}_2) ((\mathbf{p}_{23} - \mathbf{p}_{14}) \times \mathbf{f}_3) = -\beta_1 \gamma_1 \frac{(\mathbf{f}_1 \times \mathbf{f}_2)^2 (\mathbf{f}_3 \times \mathbf{f}_4)^2}{(\mathbf{f}_4 \times \mathbf{f}_1)^2} \quad (\text{A.26})$$

We deduce that the necessary and sufficient condition for the two last equations of (A.22) to hold is that β_1 be of the same sign with γ_1 . We extrapolate this partial proof and argue that:

- \Rightarrow The fact that the six equations of (A.22) hold implies that $\alpha_1, \dots, \delta_1$ all have the same sign for $i = 1$, or 2, or 3. We have proved this implication for $i = 1$ using Equation (A.26). Similar proofs exist for $i = 2$ and 3.
- \Leftarrow From Equation (A.26), if $\alpha_1, \dots, \delta_1$ all have the same sign then:

$$\mathbf{p}_{23} - \mathbf{p}_{14} = \beta_3 \mathbf{f}_2 + \gamma_3 \mathbf{f}_3$$

with $\beta_3 \gamma_3 > 0$. Equations similar to (A.26) allow us to deduce that all the six equations in (A.22) must hold.

■

A.3 Stiffness Matrix When the Fingertips Stick

Figure A.3 shows a finger F_i contacting with friction at point P_i . We assume that there is no dissipation of potential energy in grasp, so the point of contact P_i is constant. As the object is displaced by (x, y, θ) , the point P_i is mapped into its new position P'_i given by:

$$\mathbf{p}'_i = \begin{pmatrix} C\theta & S\theta \\ S\theta & C\theta \end{pmatrix} \begin{bmatrix} p_{ix} \\ p_{iy} \end{bmatrix} + \begin{bmatrix} x \\ y \end{bmatrix} \quad (\text{A } 27)$$

When the grasped object is moved away by (x, y, θ) from its equilibrium, the linear spring k_i is compressed by an amount equal to the projection of the displacement $P_i P'_i$ onto the line of action of spring k_i :

$$\begin{aligned} \sigma_i(x, y, \theta) &= \sigma_{i0} + (\mathbf{p}'_i - \mathbf{p}_i) \cdot \mathbf{k}_i \\ &= \sigma_{i0} + ((C\theta - 1)p_{ix} - S\theta p_{iy} + x) C_i \\ &\quad + (S\theta p_{ix} + (C\theta - 1)p_{iy} + y) S_i \end{aligned} \quad (\text{A } 28)$$

The first partial derivatives of the compression σ_i give the spatial vector of the spring k_i . The equilibrium equation is exactly the same as Equation (3.4). The second partial derivatives are the same, except $\partial^2 \sigma_i / \partial \theta^2$, which has a \pm sign:

$$\frac{\partial^2 \sigma_i}{\partial \theta^2} = \pm \mathbf{p}_i \cdot \mathbf{k}_i \quad (\text{A } 29)$$

The stiffness matrix of the grasp is the same as in Equation (3.8), except that the angular stiffness in K_P has a \pm sign:

$$K_P = \pm \sum_{i=1}^n f_{i0} (\mathbf{p}_i \cdot \mathbf{k}_i) \begin{pmatrix} 0 & 0 & 0 \\ 0 & 0 & 0 \\ 0 & 0 & 1 \end{pmatrix} \quad (\text{A } 30)$$

K_P therefore depends on whether the finger tips stick, or slide without friction on the grasping edge, and on whether the grasp is inside/out or outside in. The general expression of the position-dependent matrix K_P is:

$$K_P = \pm \sum_{i=1}^n f_{i0} (\mathbf{p}_i \cdot \mathbf{k}_i) \begin{pmatrix} 0 & 0 & 0 \\ 0 & 0 & 0 \\ 0 & 0 & 1 \end{pmatrix} \quad (\text{A } 31)$$

The sign is $+$ (resp. $-$) if the fingers slide (resp. stick) on the grasping edges of the object.

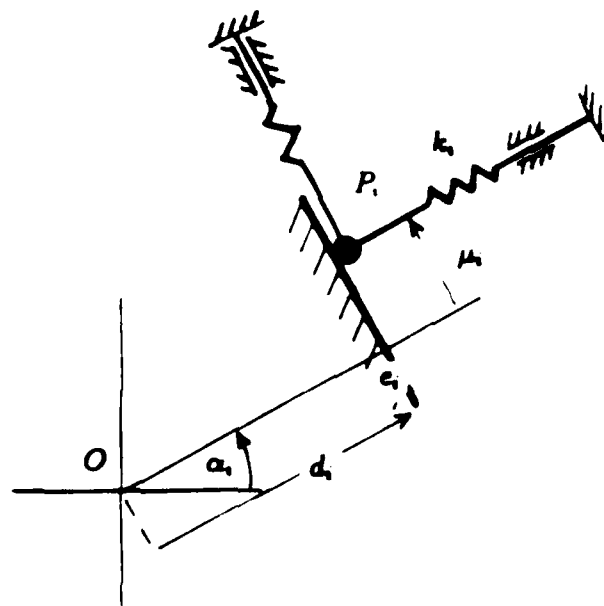


Figure A.3: A fingertip which sticks is modeled by two linear springs.

Bibliography

- Abel, J.M., Holzmann, W., McCarthy, J.M.** "On Grasping Planar Objects With Two Articulated Fingers" Proc. IEEE Intl. Conference on Robotics and Automation, St. Louis, March 1985.
- Asada, H.** "Studies on Prehension and Handling by Robot Hands with Elastic Fingers" Ph.D. Thesis, Kyoto University, April 1979.
- Baker, B.S., Fortune, S.J., Grosse, E.H.** "Stable Prehension with a Multi-Fingered Hand: Extended Abstract" Proc. IEEE Intl. Conference on Robotics and Automation, St. Louis, March 1985.
- Ball R. S.** "A Treatise on the Theory of Screws" Cambridge Univ. Press, London, 1900.
- Ben-Israel, A., Greville, T.N.E.** "Generalized Inverses: Theory and Applications" J. Wiley, New York, 1974.
- Bottema, O., Roth, B.** "Theoretical Kinematics" North Holland, Amsterdam, 1979.
- Brady, M., Hollerbach, J.M., Johnson, T.L., Lozano-Pérez, T., Mason, M.T.** (editors) "Robot Motion: Planning and Control" MIT Press, Cambridge, 1982.
- Brady, M., Paul, R.** (editors) "Robotics Research" Vol. 1, MIT Press, Cambridge, 1984.
- Brost, R.C.** "Automatic Grasp Planning in the Presence of Uncertainty" Proc. IEEE Intl. Conference on Robotics and Automation, San Francisco, April 1986.
- Buckley, S.** "Programming a Robot by Showing it What to Do" Forthcomming Ph.D. Thesis, Dept. of Elec. Eng. and Comp. Science, Massachusetts Institute of Technology, Dec. 1986.
- Chiu, S.L.** "Generating Compliant Motion of Objects with an Articulated Hand" S.M. Thesis, Dept. of Mechanical Engineering, Massachusetts Institute of Technology, June 1985.
- Cutkosky, M.R.** "Mechanical Properties for the Grasp of a Robotic Hand" CMU-RI-TR-84-24, Carnegie Mellon Robotics Institute, 1984.
- Cutkosky, M.R.** "Robotic Grasping and Fine Manipulation" Kluwer Academic Publishers, Boston, 1985.
- Cutkosky, M.R., Wright, P.K.** "Modeling Manufacturing Grips and Correlations With the Design of Robotic Hands" Proc. IEEE Intl. Conference on Robotics

and Automation, San Francisco, April 1986.

Donald, B.R. "Local and Global Techniques for Motion Planning" S.M. Thesis, Dept. of Elec. Eng. and Comp. Science, Massachusetts Institute of Technology, May 1984. Also as AI TR 791, MIT Artificial Intelligence Lab, 1984.

Erdmann, M.A. "On Motion Planning with Uncertainty" S.M. Thesis, Dept. of Elec. Eng. and Comp. Science, Massachusetts Institute of Technology, August 1984. Also as AI TR 810, MIT Artificial Intelligence Lab, 1984.

Fearing, R.S. "Touch Processing for Determining a Stable Grasp" S.M. Thesis, Dept. of Elec. Eng. and Comp. Science, Massachusetts Institute of Technology, Sept. 1983.

Fearing, R.S. "Simplified Grasping and Manipulation with Dexterous Robot hands" AI Memo 809, MIT Artificial Intelligence Lab, Nov. 1984.

Fearing, R.S. "Implementing a Force Strategy for Object Re-orientation" Proc. IEEE Intl. Conference on Robotics and Automation, San Francisco, April 1986.

Featherstone, R. "Position and Velocity Transformations Between Robot End-Effector Coordinates and Joint Angles" Intl. Journal of Robotics Research, Vol. 2, No. 2, 1983, pp. 35-45.

Featherstone, R. "Robot Dynamics Algorithms" Ph.D. Thesis, Dept. of Artificial Intelligence, Univ. of Edinburgh, 1984.

Featherstone, R. "Spatial Notation: A Tool For Robot Dynamics" D.A.I Research Paper 213, University of Edinburgh, 1984.

Goldman, A.J., Tucker, A.W. "Polyhedral Convex Cones" in "Linear Inequalities and Related Systems", Kuhn, H.W. and Tucker, A.W. editors, 1956.

Hanafusa, H., Asada, H. "Stable Prehension By a Robot Hand With Elastic Fingers" Proc. of 7th Intern. Symp. on Industrial Robots, Tokyo, Oct. 1977. Reprinted in "Robot Motion: Planning and Control", Erady et al. editors, 1982.

Hanafusa, H., Inoue, H. (editors) "Robotics Research" Vol. 2, MIT Press, Cambridge, 1985.

Hilderbrand, F.B. "Advanced Calculus for Applications" 2nd edition, Prentice-Hall, Englewood Cliffs, 1976.

Hogan, N. "Impedance Control of Industrial Robots" Robotics and Computer Integrated Manufacturing, Vol. 1, No. 1, 1984.

Hollerbach, J.M., Narasimhan, S. "Finger Force Computation Without the Grip Jacobian" Proc. IEEE Intl. Conference on Robotics and Automation, San Francisco, April 1986.

Hunt, K.H. "Kinematic Geometry Of Mechanisms" Clarendon Press, Oxford, 1978.

Jacobsen, S.C., Wood, J.E., Knutti, D.F., Biggers, K.B. "The Utah MIT Hand: Work in Progress" Intl. Journal of Robotics Research, Vol. 3, No. 4, 1984, pp. 21-50.

Jacobsen, S.C., Wood, J.E., Knutti, D.F., Biggers, K.B., Iversen, E.K. "The Version I Utah MIT Dextrous Hand" in "Robotics Research" Hanafusa H., Inoue, H. eds., 1985, pp. 301-308.

Jameson, J.W. "Analytic Techniques for Automated Grasps" Ph.D. Thesis, Dept. of Mechanical Engineering, Stanford University, June 1985.

Kerr, J.R. "An Analysis of Multi-Fingered Hands" Ph.D. Thesis, Dept. of Mechanical Engineering, Stanford University, Jan. 1985.

Kobayashi, H. "Grasping and Manipulation of Objects by Articulated Hands" Proc. IEEE Intl. Conference on Robotics and Automation, San Francisco, April 1986.

Kuhn, H.W., Tucker, A.W. (editors) "Linear Inequalities and Related Systems" Princeton Univ. Press, Princeton, 1956.

Lakshminarayana, K. "Mechanics of Form Closure" ASME Paper 78-DET-32, 1978.

Lozano-Pérez, T. "The Design of a Mechanical Assembly System" S.M. Thesis, Dept. of Elec. Eng. and Comp. Science, Massachusetts Institute of Technology, Dec. 1976. Also published as AI TR 397, MIT Artificial Intelligence Lab, 1976.

Lozano-Pérez, T. "Spatial Planning: A Configuration Space Approach" IEEE Transactions Computers, C-32, Feb. 1983.

Lozano-Pérez, T., Mason, M.T., Taylor, R.H. "Automatic Synthesis of Fine-Motion Strategies for Robots" Proc. Intl. Symposium of Robotics Research, Bretton Woods, NH. Aug. 1983. Also published in "Robotics Research", Vol. 1, Brady, M., Paul, R. editors, 1984.

Mason, M.T. "Compliance and Force Control for Computer Controlled Manipulators" S.M. Thesis, Dept. of Elec. Eng. and Comp. Science, Massachusetts Institute of Technology, May 1979. Also published as AI TR 515, MIT Artificial Intelligence Laboratory, April 1979. Reprinted in "Robot Motion: Planning and Control" Brady, M. et al. editors, 1982.

Mason, M.T. "Manipulator Grasping and Pushing Operations" Ph. D. Thesis, Dept. of Elec. Eng. and Comp. Science, Massachusetts Institute of Technology, May 1982. Also published as AI TR 690, MIT Artificial Intelligence Laboratory, June 1982.

Mason, M.T., Salisbury, J.K. "Robot Hands and the Mechanics of Manipulation" MIT Press, Cambridge, 1985.

Narasimhan, S. "Tasks with Robot Hands: Execution and Planning" Forthcoming S.M. Thesis, Dept. of Elec. Eng. and Comp. Science, Massachusetts Institute of Technology, August 1986.

Nguyen, V. "The Find-Path Problem in the Plane" S.B. Thesis, Dept. of Elec. Eng. and Comp. Science, Massachusetts Institute of Technology, June 1984. Also published as AI Memo 760, MIT Artificial Intelligence Lab, Feb. 1984.

Nguyen, V. "The Synthesis of Force-Closure Grasps in the Plane" AI Memo 861, MIT Artificial Intelligence Lab, Sept 1985. A condensed version is published in

Bibliography

- Proc. IEEE Intl. Conference on Robotics and Automation, San Francisco, 1986.
- Nguyen, V.** "The Synthesis of Stable Grasps in the Plane" A Memo, Stanford Artificial Intelligence Lab, Nov 1985. A condensed version of report to the IEEE Intl. Conference on Robotics and Automation, San Francisco, April 1986.
- Ohwovoriole, M.S.** "An Extension of Screw Theory and Its Application to the Automation of Industrial Assemblies" Ph.D. Thesis, Dept. of Mechanical Engineering, Stanford University, April 1980. Also published as AI Memo 778, Stanford Artificial Intelligence Lab, 1980.
- Ohwovoriole, E.N.** "On The Total Freedom of Planar Bodies With Direct Contact" ASME Transactions, 1984.
- Okada, T.** "Computer Control of Multi-jointed Finger System for Precise Object Handling" IEEE Transactions on Systems, Man and Cybernetics, May 1982.
- Paul, R.P.** "Robot Manipulators, Mathematics, Programming, and Control" MIT Press, Cambridge, 1981.
- Paul, R., Shimano, B.** "Compliance and Control" Proc. Joint Automatic Control Conference, Purdue University, July 1976.
- Raibert, M.H., Craig, J.C.** "Hybrid Position/Force Control of Manipulators" ASME Journal of Dynamic Systems, Measurement and Control, Vol. 102, June 1981. Reprinted in "Robot Motion: Planning and Control" Brady et al. editors, 1982.
- Rao, S.S.** "Optimization, Theory and Applications" Halstead Press, J. Wiley, 1980.
- Reuleaux, F.** "Kinematics of Machinery" Dover Press, New York, 1875.
- Roth, B.** "Screws, Motors, and Wrenches That Cannot Be Bought in a Hardware Store" in "Robotics Research", Vol. 1, Brady, M., Paul, R. editors, MIT Press, Cambridge, 1984.
- Salisbury, J.K.** "Active stiffness control of a manipulator in Cartesian Coordinates" Proc. IEEE Conference on Decision and Control, Albuquerque, Dec. 1980.
- Salisbury, J.K.** "Kinematic and Force Analysis of Articulated Hands" Ph.D. Thesis, Dept. of Mechanical Engineering, Stanford University, May 1982.
- Salisbury, J.K.** "Design and Control of an Articulated Hand" Proc. 1st Intl. Symposium on Design and Synthesis, Tokyo, July 1984.
- Salisbury, J.K., Craig, J.J.** "Articulated Hands: Force Control and Kinematic Issues" Proceedings of Joint Automatic Control Conference, Virginia, June 1981. Reprinted in "Robotics Research", Vol. 1, Brady, M., Paul, R. editors, 1984.
- Salmon, G.** "A treatise on conic sections" 6th edition Chelsea, New York.
- Salmon, G.** "A Treatise on the Analytic Geometry of Three Dimensions" 7th edition, Chelsea, New York.
- Shamos, M.I.** "Computational Geometry" Ph.D. Thesis, Dept. of Computer Science, Yale University, May 1978.

- Strang, G.** "Linear Algebra and Its Application" Academic Press, New York, 1976.
- Strang, G.** "Introduction to Applied Mathematics" Wellesley-Cambridge Press, Wellesley, 1986.
- Whitney, D.E.** "Quasi-Static Assembly of Compliantly Supported Rigid Parts" *Journal of Dynamics Systems, Measurement, and Control*, March 1982. Reprinted in "Robot Motion: Planning and Control", Brady, M. et al. editors, 1984.

END
DATE
FILMED
JAN
1988